DISS. ETH NO. 30294

Self vs Non-self-DNA discrimination in *Schizosaccharomyces pombe*

A thesis submitted to attain the degree of

DOCTOR OF SCIENCES

(Dr. sc. ETH Zurich)

presented by

Shweta Saini

MSc Bioinformatics and Applied Biotechnology

University of Mysore

born on 21.10.1993

accepted on the recommendation of

Prof. Dr. Yves Barral (Examiner)

Prof. Dr. Kirsten Bomblies (Co-examiner)

Prof. Dr. Sophie Martin (Co-examiner)

2024

Contributions

All experiments were performed and analysed by Shweta Saini, with the exception of the data shown in Figs. 8 and 9, in which the original experiments and strains were designed by Dr. Haochen Yu. In Figs. 11A and B, the time course was done and analysed by Mattia Valentini. In Fig. 12B, the strains were created by Dr. Haochen Yu. The ChIP-seq data shown in Figs. 22B, C, and 24 were sequenced by the functional genomics center and analysed by Lennart Opitz.

"It is not the strongest of the species that survives, nor the most intelligent, but the one most responsive to change." -

Charles Darwin

Table of Contents

Acknowledgements 6

Abstract 8

Abstrakt 9

1. Introduction 11

1.1. What is identity? 11

1.1.1. Identity at the Biological Level 11

1.1.2. Identity at the cellular level 12

1.1.3. Identity at the molecular level 12

1.2. Genetic identity and stability 13

1.2.1. Genetic Immunity in Prokaryotes and Archaea 14

1.2.2. Genetic Immunity in Eukaryotes 15

1.3. Hallmarks of genetic identity 16

1.3.1. DNA sequence: 16

1.3.2. Centromeres: 16

1.3.3. Epigenetic marks: 21

1.4. Exploring fission Yeast 22

1.4.1. Chromosomal Organization and nuclear architecture: 23

1.4.2. Life cycle: 27

1.4.3. Vegetative cell cycle: 27

1.4.4. Sexual cell cycle: 29

1.5. Aims of this study 32

2. Results 33

2.1. Engineering an experimental system to study chromosomal and extrachromosomal DNA dynamics 33

2.2. Self-extrachromosomal DNA is distinguished from non-self-extrachromosomal DNA. 35

2.3. Self-extrachromosomal DNA circles segregate more symmetrically with time 37

2.4. Self-extrachromosomal DNA circles segregate symmetrically regardless of their original position in the genome 41

2.5. Self-extrachromosomal DNA circles stay in close proximity to SPBs 42

2.6. Self-extrachromosomal DNA circles interact with microtubules via lateral attachment 44

2.7. Self-extrachromosomal DNA circles are stable during meiosis 47

2.8. Chromosome segregation machinery plays a role in the segregation of self-extrachromosomal DNA circles 54

2.9. Centromere and kinetochore proteins show mild localisation to the self-extrachromosomal DNA foci during mitosis.....56

2.10. Cnp1 marks the chromosomal and the extrachromosomal DNA for memory: 59

2.11. Cnp1 marking for memory is a global phenomenon: 62

3. Discussion 64

3.1. DNA is distinguished based on its origin 64

3.2. Non-self-DNA is eliminated rapidly from the population, whereas Self-DNA is not 65

3.3. Self-extrachromosomal DNA is stable both during mitosis and meiosis 66

3.4. Cnp1 marks the DNA that is prone to making extrachromosomal DNA circles. 67

3.5. Cnp1 is essential for the clustering and symmetric segregation of self-extrachromosomal DNA circles 69

3.6. Role of microtubules in symmetric segregation of extrachromosomal DNA.....70

3.7. Working model.....71

3.8. Why segregate self-extrachromosomal DNA symmetrically? 72

4. Materials and Methods 73

5. References 82

Acknowledgements

I am deeply grateful to Yves for his unwavering guidance, invaluable insights, and steadfast support throughout this journey. His expertise, feedback, and encouragement have not only shaped the trajectory of this thesis but have also contributed significantly to my personal and intellectual growth. I am profoundly thankful for his dedication, patience, and belief in my abilities. My appreciation also goes to Ruth for her perspectives and suggestions for new research papers and for organising the journal club, which has been instrumental in my learning and growth.

I extend my sincere gratitude to my committee members, Iva Tólic, Sophie Martin, and Kirsten Bomblies, for their encouraging words, constructive feedback, and enriching discussions. Their contributions have been invaluable and inspiring.

My sincere appreciation extends to all current and past members of Barral and Kroschewski labs for their valuable contributions and insightful discussions throughout my time in the lab. I cannot imagine my PhD journey without all your support. Special mention goes to Hoachen Yu, whose initiation of this project paved the way for my work, Mattia Valentini for introducing me to the fascinating realm of fission yeast and extrachromosomal DNA and Hirohisa Ebina for generously sharing his profound knowledge of fission yeast and cell division. Engaging conversations, both professional and personal, with Rupali, Madhurima, Ankita, Hassan, Rachel, Nana, Anna, Hiro and Mihailo have greatly enriched my academic journey. I especially want to thank Hassan for always being a constant support.

I am thankful to Ankita and Hiro for their valuable feedback on this thesis and to Lina for assisting with translating my abstract. I also thank all the IBC staff members and ScopeM team members, especially Tobias and Liz, for their help and support.

A heartfelt thanks is also extended to my dedicated apprentices, Lina and Matilda; I hope that our time together has been as enriching for you as it has been for me.

My deepest appreciation goes to my beloved family, including my Nanaji, Mummy, Divyam, Jyotsna and Sheetal, for their constant support, love, and motivation, which sustained me through every challenge in life. Special appreciation goes to Mayank for his immense love and support during my PhD journey and for pretending to be as interested in biology as I am. I am grateful to Rupali, Anil, Aadu and Avu for their love and support, which eased the beginning of my PhD journey. I also extend my heartfelt thanks to Budha, Ma, and Baba for igniting my

passion for science and being supportive at crucial times. All your unwavering belief in me, endless encouragement, and understanding during the ups and downs of this academic endeavour have been an invaluable source of strength and inspiration.

This thesis is a culmination of the collective efforts, encouragement, and support of all those who have been a part of my academic and personal journey. I am profoundly grateful to each and every one of you. Thank you.

Abstract

Our environment is filled with DNA originating from various sources, such as secreted mucous, gametes, skin, hair and decomposing organisms. When these external DNA molecules enter a cell, they can potentially pose harm. Organisms must, therefore, distinguish between self and non-self-DNA to survive and neutralise or eliminate the latter. While we have a deep understanding of the immune systems in multicellular eukaryotes, prokaryotes, and archaea, our knowledge of how unicellular eukaryotes defend against unwanted intruders is somewhat limited. Using *Schizosaccharomyces pombe*, fission yeast, we aim to explore these immune mechanisms that specialise in discriminating between the self and the non-self.

Previous studies from our lab indicated that *S. pombe* can differentiate chromosomal DNA from foreign extrachromosomal DNA circles and treat them differently. Building on this, we aimed to determine if self-extrachromosomal DNA circles originating from within the genome undergo similar discrimination. And if they do, how is the identification achieved.

We confirmed that *S. pombe* can indeed differentiate between extrachromosomal DNA, depending on their origin. Self-extrachromosomal DNA circles are identified as self and evenly distributed among dividing cells, while foreign ones are eliminated from the population. We found that the self-identification of chromosome-borne DNA circles is mediated by the nucleation of Cnp1 molecules, leading to their symmetric segregation via lateral attachments to microtubules during mitosis. Disruption of Cnp1 nucleation by *sim3Δ* mutants impairs the propagation of self-extrachromosomal DNA circles. Additionally, we observed that Cnp1 is not limited to endogenous centromere locations but is distributed throughout the genome.

Based on our findings, we propose that Cnp1 is widely distributed on chromosomes, especially at sites prone to recombination, such as the rDNA locus. Upon excision, the presence of Cnp1 molecules enables self-extrachromosomal DNA circles to nucleate additional Cnp1 at the same site, potentially forming a functional neocentromere and ensuring symmetric segregation. This model fits *S. pombe*, allowing it to maintain homeostasis by preventing gene loss via extrachromosomal DNA recombination and reducing toxicity associated with extrachromosomal DNA accumulation, as observed in *Saccharomyces cerevisiae*.

Abstrakt

Unsere Umwelt ist voller DNA aus verschiedenen Quellen, beispielsweise aus abgesondertem Schleim, Gameten, Haut, Haaren und zersetzenden Organismen. Wenn diese externen DNA-Moleküle in eine Zelle gelangen, können sie möglicherweise Schaden anrichten. Organismen müssen daher zwischen Selbst- und Nicht-Selbst-DNA unterscheiden, um zu überleben und letztere zu neutralisieren oder zu eliminieren. Während wir über ein tiefes Verständnis des Immunsystems in mehrzelligen Eukaryoten, Prokaryoten und Archaeen verfügen, ist unser Wissen darüber, wie einzellige Eukaryoten sich gegen unerwünschte Eindringlinge verteidigen, begrenzt. Mit Hilfe der Hefe *Schizosaccharomyces pombe* wollen wir diese Immunmechanismen erforschen, die auf die Unterscheidung zwischen dem Selbst und dem Nicht-Selbst spezialisiert sind.

Frühere Studien aus unserem Labor zeigten, dass *S. pombe* chromosomale DNA von fremden extrachromosomalen DNA-Kreisen unterscheiden und diese unterschiedlich behandeln kann. Darauf aufbauend wollten wir testen, ob extrachromosomale Selbst-DNA-Kreise, die aus dem Genom stammen, einer ähnlichen Diskriminierung unterliegen. Und wenn ja, wie wird diese Identifizierung erreicht?

Wir haben bestätigt, dass *S. pombe* je nach Herkunft tatsächlich zwischen extrachromosomaler DNA unterscheiden kann. Extrachromosomale Selbst-DNA-Kreise werden als selbst identifiziert und gleichmäßig auf sich teilende Zellen verteilt, während fremde DNA-Kreise aus der Population eliminiert werden. Wir konnten zeigen, dass die Selbst-Identifikation von chromosomenbasierten DNA-Kreisen durch Cnp1-Moleküle vermittelt wird, was zur symmetrischen Segregation der DNA über seitliche Bindungen an Mikrotubuli während der Mitose führt. Eine Störung der Cnp1-Keimbildung in *sim3Δ*-Mutanten beeinträchtigt die Verteilung extrachromosomaler Selbst-DNA-Kreise. Darüber hinaus haben wir beobachtet, dass Cnp1 nicht auf endogene Centromerpositionen beschränkt ist, sondern im gesamten Genom verteilt ist.

Basierend auf unseren Erkenntnissen schlagen wir vor, dass Cnp1 auf Chromosomen weit verbreitet ist, insbesondere an Stellen, die zur Rekombination neigen, wie zum Beispiel dem rDNA-Locus. Nach dem Ausschneiden ermöglicht das Vorhandensein von Cnp1-Molekülen extrachromosomalen Selbst-DNA-Kreisen die Keimbildung von zusätzlichem Cnp1 an derselben Stelle, wodurch möglicherweise ein funktionelles Neocentromer gebildet und eine

symmetrische Segregation sichergestellt wird. Dieses Modell ermöglicht *S. pombe* die Aufrechterhaltung der Homöostase, indem es den Genverlust durch extrachromosomale DNA-Rekombination verhindert und die Toxizität durch Ansammlung extrachromosomaler DNA verringert, wie sie bei *Saccharomyces cerevisiae* beobachtet wird.

1. Introduction

1.1. What is identity?

At a fundamental level, identity refers to the characteristics, qualities, and experiences that define an individual (Montévil & Mossio, 2020). Various factors, including biological and environmental influences, can shape identity. An important facet of identity is identifying what is the self and what is the non-self.

1.1.1. Identity at the Biological Level

Identity at the biological level encompasses the distinctive amalgamation of genetic, physiological, and anatomical attributes that differentiate one individual from another. Each person inherits a unique genetic blueprint from their parents, shaped by millions of years of evolutionary selection(Emerson & Li, 2010; Lewontin, 1974). Furthermore, every organism embarks on a singular developmental journey from birth to old age, influenced by genetic predispositions and environmental stimuli. Additionally, individuals harbour a distinct set of microbiotas, which play multifaceted roles in maintaining health and regulating physiological processes (Sender et al., 2016). This intricate interplay between genetic, physiological, anatomical, developmental, microbial, and environmental factors contributes to the complexity of identity at the biological level, underscoring the uniqueness of each individual within the global ecosystem.

Each organism's uniqueness determines its ability to thrive in its environment. Their identity dictates the acquisition of traits crucial for adaptation, such as camouflage, thermoregulation and resistance to pathogens (Endler, 1986). Additionally, individual differences influence genetic variations that confer adaptive advantages, particularly in challenging environments where survival is at stake (Stearns, 1994). Furthermore, biological identity shapes the interactions between organisms and other species within their ecosystems. Predator-prey dynamics, competition for resources, and symbiotic relationships are all influenced by the specific characteristics of each organism involved (Connell, 1980).

1.1.2. Identity at the cellular level

At the cellular level, identity refers to the unique characteristics and functions inherent to the cells and tissues within an organism. Cells display a range of identities determined by their specialised processes, structures, and locations (Uzman, 2003). For example, neurons are specialised for transmitting electrical signals, whereas muscle cells are optimised for contraction. Although all cells within an organism share the same genetic makeup, differential gene expression patterns across cell types result in distinct protein profiles that define cellular identity (Lodish, 2000). Furthermore, certain cells possess plasticity, allowing them to adjust their identity and function in response to developmental cues, injuries, and environmental signals (Linder & Mostoslavsky, 2017).

Although cells within an organism possess distinct identities, their collective performance in specialised functions is essential for the organism's survival and maintenance (Uzman, 2003). For example, coordinated intestinal cells support nutrient uptake, while a well-balanced immune system facilitates the elimination of pathogens. Immune cells such as macrophages, T cells, and B cells possess unique identities that enable them to recognise and neutralise pathogens (Janeway, 2001). These cells express specific receptors capable of detecting antigens on pathogen surfaces, triggering an immune response to eradicate the threat. Conversely, epithelial cells act as physical barriers against pathogen entry into the body. Equipped with specialised junctions and secretory mechanisms, these cells enhance barrier function and safeguard the underlying tissues from harm.

1.1.3. Identity at the molecular level

Molecular identity originates from a specific DNA sequence comprising an organism’s genome (Uzman, 2003). Along with DNA, RNA, proteins, metabolites, and signalling molecules collectively determine the molecular identity. This genetic information, inherited from parents and shaped by evolutionary selection, dictates an organism’s traits and characteristics. Variations in gene expression patterns, enzymes and molecules involved in metabolic pathways, signalling molecules, and epigenetic modifications all contribute to molecular identity.

An important component of molecular identity is genetic identity, which is the unique genetic makeup of the organism. Genetic identity profoundly influences an organism’s ability to adapt

to changing environments, resist infections, and compete for resources, ultimately affecting its survival. For instance, certain individuals harbour genetic variants that bolster their immune responses, providing heightened defences against pathogens. Conversely, others possess genetic predispositions that weaken their immune functions, rendering them more vulnerable to infections.

Given the pivotal role of genetic/molecular identity in determining cellular and biological identity, it becomes essential for organisms to protect their genetic identity to survive. Any changes or disruptions to genetic identity can profoundly affect cellular functions, organismal health and population viability. By safeguarding genetic integrity, organisms can maintain the stability, resilience, and adaptability necessary to thrive in their environment and ensure the continuity of life processes across generations.

1.2. Genetic identity and stability

In the intricate landscape of life, the ability to differentiate what belongs to oneself (self) and what doesn't (non-self) is a biological necessity. The integrity of the organism, the stability of cellular activity, and the very survival of the organism hinges upon the precise execution of this discriminatory function. The consequences of misidentification can be profound. Failure to recognise and appropriately respond to foreign intruders can lead to organisms' demise. Virtually all organisms, from bacteria to complex eukaryotes, possess a recognition system that allows them to discriminate between self and nonself and possess effective mechanisms to defend themselves from unwanted non-self (S. Gonzalez et al., 2011).

DNA is widely present in the environment (Trevors, 1996) , originating from various sources such as secreted mucous, gametes, skin, hair, and decomposing organisms. Studies have shown that oceanic concentrations of dissolved DNA range from 0.2 to 19 µg/lt seawater with a molecular weight of up to 35 kbp (DeFlaun et al., 1987). Additionally, DNA contribute to approximately 10% of humic-bound organic phosphate in mineral soil (Baker, 1977). Though natural transformations facilitated by environmental extracellular DNA (eDNA) serve as a major horizontal gene transfer(HGT) mechanism in prokaryotes, such occurrences are rare in eukaryotes (Arber, 2000; Dubnau, 1999; Lorenz & Wackernagel, 1994). In eukaryotes, HGT prominently occurs through endosymbiosis, transfections, and infections (Andersson, 2005; Keeling & Palmer, 2008; Lacroix & Citovsky, 2016; Rancurel et al., 2017).

While HGT can facilitate evolutionary processes (Koonin, 2016), it also poses risks by introducing unwanted genetic elements that may compromise an organism's fitness. An example of such an adverse biological event is acquiring transposable elements (TEs) in the human genome (Deniz et al., 2019). The LINE (L1) element, an active TE in the human genome, is implicated in various human diseases by activating dormant promoters or dysregulating the expression of oncogenes and tumour suppressor genes (Ardeljan et al., 2017; Briggs et al., 2018; Emamalipour et al., 2020). Apart from cancer, TEs are also implicated in the pathogenesis of various well-known genetic, metabolic, and neurological diseases (Campos et al., 2019; Castellano-Castillo et al., 2019; Costello & Schones, 2018; Emamalipour et al., 2020; Payer & Burns, 2019, 2019; Turcot et al., 2012).

Given the potential hazard of the free flow of DNA into an organism from the environment or other sources, organisms have evolved mechanisms to discern and eliminate incoming unwanted genetic intruders, thereby safeguarding genome integrity and establishing a form of genetic immunity. The defence mechanisms can vary among different species and are influenced by their evolutionary history and ecological niche. The fundamental premise of this kind of immune system is the ability to distinguish self from non-self, allowing for a targeted immune response.

1.2.1. Genetic Immunity in Prokaryotes and Archaea

A well-known example of such genetic immunity is the restriction-modification system in bacteria, which recognises structural features on specific sequences of DNA base and targets DNA identified as "Foreign" (Dimitriu et al., 2020). This system creates an immunological defence barrier from invading bacteriophages and, potentially, eDNA (Arber, 1965; Arber & Dussoix, 1962; Arber & Linn, 1969; Thomas & Nielsen, 2005). In this case, the bacteria genome encodes methyltransferase enzymes that methylate DNA at specific positions and restriction enzyme endonuclease that specifically recognises and cleaves unmethylated DNA molecules. Consequently, the host's own genome stays protected, but the incoming unwanted DNA molecules are digested (Vasu & Nagaraja, 2013). The restriction-modification system serves as an innate immune system.

CRISPR-Cas is another kind of genetic immunity found in these organisms which is adaptive. Most prokaryotes and all the archaea have CRISPR adaptive immune systems. This kind of immunity requires exposure to a mobile genetic element. Initial exposure creates a memory

of the infection in the form of CRISPR arrays, which can be recorded onto the host DNA by recombining short sequences from a foreign genome. Using Cas enzymes, these sequences are then used to detect and eliminate the mobile genetic elements in subsequent infections (Emamalipour et al., 2020). This kind of immune system distinguishes itself based on the memory it creates after encountering it.

1.2.2. Genetic Immunity in Eukaryotes

Our understanding of immune responses in eukaryotes has been focused on protein ligands, whereas immune activation against nucleic acids is a relatively new field of study. While prokaryotes and archaea have well-established mechanisms for distinguishing self from non-self in terms of nucleic acid, this aspect remains poorly understood in eukaryotes.

Eukaryotes typically target intruders at the gene expression level, employing defence machinery to impede the transcription and replication of non-self RNA molecules. This defence mechanism predominantly involves RNA interference (RNAi), utilising small regulatory RNA molecules like microRNAs (miRNAs) or small interfering RNAs (siRNAs) to guide the degradation of complementary RNA sequences, thereby suppressing gene expression (Gammon & Mello, 2015; Holoch & Moazed, 2015; Szittya & Burgyán, 2013; Zhou & Rana, 2013). Additionally, eukaryotes utilise the distinctive structure of viral mRNA caps to differentiate self-RNA from non-self RNA, activating polyA-binding complexes that trigger an immune response leading to the elimination of non-self RNA.

Despite the well-studied mechanisms for distinguishing self-RNA from non-self-RNA, there remains a significant gap in our understanding of how eukaryotes sense self-DNA from non-self-DNA. Multicellular eukaryotes employ various receptors to detect nucleic acids, such as toll-like receptors (TLRs), which can differentiate self and non-self-nucleic acids and induce the production of crucial immune mediators like cytokines, which eliminate them (Barbalat et al., 2011). Another critical genetic immune mechanism is the cGAS-STING pathway, which is activated when the enzyme cGAS (cyclic GMP-AMP synthase) detects cytoplasmic DNA, such as that from viruses or cellular damage. This pathway triggers a cascade of events culminating in the production of interferons, which initiate an antiviral response by inducing the expression of interferon-stimulated genes (ISGs) (Ishikawa et al., 2009). These antiviral responses can be anywhere from degrading the DNA to apoptosis. However, these pathways

and their associated molecules, such as cGAS and STING, are a late evolutionary acquisition found mostly in metazoans.

While these pathways function effectively in multicellular organisms, where they can activate a systemic response and eliminate single infected cells to protect the multicellular individual, the mechanisms by which unicellular eukaryotes safeguard their genome, where a single cell represents an organism remain largely unknown.

1.3. Hallmarks of genetic identity

1.3.1. DNA sequence:

DNA sequence is the fundamental basis of genetic identity, providing the blueprint that distinguishes individuals within a species and across different species. It contains the genetic information necessary for building and maintaining organisms, dictating various traits such as physical characteristics, physiological functions, and disease susceptibility. Genetic variation within populations arises from differences in DNA sequence, including mutations, genetic recombination, and other processes. This variation contributes to individuality and enables organisms to adapt to changing environments and evolutionary pressures.

1.3.2. Centromeres:

Since the survival of all organisms depends on maintaining the integrity of their genomes within every cell. Cells must, therefore, accurately segregate their replicated genetic material during each cell division. Eukaryotes organise their genomes into physically distinct chromosomes, which replicate during the S phase and condense during the prophase of mitosis to form paired sister chromatids. During mitosis, a crucial connection forms between each sister chromatid and microtubules of the mitotic spindle, facilitating the segregation of one copy of each chromatid to the daughter cell. Each chromosome has a specific DNA locus, the centromere, that serves as the focal point of this connection (Barra & Fachinetti, 2018; Westhorpe & Straight, 2015).

The centromere, initially identified by Flemming (1882 (Flemming, 1882)), is vital for chromosome association with spindle microtubules and subsequent segregation during cell division. Given that multiple spindle attachment points (kinetochores) per chromatid often lead to chromosome missegregation in most organisms, it is imperative that this complex

machinery be assembled at a single site on each chromosome (except for holocentromeres-explained later). Failures in correct kinetochore assembly, microtubule attachment, or sister-chromatid cohesion can result in events of chromosome loss and gain, which can have severe consequences (Allshire & Karpen, 2008a; Sundararajan & Straight, 2022; Westhorpe & Straight, 2015). Such failures may drive tumour formation in somatic mammalian cells (during mitotic division) (Weaver & Cleveland, 2007). Similarly, defective chromosome segregation during meiosis can profoundly impact human fertility, with a notable proportion of recognised human pregnancies being aneuploid (Hassold & Hunt, 2001).

Though centromeres are quite well studied, the way centromeres are maintained as a unique locus on chromosomes is not understood (Black & Cleveland, 2011). Different organisms have diverse ways of specifying their centromere. In some yeasts, like *S. cerevisiae*, the centromere is entirely genetically specified. Others, like *S. pombe*, have centromeres that are genetically specified but without clear sequence specificity (Polizzi & Clarke, 1991). In other cases, like *Candida albicans*, centromeres are entirely inherited epigenetically(Ketel et al., 2009). In multicellular organisms, the sequences responsible for specifying centromeres vary widely. For instance, centromeres can be identified in humans by arrays of tandem alpha satellite repeat sequences, although neocentromeres can also form without these arrays (Ahmad & Henikoff, 2002). In rice, centromeres can consist entirely of repeating sequences or almost entirely lack them (Nagaki et al., 2004). *Drosophila* centromeres primarily comprise pentameric or short repeating sequences, but no single satellite sequences are found. In *Caenorhabditis elegans*, centromeres take up most of the length of chromosomes, and no specific sequence determines their location (Buchwitz et al., 1999; Henikoff & Furuyama, 2012; Yuen et al., 2011).

Despite the variety of sequences found at centromeres, a feature common to almost all eukaryotic cells is the presence of centromere-specific histone variant H3 (cenH3)(Malik & Henikoff, 2009). Centromeric nucleosomes are identifiable by the presence of a histone variant called cenH3 (e.g., CENP-A in humans, Cnp1 in *S. pombe*), which replaces the usual histone H3. While canonical H3 and H3.3 histones are highly conserved across species, cenH3 histones exhibit noticeable divergence, particularly in their N-terminal tails of varying lengths and long Loop 1 regions (Henikoff & Smith, 2015). Despite these significant sequence differences between species, there are no apparent functional disparities in kinetochore formation, as demonstrated by the ability of budding yeast cenH3 (Cse4) to substitute for

human CENP-A effectively (Henikoff & Furuyama, 2012; Wieland et al., 2004). There are different kinds of centromere found in organisms, as described below:

Holocentromeres:

Holocentromeres, as depicted in Figure 1A, are distinguished by their continuous distribution along the entire chromosome, facilitating microtubule attachment throughout the chromosome during cell division. They are predominantly observed in specific plant species, including representatives of the genera *Luzula* (woodrushes) and *Rhynchospora* (beak sedges) (Heckmann et al., 2013; Hofstatter et al., 2022). Additionally, holocentromeres have been documented in certain nematode species, such as *Caenorhabditis elegans*, and in various insects like butterflies and grasshoppers (Buchwitz et al., 1999; Costa et al., 2023; Pazhenkova & Lukhtanov, 2023; Steiner & Henikoff, 2014). The presence of holocentromeres in species boasting large and complex genomes suggests potential advantages in terms of genome stability and organisation.

Monocentromeres:

Monocentromeres are the typical centromeres found in most eukaryotic organisms. They are characterized by their single, localized region on the chromosome where kinetochores assemble (Figure 1B). Monocentromeres are prevalent across diverse organisms, including plants, animals, and most fungi. They are further characterized by point centromeres and regional centromeres.

Point Centromeres:

Point centromeres are primarily found in the *Saccharomycotina* subphylum of fungi, such as *Saccharomyces cerevisiae* (Figure 1C). In *S. cerevisiae,* the centromere is approximately 125 bps and contains three conserved DNA elements: CDEI, CDEII, and CDEIII (Neitz & Carbon, 1985). Characterised by a single, defined DNA sequence, point centromeres have the ability to genetically impart centromeric function onto any DNA segment to which they are transferred (Malik & Henikoff, 2009).

Regional Centromeres:

Regional centromeres, as shown in Figure 1D, also known as epigenetically defined centromeres, are found in a wide range of eukaryotic organisms, from Fission yeast to humans. Unlike point centromeres, regional centromeres are defined by significantly larger, more diffuse regions of DNA spanning several kilobases to megabases in length. While most regional centromeres consist of repetitive DNA sequences such as satellite DNA and tandem repeats interspersed with unique DNA sequences (Henikoff et al., 2001), neocentromeres can also exist without these repeats. These centromeres are established through epigenetic mechanisms and do not necessitate the presence of a specific conserved sequence (Malik & Henikoff, 2009). Remarkably, despite their essential role, these centromeres exhibit notable flexibility concerning their chromosomal position and function.

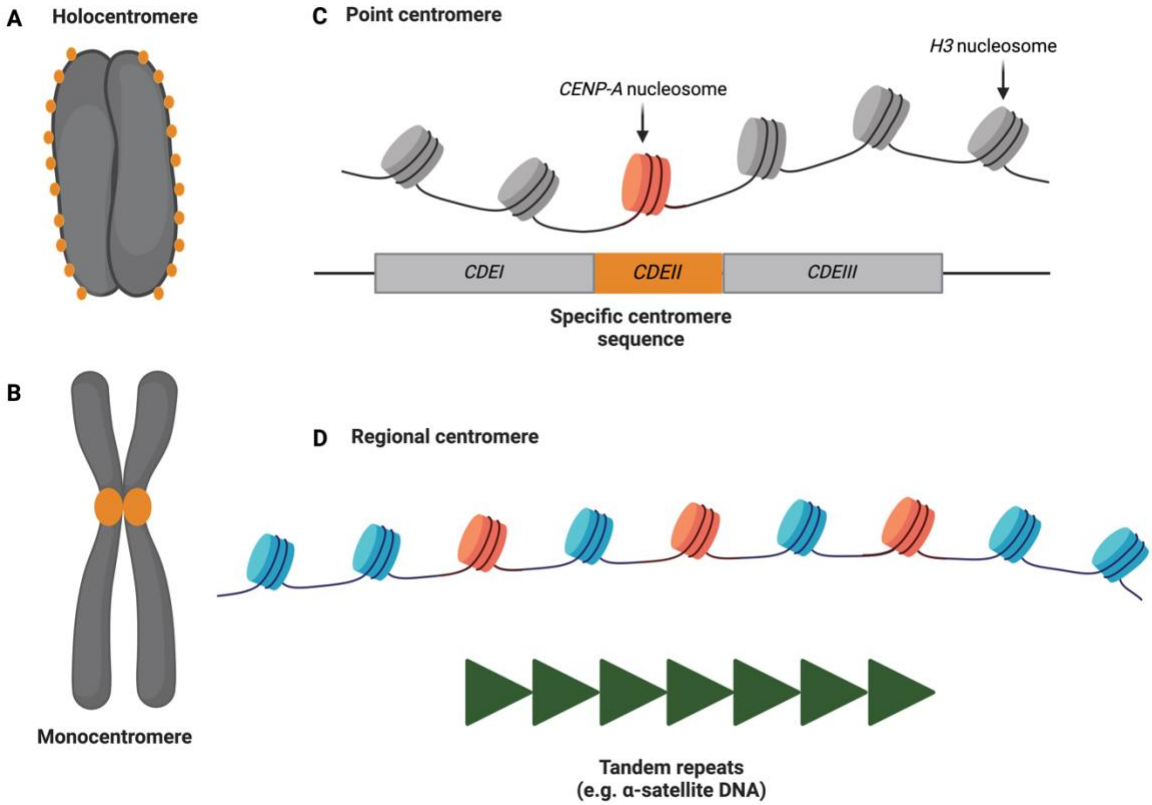

Figure 1: Variety of centromere found in eukaryotes. Holocentric chromosomes feature a diffuse centromere spread across the entire chromosome length. In contrast, monocentric chromosomes possess a centralised centromere, observable as a constriction during mitosis, known as the primary constriction. Monocentric chromosomes can be further categorised into point centromeres and regional centromeres. Point centromeres harbour specific DNA sequences necessary for centromere function, exemplified by the *Saccharomyces*

(figure legend continued on next page)

hand, encompass large repetitive DNA regions, like α-satellite DNA in primates, facilitating the assembly of multiple CENP-A nucleosomes. Based on (McKinley & Cheeseman, 2016).

Though centromeres are studied quite extensively, the mechanism responsible for ensuring the presence of one and only one centromere per chromosome remains unclear (except in Holocentromeres) (Henikoff & Furuyama, 2012). The regulated deposition of CENP-A nucleosomes plays a critical role in ensuring the epigenetic inheritance of centromeres, maintaining their position on each chromosome. Many organisms employ strategies to restrict CENP-A deposition to centromeric regions to prevent inappropriate attachments to the mitotic spindle (McKinley & Cheeseman, 2016). In *S. cerevisiae*, mislocalised CENP-A is eliminated through a coordinated mechanism involving the FACT chromatin remodeler and the E3 ubiquitin ligase Psh1 (Pob3/Spt16 histone-associated 1), which targets ectopic CENP-A for degradation(Collins et al., 2004; Deyter & Biggins, 2014). Similarly, in fission yeast, the proteasome subunit Rpt3 (regulatory particle triphosphatase 3) interacts with CENP-A, limiting the size of the CENP-A centromeric domain (Kitagawa et al., 2014).

While CENP-A plays a crucial role in most centromeres, it is not the exclusive determinant of centromere specification. Some organisms, such as trypanosomes and certain insects with holocentric chromosomes, lack CENP-A homologs, suggesting alternative mechanisms for centromere specification have evolved (Akiyoshi & Gull, 2014; Drinnenberg et al., 2014). Even in organisms containing CENP-A, additional molecular factors contribute to defining an active centromere, including the characteristics of the underlying DNA sequence, the composition of surrounding chromatin, and post-translational modifications of CENP-A itself. Furthermore, CENP-A nucleosomes are often found at non-centromeric sites throughout human and *S. pombe* chromosomes (Bodor et al., 2014; Castillo et al., 2013; McKinley & Cheeseman, 2016), indicating that the presence of CENP-A alone does not suffice for centromere formation. All these observations suggest multiple layers of regulation, ensuring only one site assembles a fully functional centromere (except for Holocentromeres). The presence of additional CENP-A localisation might have a role in genomic stability that is yet to be uncovered.

1.3.3. Epigenetic marks:

Epigenetic marks play a crucial role in establishing and maintaining the identity of the genome. For instance, DNA methylation on the fifth position of cytosine serves as a stable epigenetic modification that can be passed down through multiple cell divisions. While dynamic, during mammalian development and cell differentiation, certain DNA methylation patterns may persist, acting as a form of epigenetic memory. These methylation profiles are valuable for lineage classification and quality assessment of stem cells like embryonic stem cells, induced pluripotent cells, and mesenchymal stem cells (Kim & Costello, 2017). In cancer initiation and progression, mutations or dysregulation of chromatin regulators lead to genome-wide and gene-specific alterations in DNA methylation. Early abnormal methylation patterns emerging during transformation tend to endure throughout tumour evolution. Moreover, variations in DNA methylation across tumor regions reflect the history of cancer cells and their interaction with the tumor microenvironment. (Kim & Costello, 2017). All these indicate the importance of epigenetic marks in maintaining the genetic integrity of the cells.

Another example of epigenetic marks is histone modifications, which are Chemical modifications to histone proteins, such as acetylation, methylation, phosphorylation, ubiquitination, sumoylation, etc., which regulate chromatin structure and gene expression. Histone modifications can either promote or repress transcription by altering the accessibility of DNA to transcriptional machinery (Baan, 2009). Specific combinations of histone modifications form epigenetic "codes" that determine the functional state of chromatin and contribute to the maintenance of cellular identity and lineage specification (Z. J. Chen et al., 1996; Strahl & Allis, 2000; Vazquez-Martin et al., 2016).

1.4. Exploring fission Yeast

Schizosaccharomyces pombe, commonly known as fission yeast, is a small, rod-shaped unicellular eukaryotic microorganism that is a good model organism for understanding the regulation and conservation of the eukaryotic cell cycle (Vyas et al., 2021b). Initially isolated from beer by Saare and colleagues, it was subsequently purified in the early 1890s by Paul Linder and colleagues. The pivotal work of Ur Leupold, a Swiss scientist regarded as the father of *S. pombe*, laid the foundation for understanding the genetic basis of the mating type system in this organism in the 1940s. Leupold's isolation of the ancestral strains, 968 h^{90}, 972 h^{-} and 975 h^{-} forms the basis of nearly all modern strains used today (Leupold, 1949).

S. pombe and *S. cerevisiae* both belong to the Ascomycota group of fungi, which has a distinctive feature of forming sexual spores within specialised structures called ascus. Despite their common ancestry, these yeasts diverged evolutionarily approximately 330-420 million years ago. Protein and DNA sequence analysis suggest that the *Schizosaccharomyces* genus, to which *S. pombe* belongs, is an ancient ascomycete (*Taphrinomycetes*) with origins dating back to the early radiative evolution of ascomycetes, possibly near the divergence between animals and fungi. This implies that the evolutionary distance between *S. pombe* and *S. cerevisiae* is comparable to the distance between either of these yeasts and mammals (Heckman et al., 2001; Sipiczki, 2000).

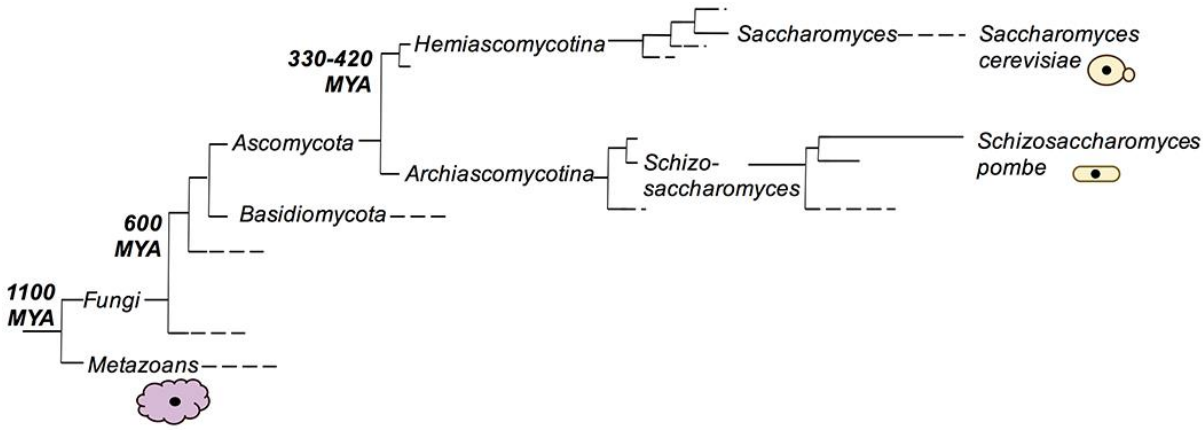

Figure 2: The phylogenetic tree *S. cerevisiae* has experienced a greater number of divergent events and is phylogenetically more distant from their common ancestor at the metazoan-fungi branching point compared to *S. pombe*. Taken from (Vyas et al., 2021a)

However, based on its biological characteristics, *S. pombe* is considered a more ancient yeast than *S. cerevisiae*, as it has undergone fewer evolutionary changes since the divergence from its common ancestors. For instance, *S. cerevisiae* has lost more than 300 genes and several

biological processes that are conserved between *S. pombe* and complex eukaryotes (Aravind et al., 2000; Hoffman et al., 2015; Wood, 2006).

These distinctions underscore *S. pombe's* significance as a model organism for exploring biological processes that bridge unicellular eukaryotes to metazoans, offering valuable insights into fundamental cellular mechanisms. *S. pombe*, unlike *S. cerevisiae*, shares common features with metazoans, including gene structure, chromatin dynamics, presence of RNA interference, and epigenetically defined centromeres. For this reason, it is also regarded as a "micromammal"(Vyas et al., 2021a) .

1.4.1. Chromosomal Organization and nuclear architecture:

The *S. pombe* genome is approximately 13.8 Mb, which is packed in the form of three large chromosomes of size 5.7, 4.6, and 3.5 Mb. In *S. pombe,* the telomeric organisation displays a higher level of complexity, mirroring that found in metazoans. The telomeres comprise a 300 bp stretch containing repeating units of 8-11 bp conserved sequences, culminating in a single-stranded 5' overhang sequence. Chromosomes I and II feature telomeric regions flanked by 20-40 kb of repetitive subtelomeric (STE) sequences. While no subtelomeric sequences have been identified in Chromosome III, it harbours approximately ~1.2 Mb of ribosomal DNA between its arms. Additionally, replication origin (oriC) sites in *S. pombe* exhibit conserved higher-order features, with around 1200 oriC sites identified, though only a subset is utilised in each replication cycle. Analogous to metazoans, oriC sites vary in length (0.5 to 3 kb) and replication efficiency (Vyas et al., 2021a).

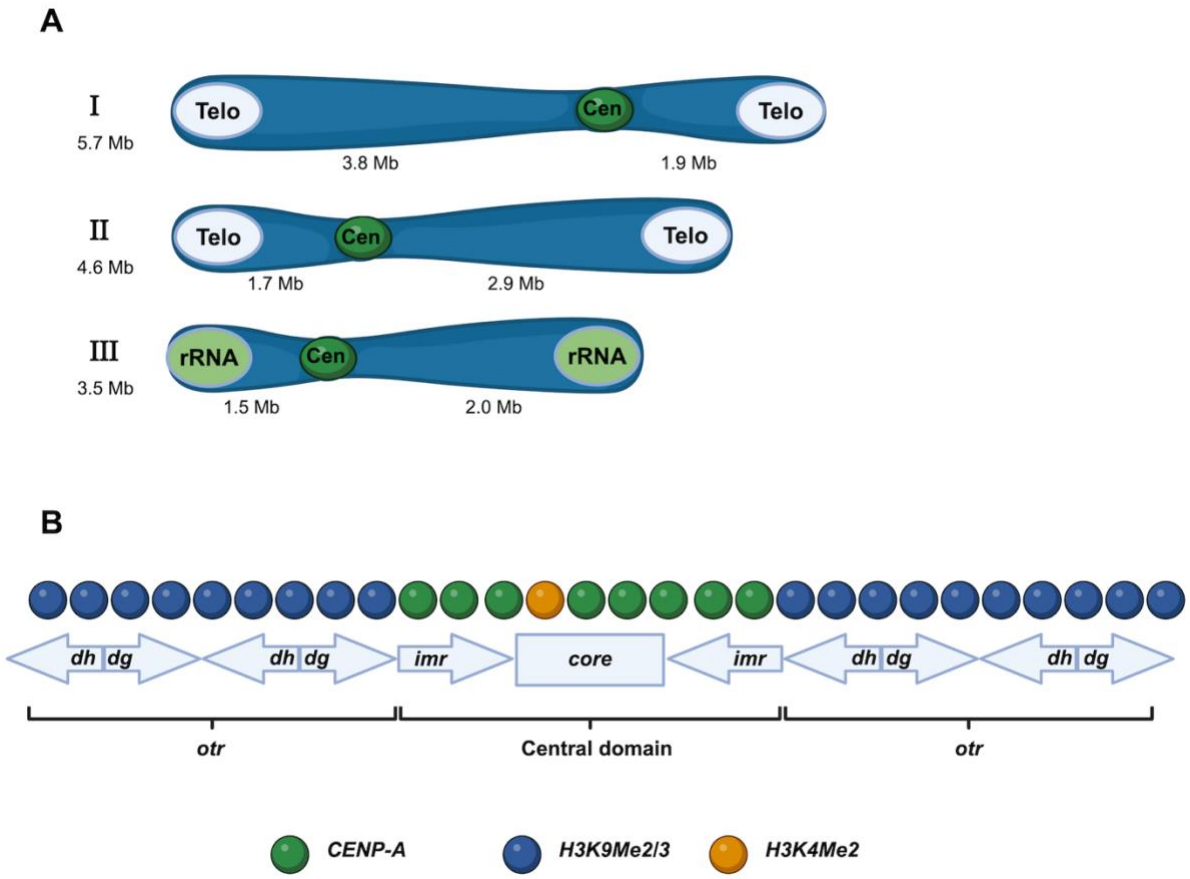

Figure 3: Chromosomal and Centromeric organisation of *S. pombe*. (A) The genome of the fission yeast *S. pombe* consists of three chromosomes. Chromosomes I and II share a telomere repeat sequence, whereas chromosome III lacks this sequence; instead, its telomeric repeats are flanked immediately by repeats of ribosomal RNA genes. All three chromosomes, however, share a common centromeric repetitive sequence represented in B. In visual representations, telomere repeats are depicted by a light blue circle labelled 'Telo', centromeres by a green circle labelled 'Cen', and repeats of ribosomal RNA genes by a light green circle labelled 'rRNA'. Based on (Hiraoka, 1998). (B) The complexity of *S. pombe* centromeres features a central domain composed of a central core flanked by innermost repeat (*imr*) regions. Surrounding the central domain are outer repeat regions (*otr*), which primarily contribute to the heterochromatinisation of the centromere. The coloured circles depicted above the centromeric sequences represent the enriched histone types associated with the centromeric domain. It's important to note that centromere lengths, histone sizes, and histone numbers are not depicted to scale. The broad arrows indicate various repetitive elements found at centromeres.

Furthermore, *S. pombe* centromeres are quite large compared to *S. cerevisiae*, with Cen I at 35 Kbp, Cen II at 65 Kbps, and Cen III at 110 Kbps. Each chromosome's centromeric region comprises a ~4kb central core (*cc*) region flanked by two distinct repetitive domains. The cc domain is associated with the centromere-specific histone H3 variant, Cnp1/CENP-A. Immediately flanking the cc sequences are the innermost repeats (*imr*) regions, while the outer repeat (*otr*) sequences delineate the boundaries of the centromeric heterochromatin. The *otr* region typically comprises varying numbers of *dg* and *dh* repetitive elements (Allshire & Karpen, 2008b; Matsuda et al., 2017; Vyas et al., 2021b; Westhorpe & Straight, 2015).

S. pombe genome contains *Tf2* retrotransposon and around 300 long terminal repeats (LTRs), which are dispersed throughout the genome. These LTRs and *Tf2* retrotransposons are suppressed by CENP-B homolog Abp1, which recruits histone deacetylases (HDACs) at the sites and silences them (Cam et al., 2008).

The nucleus of *S. pombe* is ~2µm, in which the chromosomes are spatially organised. During interphase, the three chromosomes adopt a Rabl-like arrangement, where centromeres gather and attach to the nuclear envelope (NE) beneath the spindle pole body (SPB), while telomeres connect to distant NE sites opposite the SPB (Funabiki et al., 1993; Gallardo et al., 2019) (Figure 4). The attachment of centromeres to the SPB/Inner nuclear membrane protein (INM) Sad1 during interphase is mediated by the protein Csi1 that bridges sad1 to outer kinetochore proteins (Hou et al., 2012). Additionally, the association of telomeres with the NE is facilitated by the INM protein complex Bqt3-Bqt4, which binds the telomere protein Rap1 during interphase (Chikashige et al., 2009).

The mating-type locus resides at the nuclear periphery near centromeres (Noma et al., 2001). Chromosome III ends housing rDNA repeats that organise the nucleolus, a specialised nuclear region for rRNA gene expression and ribosome assembly (Uzawa & Yanagida, 1992)(Figure 4). This interphase chromosome configuration results from numerous interactions involving various inner nuclear membrane (INM) proteins and linkers of nucleoskeleton and cytoskeleton (LINC) complexes with specific chromatin domains (Matsuda et al., 2017). Additionally, chromatin-NE interactions occur at several other loci, including polymerase III (pol III)-transcribed genes like tRNAs and 5sRNA genes or Long Terminal Repeats (LTR) of retroviruses within the fission yeast genome (Alfredsson-Timmins et al., 2007; Ebrahimi et al., 2018; Gallardo et al., 2019; Iwasaki et al., 2010; Noma et al., 2006; Woolcock et al., 2012). Consequently, the NE, facilitated by its INM proteins, serves as a scaffold for chromatin, confining its movement and contributing to the spatial arrangement of fission yeast chromosomes within the nucleus.

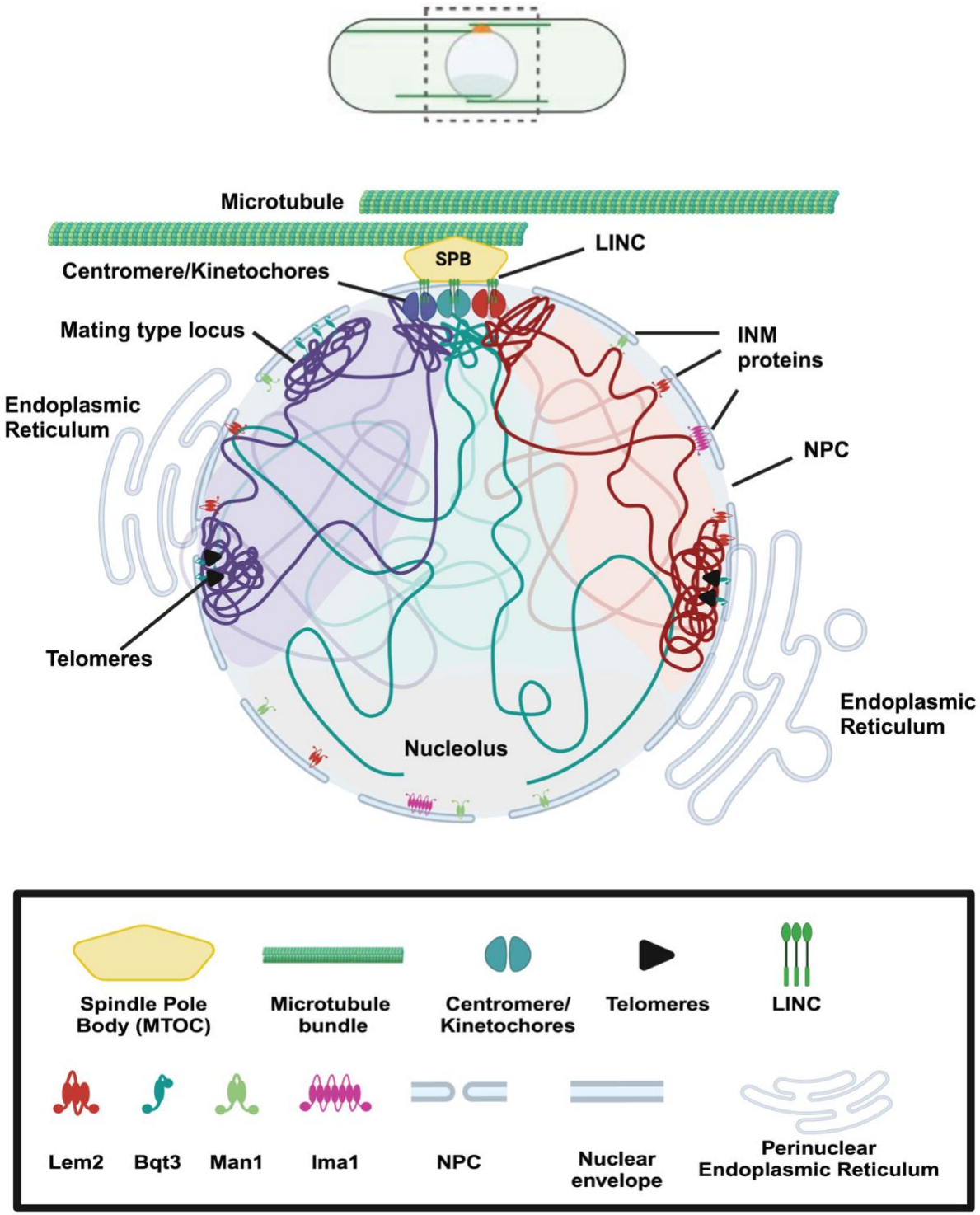

Figure 4: Diagram depicting the nucleus of a fission yeast. Above, a schematic of the entire cell is shown, while below, a close-up of the region outlined by dashed lines is displayed. Chromosome organisation is depicted globally, with centromeres located beneath the spindle pole body (SPB), telomeres, and nucleolus situated at a distance. Chromatin interacts with the nuclear envelope (NE) through various genomic elements binding to inner nuclear membrane (INM) proteins and linker of nucleoskeleton and cytoskeleton (LINC) complexes. The NE seamlessly merges with the perinuclear endoplasmic reticulum. The SPB, along with other microtubule organising centers (MTOCs), coordinates antiparallel arrays of microtubules (MTs). Based on (Gallardo et al., 2019).

1.4.2. Life cycle:

The fission yeast *S. pombe* can be grown at 18°C-36°C in minimal or rich media with a generation time ranging from 2 to 4 hours. It can live as diploid or haploid, but in the natural environment, it tends to live in the haploid form (Forsburg, 2003). The life cycle of *S. pombe* consists of asexual (vegetative) and sexual phases (Forsburg & Nurse, 1991; *Molecular Biology of the Fission Yeast*, 2012).

1.4.3. Vegetative cell cycle:

Schizosaccharomyces pombe cells exhibit a cylindrical shape with roughly hemispherical ends and a diameter of approximately 3.5 µm during exponential growth on a nutrient-rich medium. Newly born cells measure around 8 µm in length and undergo continuous growth throughout most of the cell cycle without any changes in width. Consequently, estimating a cell's age (time elapsed since birth) is facilitated by measuring its length. Upon reaching a length of about 15 µm, cells undergo closed mitosis, with the nucleus situated close to the cell's center. Following nuclear division, a septum forms at the medial position, which subsequently cleaves to generate two daughter cells. Nuclear DNA replication promptly follows mitosis, with a short G1 phase occurring between mitosis and cell separation(Nasmyth et al., 1979). Consequently, two unreplicated nuclei coexist in the cell until septum cleavage. S phase coincides with the presence of the septum, rendering newborn daughter cells already in the G2 phase, harbouring fully replicated chromosomes. Subsequently, after cytokinesis, cells remain in the G2 phase, which encompasses about three-quarters of the cell cycle, preceding the next mitosis. Hence, virtually every haploid cell within a proliferating population harbours two copies of the chromosomal complement.

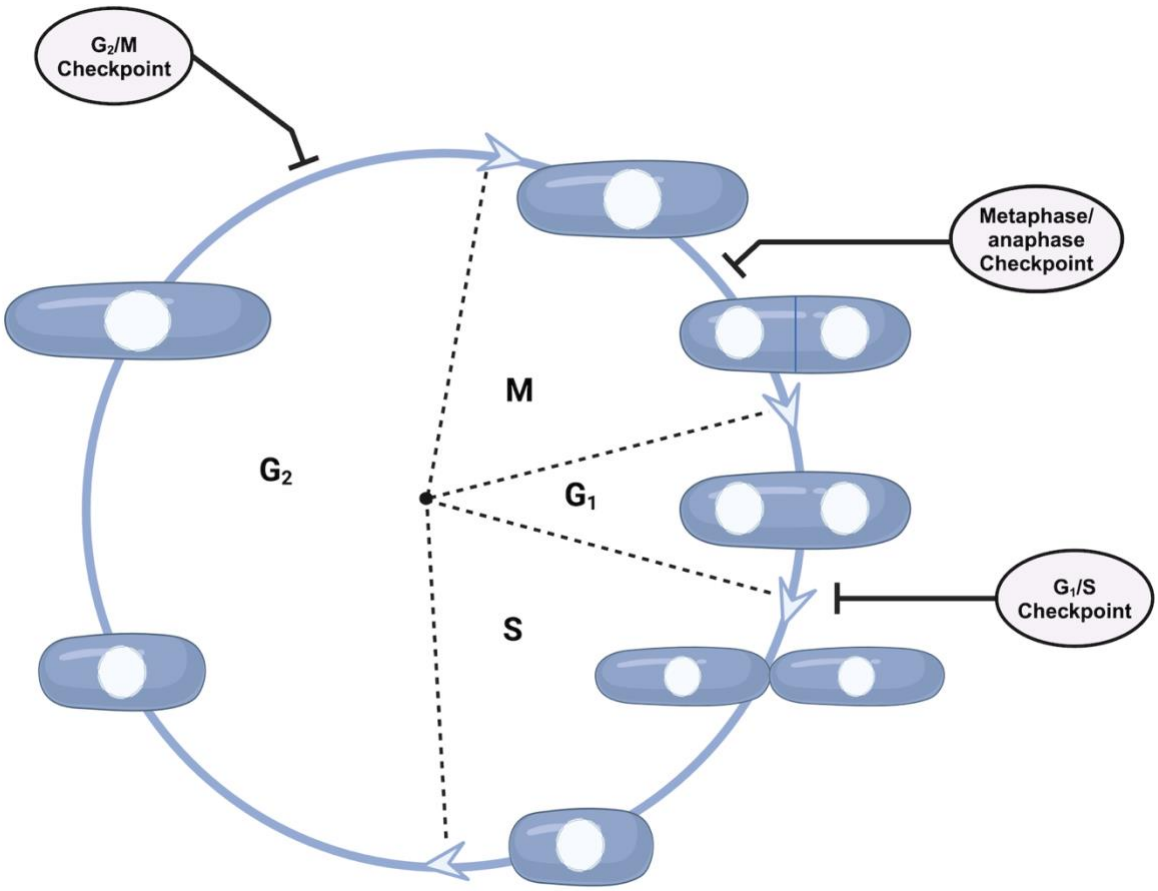

Figure 5: *S. pombe* vegetative life cycle with checkpoints: During exponential growth, cells spend around 70% of the cell cycle in the G2 phase, with the remaining 10% allocated to each other. Each checkpoint ensures the cell cycle progresses only when the conditions are suitable. Based from (Gómez & Forsburg, 2004; Sveiczer, 2004).

To prevent genetic and physiological abnormalities, checkpoints operate throughout the cell cycle. *S. pombe,* like most eukaryotes, has the following cell-cycle checkpoints: at the G1/S transition, the G2/M transition, and the metaphase/anaphase transition during mitosis (Figure 5). Before entering S-phase, a G1 cell evaluates nutrient availability; if inadequate, the cell remains in G1. Simultaneously, in the presence of mating pheromones, the cell may initiate sexual differentiation instead of proceeding with a mitotic cycle (discussed later). Additionally, a small G1 yeast cell must reach a critical size before progression. This size control at G1/S is subtle in rapidly growing, wild-type *S. pombe* cells, which primarily measure size at the G2/M transition. If the cell is too small, the G2/M checkpoint postpones entry into mitosis. Another mechanism at the G2/M checkpoint ensures mitotic delay if DNA damage or incomplete replication occurs. The third checkpoint ensures that sister chromatid segregation

(anaphase) does not commence until all chromosomes align correctly on the mitotic spindle (metaphase). These checkpoints hinder cell cycle progression by disrupting interactions that activate or deactivate cyclin-dependent serine/threonine protein kinase cdc2 *(Hayles & Nurse, 2016; Sveiczer, 2004).*

An interesting characteristic of *S. pombe* is that unlike S. cerevisiae, which divides through asymmetrical budding, *S. pombe* elongates at the tip and divides through medial fission, maintaining a relatively constant cell diameter. This growth polarity enables the convenient and precise tracking of cell cycle stages by measuring cell size, particularly cell length, facilitating detailed analysis of control in cell cycle progression (Vyas et al., 2021a).

Notably, diploid *S. pombe* cells exhibit a wider morphology (~4.4 µm) than haploid cells and undergo cytokinesis at approximately 24 µm, rendering them nearly double the volume of haploid cells (Hoffman et al., 2015).

1.4.4. Sexual cell cycle:

In addition to its vegetative growth phase, *S. pombe* also undergoes a sexual cycle, meiosis. When faced with nutrient starvation, two haploid cells of compatible mating types initiate mating, a process known as conjugation (Egel & Egel-Mitani, 1974). This involves the adhesion of cells followed by the digestion of the walls separating them, resulting in the formation of a single fusion cell containing the nuclei of both parents (Hoffman et al., 2015). Subsequently, the nuclei fuse to create a zygote, a singular cell harbouring a diploid nucleus. Following nuclear fusion, the nucleus undergoes elongation and oscillates between the cell poles. This elongated nucleus is commonly called the "horsetail" nucleus due to its distinctive shape. Within this structure, meiotic DNA synthesis and recombination take place (Asakawa et al., 2007). After this horsetail movement, the nucleus proceeds down the meiosis, yielding four haploid nuclei. These nuclei are then encased in a spore wall, forming an ascus containing four spores within the zygote's shell. Zygotic asci often exhibit a bent shape, reflecting the angle between the fused cells that gave rise to the zygote. In contrast, azygotic asci, originating from vegetative diploid cells, are typically short and linear. Upon exposure to a growth medium, the ascus wall disintegrates, allowing the spores to germinate and develop into vegetative cells that resume mitotic growth (Hoffman et al., 2015).

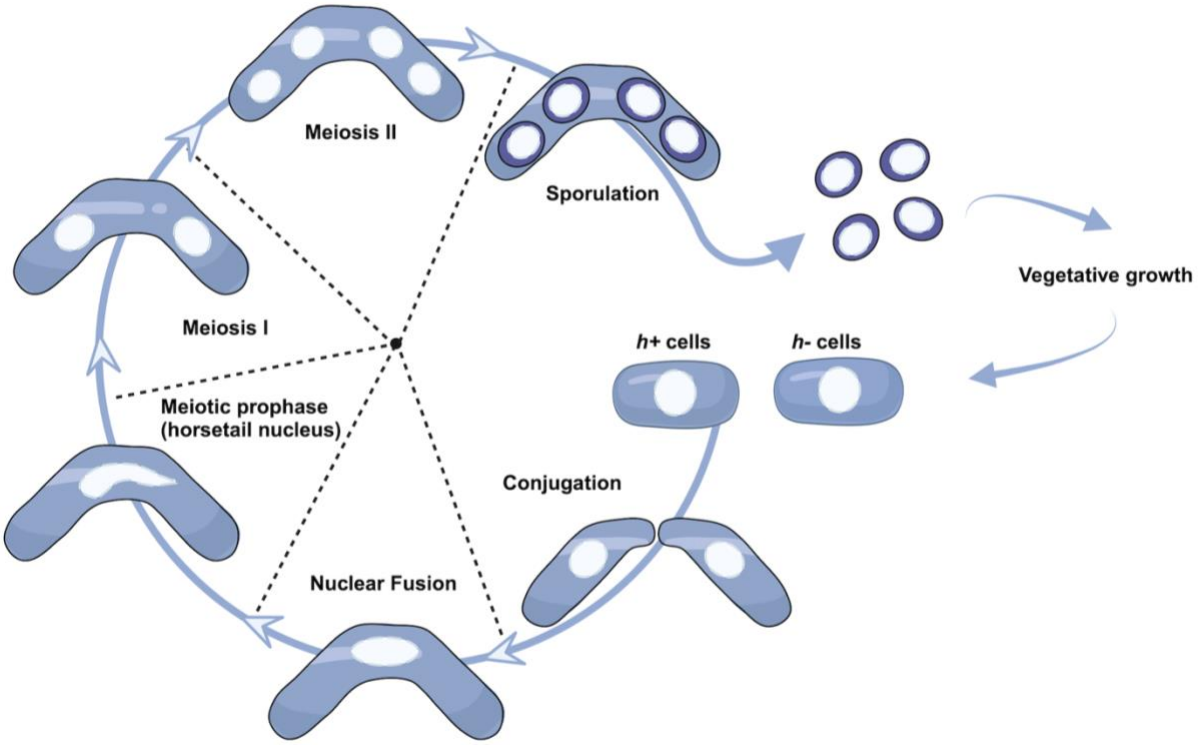

Figure 6: *S. pombe* sexual life cycle: When deprived of nitrogen sources, haploid cells of the *h+* and *h-* mating types halt in G1 and release mating pheromones to cells of the opposite mating type. Upon detecting the pheromones, the cells elongate towards each other, leading to fusion (conjugation), followed by fusion of their haploid nuclei. Subsequently, the fused diploid nucleus elongates (referred to as the horsetail nucleus) and oscillates between the cell ends (meiotic prophase). Meiotic DNA replication initiates during this phase, resulting in a nucleus containing 4C DNA content. Once movement subsides, the nucleus proceeds through the first and second meiotic divisions, yielding four 1C nuclei. Based on (Asakawa et al., 2007).

Importantly, during meiosis, there is a notable repositioning of centromeres and telomeres within the nucleus (Chikashige et al., 1994; Hiraoka, 1998; Scherthan et al., 1996). Prior to meiosis, centromeres aggregate near the spindle-pole body, while telomeres attach to the nuclear membrane, exhibiting a typical Rabl orientation (Figure 7A). Conversely, upon entering meiosis, telomeres migrate to the SPB, and centromeres disassociate from the SPB, adopting a bouquet configuration (Figure 7B). During nuclear fusion, haploid nuclei come close, with the telomere-SPB cluster positioned at the forefront of each nucleus. After nuclear fusion, telomeres remain clustered at the SPB, which now resides at the leading edge of the elongated nucleus, oscillating between the cell poles for about 2-3 hrs. until the first meiotic division (Chikashige et al., 1997). The repositioning phenomenon of centromeres and telomeres is also observed in meiotic cells across a wide range of eukaryotes, spanning from

yeasts and plants to animals, including humans (Bass et al., 1997; Loidl & Scherthan, 2004; Trelles-Sticken et al., 1999).

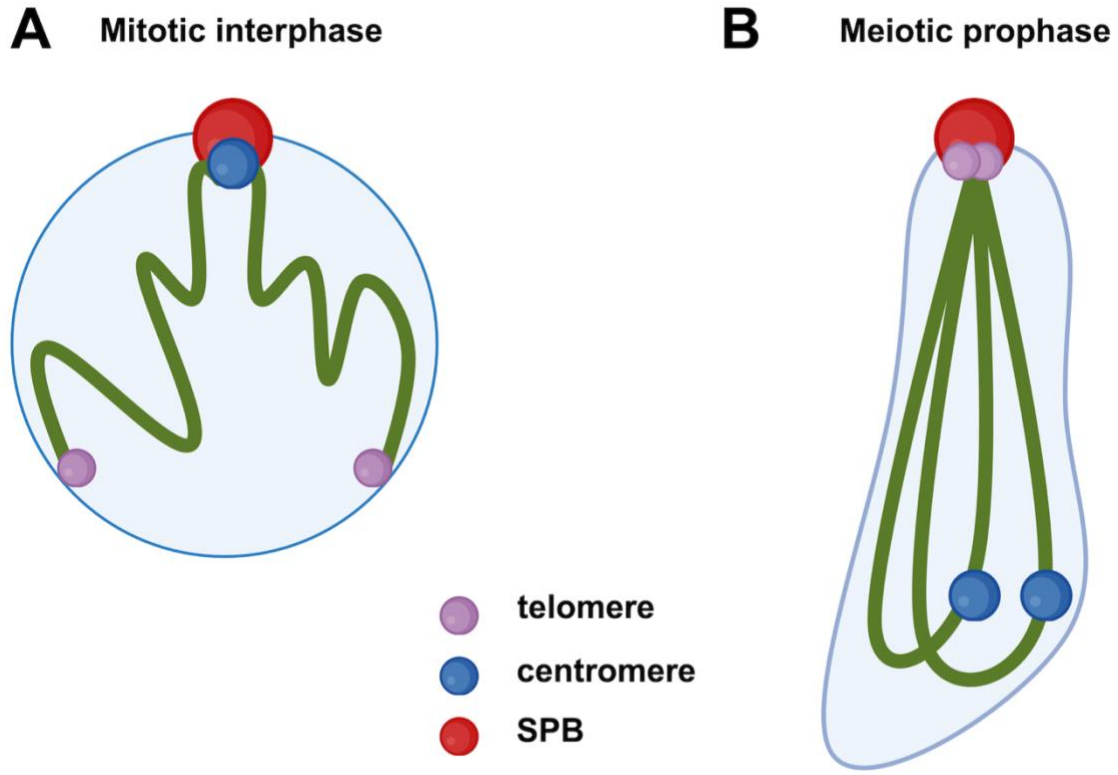

Figure 7: Spatial arrangement of *S. pombe* chromosomes. Schematic representation of centromere and telomere positions in the nucleus in mitotic interphase (A) and meiotic prophase (B) with a chromosome represented by the green line.

The wild-type *S. pombe* strains predominantly have homothallic mating type h_{90}. In these cells, the mating-type locus (mat) contains three copies of information, one actively expressed and the other transcriptionally silenced. *S. pombe* h_{90} cells have the ability to transfer genetic information from either of the silent loci to the expressed locus. This results in a population of cells within a clone expressing either one or the other mating type, facilitating mating. This genetic diversity may confer an advantage in surviving starvation conditions in the wild by enabling the production of spores. Additionally, *S. pombe* cells can also be heterothallic, requiring a mating partner of the opposite mating type (Hoffman et al., 2015; Leupold, 1949).

1.5. Aims of this study

DNA is ubiquitous in the environment and can enter a living organism via different means. This poses a risk to the sanctity of the organism's genome. As a result, different organisms developed different strategies to deal with unwanted genetic intruders, ensuring they maintain genome integrity. A consequence of such a mechanism is low transformation efficiency in most eukaryotic model organisms that we work with. A fundamental step in dealing with genetic intruders is identifying what self is and what is not. In this study, we utilised the symmetrically dividing yeast, *Schizosaccharomyces pombe,* to explore the possible self-defining factors that might contribute to distinguishing self from non-self-DNA and maintaining the genome integrity.

Utilising extrachromosomal DNA as a source of self and non-self-DNA, we explore whether *S. pombe* can distinguish one from the other. Previous work from our lab has shown that *S. pombe* can distinguish chromosomal DNA from foreign extrachromosomal DNA circles and sort them differently. Expanding on this, we aim to explore whether extrachromosomal DNA circles originating from the organism's genome undergo treatment similar to that of foreign ones, shedding light on potential discrimination mechanisms in unicellular eukaryotes.

The objectives of this study are:

- Determine whether *S. pombe* can discern between self-DNA and non-self-DNA.
- Investigate the fate of both self and non-self-DNA during mitosis and meiosis within the cell.
- Dissect the mechanisms underlying the recognition of self-DNA by *S. pombe*, aiming to uncover the molecular processes involved in distinguishing between endogenous and exogenous DNA.

2. Results

2.1. Engineering an experimental system to study chromosomal and extrachromosomal DNA dynamics

While extrachromosomal DNA circles are abundantly present in most eukaryotes (Cao et al., 2021; Sinclair & Guarente, 1997; Zhao et al., 2022), their occurrence in *S. pombe* is not as pronounced. This posed a challenge in investigating the dynamics and implications of extrachromosomal DNA circles in *S. pombe*.

To overcome the imitation and investigate the response of *S. pombe* to self and non-self-extrachromosomal DNA, we designed a system enabling their generation, visualization, and tracking. A reporter plasmid was engineered using the pBluescript-KS-II backbone, featuring a bacterial origin of replication for high copy number amplification in bacterial hosts and an autonomously replicating sequence *ars1* from *S. pombe* to support replication in the same organism (Bolivar et al., 1977; Clyne & Kelly, 1995). The selection marker *LEU2* from *S. cerevisiae* was chosen to complement the *S. pombe leu1-32* auxotroph mutant, reducing the likelihood of homologous recombination (Keeney & Boeke, 1994). Incorporating a tetracycline operon and repressor (TetO-TetR)-based tagging system, we inserted two arrays of 256 Tet-operator (*tetO*) sequences separated by a gentamicin resistance cassette into the construct (Figure 8A). Due to being highly repetitive, this construct was prone to recombine in bacterial hosts (Polleys & Freudenreich, 2021) and was selected for intact *tetO* arrays using the gentamicin resistance cassette. The plasmid construct was then transformed into cells expressing TetR fused with GFP and a nuclear localization signal, facilitating visualization due to TetR's high affinity for *tetO* repeats (Figure 8B). This setup allowed for studying the replicating non-self-extrachromosomal DNA over generations.

Additionally, we created a strain where the construct was integrated into Chromosome II using wild type *his7* sequence from *S. pombe* flanked by two *LoxP* sites. This modified construct, integrated into cells with the *his7-366* mutation, served to label Chromosome II (Figure 8D). We excised this integrated construct using the *cre*-LoxP recombination system (Sauer & Henderson, 1988). To control the excision of the construct from the chromosome, we introduced the β-estradiol-inducible Cre recombinase (hereafter creEBD) into the same

strain. Activation of Cre recombinase by β-estradiol efficiently led to the excision of circles from the chromosomes, as verified by microscopy (Figure 8E). Since there were tandem insertions of the construct at the locus by homologous recombination, we ended up clones with more than one integration. For this study, we chose to work with a clone with three integrations, as they appeared suitable for visualization and tracking. This system served as a model for generating and tracking replicating self-extrachromosomal DNA.

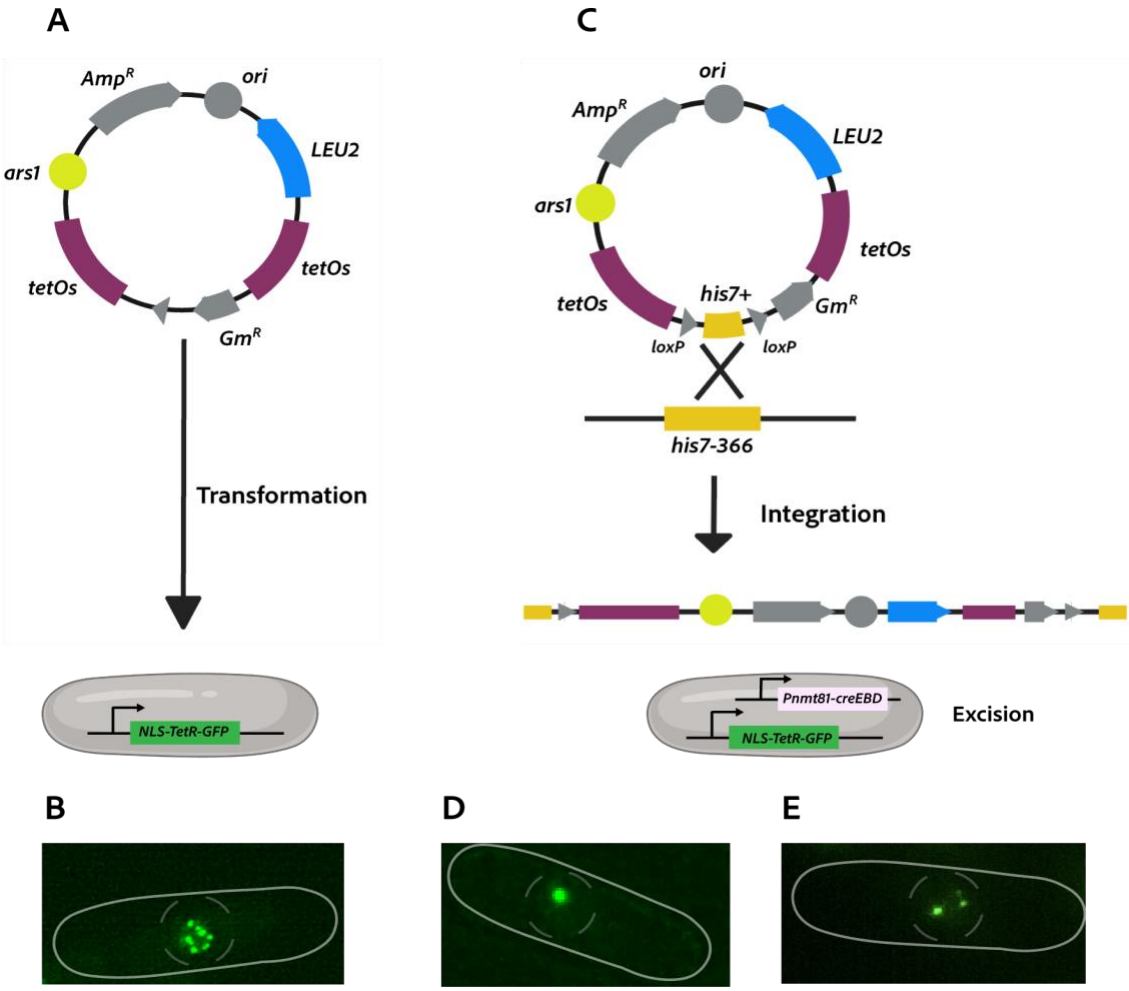

Figure 8: A reporter system to generate, visualise, and track self and non-self-extrachromosomal DNA in *S. pombe*. Schematic representation of the DNA circles used in this study. (A) Illustration of the non-self-extrachromosomal DNA construct depicting important sequences. The construct is transformed into *S. pombe* strains stably expressing NLS-TetR-GFP proteins. (B) Example of fluorescence microscopy image depicting transformed DNA circles as bright DNA foci. (C) Illustration of the construct used to create self-extrachromosomal DNA circles. The construct was integrated at the Chr. II *his7* locus into the strain stably expresses NLS-TetR-GFP and CreEBD proteins. (D) A representative fluorescence microscopy image depicting integrated DNA construct as a single bright focus. (E A representative fluorescence microscopy image of a cell treated with β-estradiol, which activates Cre recombinase and eventually leads to the excision of the integrated construct. Images are maximum projections of 15 Z sections 0.2 µm apart. The white continuous and dotted lines in B, D, and E represent the outlines of cells and nuclei, respectively.

2.2. Self-extrachromosomal DNA is distinguished from non-self-extrachromosomal DNA.

Non-self-extrachromosomal DNA circles were modeled by transformation, whereas self-extrachromosomal DNA circles were created by excising the integrated construct by activating Cre recombinase. To serve as a control, the construct integrated at Chr. II was utilized to observe the behavior of Chr. II.

The segregation of chromosomal and extrachromosomal DNA (self and non-self) foci was closely monitored during mitosis. Interestingly, both types of extrachromosomal DNA circles exhibited dynamic behavior. In cells with the labeled chromosome II locus, 100% of the cells symmetrically segregated the DNA foci exclusively, maintaining a 1 to 1 ratio (Figure 9B). In contrast, extrachromosomal DNA circles coming from outside (non-self) were frequently segregated asymmetrically, with one daughter inheriting all or more DNA circles than the other ratio (Figure 9A). These results were consistent with the previous studies that analysed various vectors in *S. pombe* (Heyer et al., 1986; Sakaguchi & Yamamoto, 1982, Valentini, unpublished). Remarkably, despite having almost the same DNA sequence as the transformed extrachromosomal DNA circles, chromosome-borne self-extrachromosomal DNA circles demonstrated symmetric segregation (Figure 9). Segregation patterns were assessed based on the number of foci observed per daughter. Although the intensities of foci varied, indicating non-uniform labeling with TetR-GFP, the presence of DNA foci in one daughter versus their absence in another provided a reliable measure of the DNA segregation pattern.

Interestingly, both kinds of extrachromosomal DNA segregation patterns were virtually identical regardless of whether selection (EMM-leu) or non-selection (EMM complete) media was used. This suggests that the segregation behavior is not influenced by the selection of the extrachromosomal-DNA-borne marker *LEU2*. Furthermore, we observed that on the selection medium, when extrachromosomal DNA segregated asymmetrically, daughter cells lacking extrachromosomal DNA did not immediately die but instead underwent a few additional cell divisions. This phenomenon could indicate the persistence of leucine transcripts encoded by extrachromosomal DNA. Previous studies have reported that plasmid-coded products, particularly auxotrophic markers, exhibit considerable persistence for generations (Boeke et al., 1984; Heyer et al., 1986). Based on these observations, we opted

to continue using selection media for segregation analysis, as it maintained a consistent population of extrachromosomal DNA-containing cells.

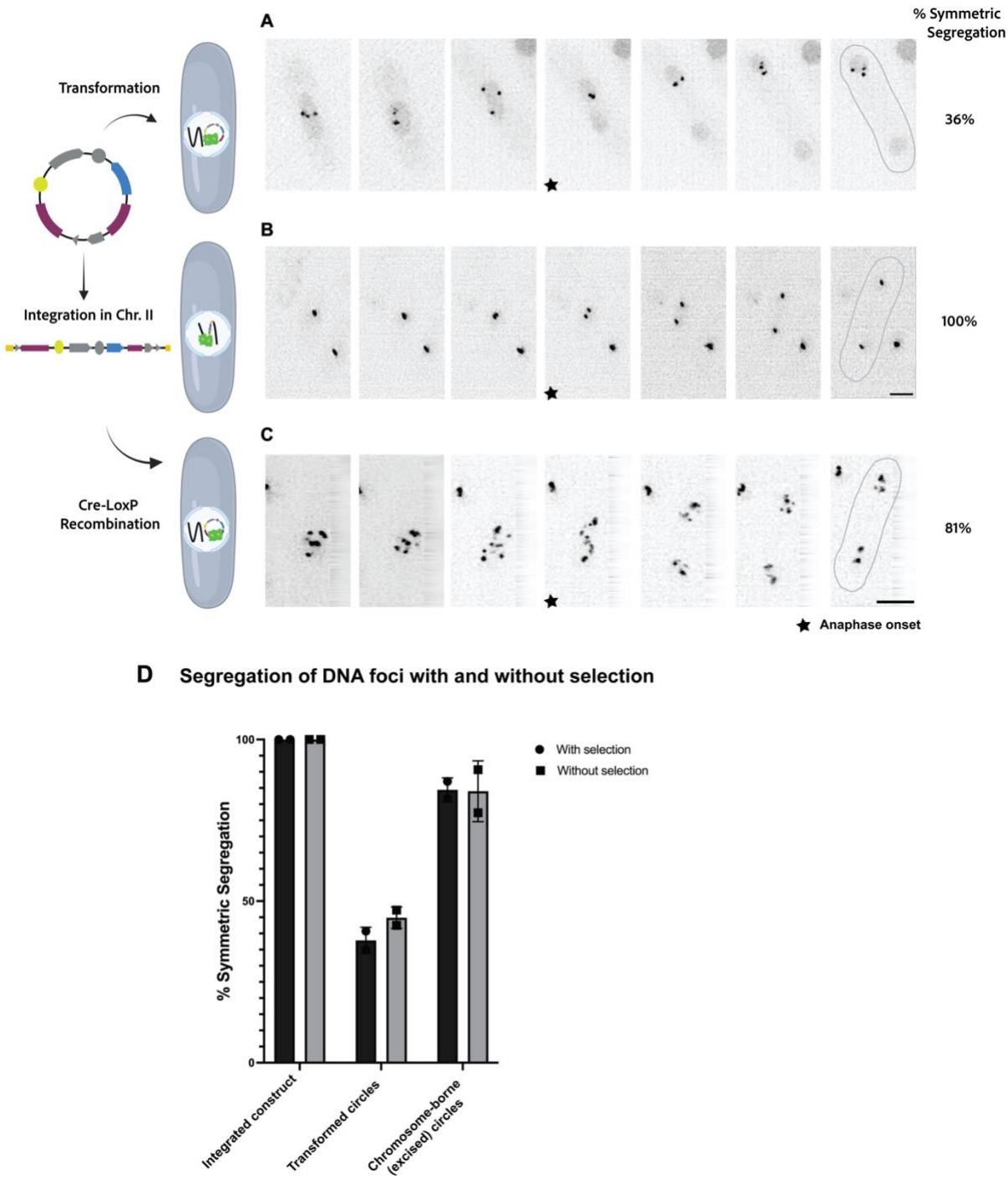

Figure 9: Segregation of self and non-self-extrachromosomal DNA in *S. pombe*. Fluorescence microscopy time-lapse images of cells undergoing mitosis. (A) Complete loss of non-self-extrachromosomal DNA circles from one daughter by asymmetric segregation. (B) Segregation of integrated construct in Chr. II depicting its faithful distribution. (C) Symmetric segregation of self-extrachromosomal DNA circles after its excision from Chr. II using

(figure legend continued on next page)

Cre-mediated recombination. Images are maximum projections of 12 Z sections 0.4 µm apart. Time resolution is 2 min/frame. The scale bar is 3 µm. (D) Quantification of symmetric segregation of various DNA molecules during mitosis in media with and without selection. Columns show the mean of replicates. Error bars show SEM.

The segregation pattern of these extrachromosomal DNA circles suggested that *S. pombe* can differentiate DNA based on its origin rather than its sequence, as the sequences of both types of extrachromosomal DNA circles were almost identical (Figures 8A, 8C). Transformed DNA circles, or non-self-DNA, were asymmetrically segregated and not propagated any further, while chromosome-borne self-DNA circles were symmetrically segregated and faithfully propagated in subsequent generations.

2.3. Self-extrachromosomal DNA circles segregate more symmetrically with time

Our approach to modeling non-self-extrachromosomal DNA circles, as previously outlined, involved transforming the construct into a compatible strain. It usually takes 3 to 4 days for the emergence of clones before conducting imaging. In contrast, self-extrachromosomal DNA circles could be visualized within a few hours following their excision from the chromosome by the Cre recombinase. This temporal difference between the experimental conditions prompted us to refine our methodologies to enable the observation of both types of circles under comparable conditions.

Two potential strategies were considered to achieve this optimization: immediate observation of cells post-transformation for non-self-extrachromosomal DNA or excising self-extrachromosomal DNA and observing them 3-4 days later. Due to the harsh conditions cells experience during transformation, they require substantial recovery time, rendering immediate imaging difficult. Consequently, we opted to observe self-extrachromosomal DNA circles 3-4 days post-excision.

To facilitate this, our experimental design involved excising the integrated construct with β-estradiol treatment for a defined period (6-16 hours), followed by streaking them on a selection plate to allow individual clones to emerge. It typically took approximately 3 days at 30°C for the clones to become visible and ready for imaging. This ensured that both types of circles could be observed under similar experimental conditions and eliminated any bias that might come due to different temporal conditions (Figure 10A).

Upon examination of the clones 3 days post-excision, the following key differences were observed between the cells a few hours and 3 days post-excision:

- Immediately after excision, multiple small foci per daughter were observed compared to a single dot when they were integrated (Figure 10B). However, 3 days post-excision, fewer foci were apparent, indicating foci clustering over time (figure 10C, 10E). The clustered foci also appeared brighter than individual foci from a few hours of excision (Figure 10C).
- The segregation of extrachromosomal DNA circles was more symmetrical (~91%) 3 days post-excision compared to a few hours post-excision (~80%), suggesting a time-dependent mechanism stabilising their symmetric segregation (Figure 10D).

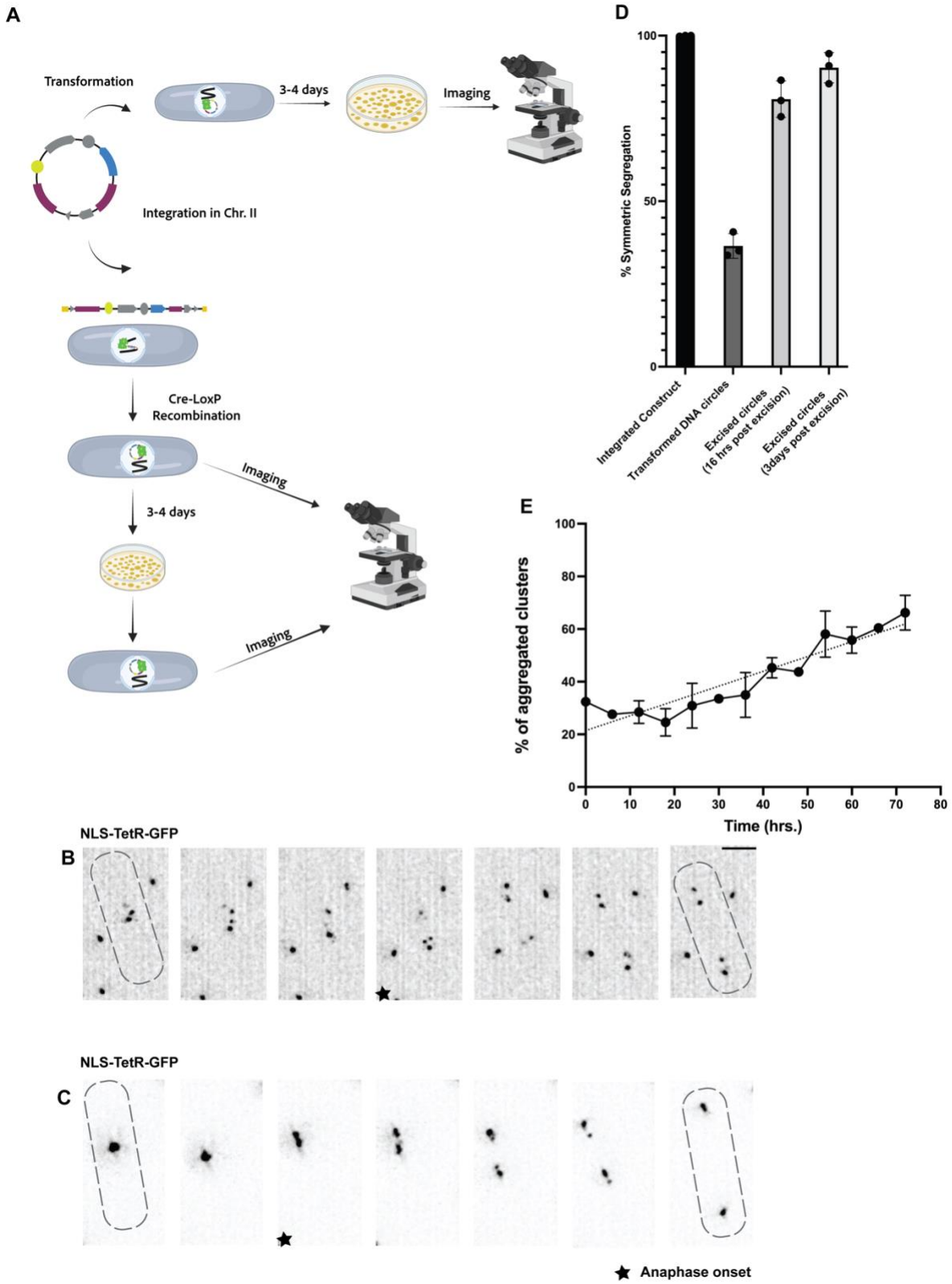

Figure 10: Symmetric segregation of self-extrachromosomal DNA circles increases with time. (A) Illustration of the experimental setup. (B) Segregation of self-extrachromosomal DNA circles right after its excision from Chr. II using Cre-mediated recombination. (C) Segregation of self-extrachromosomal DNA circles 3 days after its excision from Chr. II. Images are maximum projections of 15 Z sections 0.2 µm apart. Time resolution is

(figure legend continued on next page)

2 min/frame. The scale bar is 3 µm. The dotted lines in (B) and (C) represent the outline of the cells. (D) Quantification of symmetric segregation of various DNA molecules during mitosis. Columns show the mean of replicates indicated by dots. Error bars show SEM. (E) The quantification of single clusters observed per daughter in a time dependent manner. The number of foci clusters was quantified starting from 6 hours of excision. Error bars show SEM.

To further explore whether this symmetric segregation was transient or actively maintained, we compared the segregation of self-extrachromosomal DNA to non-self-extrachromosomal DNA over a longer time period. Clones obtained 3 days post-transformation and 3 days post-excision were inoculated into non-selection liquid media (EMM complete) at 30°C and monitored every 6 hours for 72 hours. The experiment was designed without selection pressure to ensure the correct quantification of cells losing the extrachromosomal DNA circles. The loss rate of circles was calculated using linear regression, revealing that non-self-extrachromosomal DNA circles were lost significantly faster from the population than self-extrachromosomal DNA circles (Figure 11). This finding suggests an active mechanism for recognizing and maintaining self-extrachromosomal DNA while eliminating non-self-extrachromosomal DNA from the population.

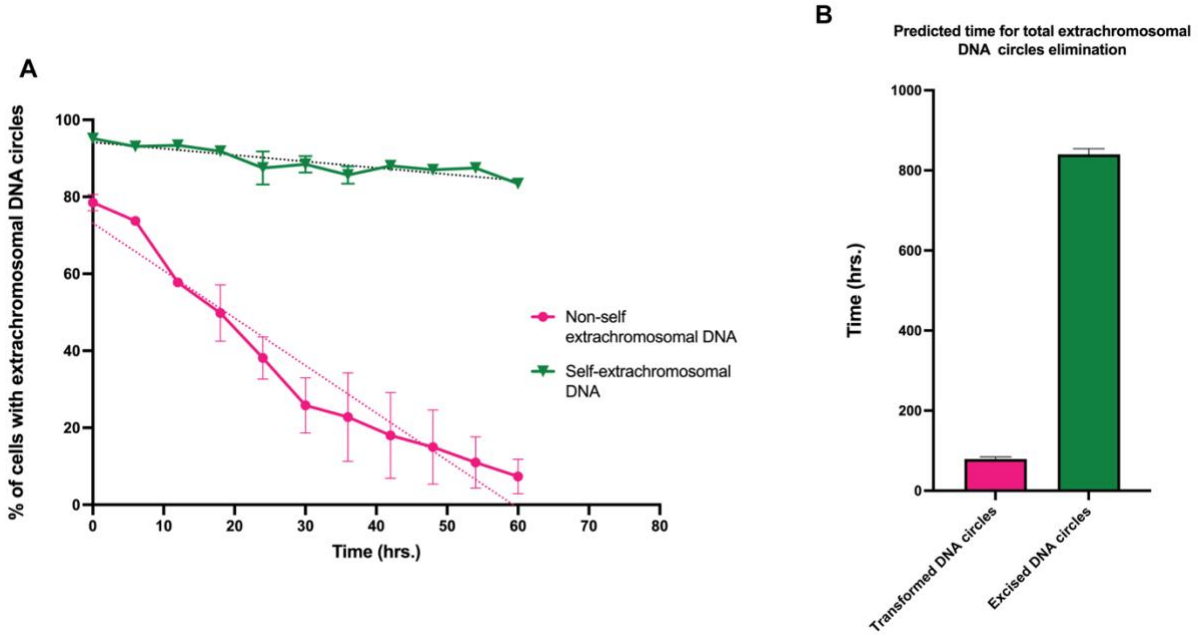

Figure 11: Non-self-extrachromosomal DNA circles are eliminated, whereas self-extrachromosomal DNA circles are maintained in the population. (A) Time course experiment of transformed and chromosome-borne self-extrachromosomal DNA depicting the percentage of cells keeping the extrachromosomal DNA circles with time in media without any selection. Quantifications were done every 6 hrs. Biological replicates were used for each time course, and more than 500 cells were counted for each time point and each biological replicate. Time point zero represent 72 hours after after β-estradiol induction. (B) Predicted time for total extrachromosomal DNA circle elimination in hours. Columns show the mean of replicates, and error bars show SEM.

2.4. Self-extrachromosomal DNA circles segregate symmetrically regardless of their original position in the genome

Next, we wanted to explore whether the observed phenotype was influenced by the insertion site or if it persisted irrespective of the origin of the extrachromosomal DNA in the genome. Extrachromosomal DNA circles naturally originate from sequences like rDNA repeats and telomere repeats in budding yeast (Møller et al., 2015). To investigate whether the origin might impact the segregation, we generated various strains wherein an identical single construct was integrated into various locations across all three chromosomes of *S. pombe* (Figure 12). Modifications to our original construct for the *his7* locus insertions via homologous recombination were made. Specifically, we replaced the *his7* sequence with the *lys1* sequence for pericentromeric insertions in chromosome I, incorporated subtelomeric fragments for subtelomeric insertions in chromosome I, utilized 18S rDNA for rDNA insertions in chromosome III, and targeted the *lys2* locus for insertion in the middle of arm of chromosome I. By utilizing these loci, By generating extrachromosomal DNA circles from the various genomic loci, we tested if the specific genomic loci, such as highly repetitive regions (e.g. rDNA and telomeric regions), affect the symmetric segregation pattern of extrachromosomal DNA circles described above.

Upon observing these strains for the segregation patterns of different chromosome-borne self-extrachromosomal DNA circles, we observed a consistent trend: all strains exhibited symmetrical segregation of extrachromosomal DNA circles, and notably, the symmetry increased over time across all scenarios (Figure 12B).

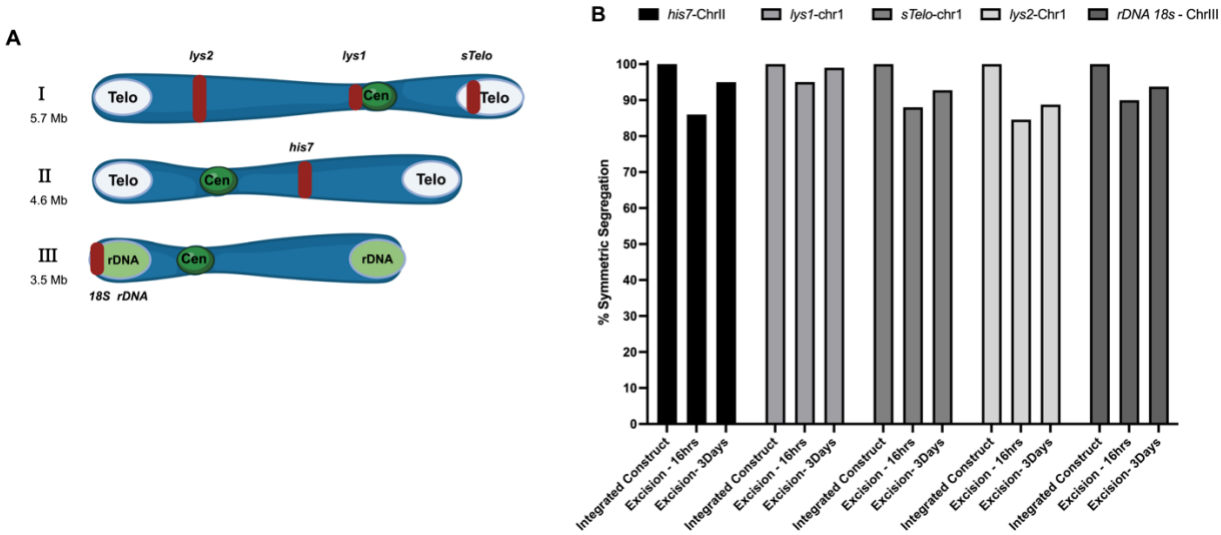

(figure legend on next page)

Figure 12: Regardless of location, chromosome-borne DNA circles segregate symmetrically. (A) Illustration of various locations used to insert the construct (B) Segregation pattern of differently originated chromosome-borne DNA circles when integrated, as soon as the excision and three days after the excision, respectively. Approximately 300 cells were counted for each experiment.

Interestingly, we observed that extrachromosomal DNA circles originating from the pericentric region of chromosome I exhibited the most symmetrical segregation a few hours after excision from the genome (Figure 12B). Three days later, they were segregating as faithfully as chromosomal DNA. This suggests that regions near the centromeres when excised, may possess unique properties that facilitate symmetric segregation immediately upon excision.

In conclusion, these observations imply that regardless of the excision location in the genome, chromosome-borne DNA circles in *S. pombe* are segregated symmetrically.

2.5. Self-extrachromosomal DNA circles stay in close proximity to SPBs

Having observed *S. pombe*'s ability to differentiate self-DNA from non-self-DNA, our attention turned to unraveling how self-extrachromosomal DNA is recognized as "self" and segregated symmetrically despite its close resemblance to transformed extrachromosomal DNA circles in terms of DNA sequence. We first aimed to investigate the behavior of self-extrachromosomal DNA circles during mitosis to gain insights into their potential mechanism for symmetric segregation. During mitosis, the centromeres interact with the mitotic spindle, moving along the spindle during prometaphase and metaphase, with sister centromeres separating in anaphase A. The spindle extension that brings the separated sister chromatids further toward the ends of the cell occurs in anaphase B immediately after anaphase A (Saitoh et al., 1997). In interphase, the centromeres cluster together and localize near the nuclear periphery at the site of SPB (specifically Sad1) (Funabiki et al., 1993).

Using this information, we utilized a spindle pole body marker, Sad1, tagged with mCherry, to delineate the cell cycle phase. This marker enabled us to ascertain whether the extrachromosomal DNA was segregating synchronously with chromosomes during metaphase or employing a distinct segregation mechanism. Cultivating the cells in liquid EMM without leucine selection media was instrumental in minimising the survival of cells lacking the extrachromosomal DNA circles. Subsequently, we conducted time-lapse fluorescent microscopy to capture all *S. pombe* cell cycle phases. Shortly after excision, the foci appeared

dispersed during interphase but like chromosomes, they were segregated symmetrically. This phenomenon became even more pronounced three days post-excision, with only 1-2 foci per daughter cell. Tracking analysis revealed that both the integrated and excised circles exhibited a trajectory resembling the spindle pole body during mitosis until telophase (figure 13). Another intriguing observation was the proximity of extrachromosomal DNA circles (3 days post excision) to the SPB, suggesting their chromosome-like behavior. This proximity was consistent during interphase and mitotic phases following anaphase A. This kind of behavior is seen in chromosomes as centromeres localize near SPB during interphase and mitotic phases after anaphase A.

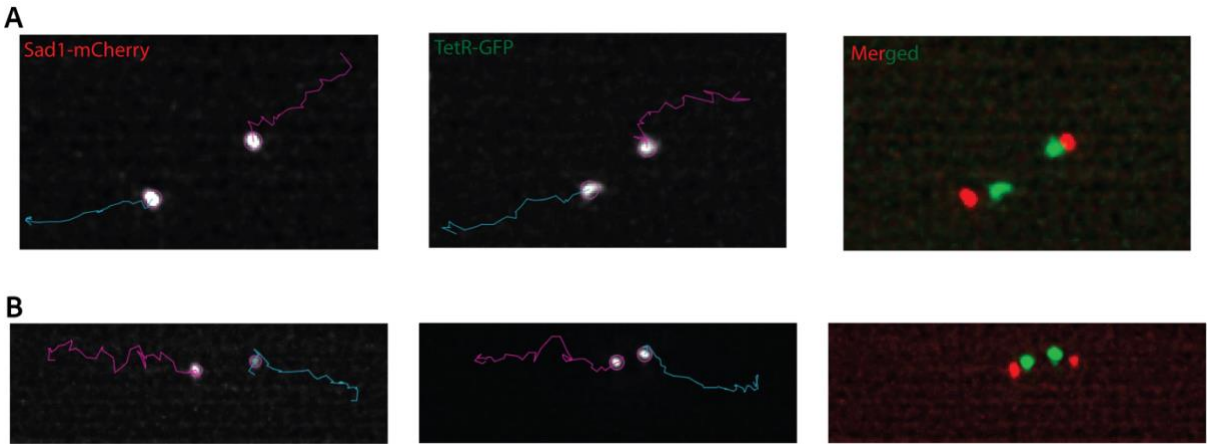

Figure 13: Self-extrachromosomal DNA circles follow a trajectory similar to chromosomal DNA. The spindle pole body is visualized with Sad1-mCherry and DNA with TetR-GFP. (A) The trajectory of the integrated construct at *his7* locus of chromosome II with spindle pole body (SPB). (B) The trajectory of the 3 days excised extrachromosomal DNA circles with spindle pole body. The time resolution is 30sec/frame; images are maximum projections of 9 Z sections 0.4 µm apart.

So far, the segregation and localization of self-extrachromosomal DNA circles closely resembled that of chromosome II, prompting the question: could the excised circles reintegrate into the genome? This seemed less likely for several reasons: First, the DNA sequence between transformed DNA circles and excised circles is almost identical (Figure 8), and it is unlikely that integration happens with the same sequence fo they are excised from the genome and not for the transformed ones. Second, there is minimal homology between the extrachromosomal DNA circles and the *S. pombe* genome, making homologous recombination unlikely. It has been reported that for efficient homologous recombination in *S. pombe,* a homology of at least 60-80 bp is required (Bähler et al., 1998; Krawchuk & Wahls, 1999). Additionally, it has been reported that if there is little homology between a circular piece of DNA and the *S. pombe* genome, they are usually maintained as episomes (Grallert et

al., 1993). Studies characterising different plasmid vectors in *S. pombe* also revealed that vectors with little homology to the *S. pombe* genome can be maintained in a non-integrative manner; these vectors can replicate autonomously and are stable with high copy numbers (Heyer et al., 1986; Sakaguchi & Yamamoto, 1982). Third, the presence of multiple extrachromosomal DNA foci suggests that even if some circles integrate through non-homologous recombination, they cannot account for all the other dynamic foci that we observe in a single nucleus, so there are bound to be some unintegrated ones. Fourth, if the non-homologous integration occurred, we would expect to see 100% symmetric segregation, which is not observed. 15-20% of cases segregate asymmetrically, indicating that self-extrachromosomal DNA circles do not integrate into chromosomes. This observation suggests that once excised, the circles remain separate from the genome, a notion further supported in subsequent sections.

2.6. Self-extrachromosomal DNA circles interact with microtubules via lateral attachment

Given the evident interaction between extrachromosomal DNA circles and the spindle pole body (SPB) during mitosis, we aimed to investigate whether these circles could also interact with microtubules to facilitate symmetric segregation. To explore this, we developed a strain expressing α-tubulin, Atb2 tagged with mCherry. Atb2 plays a pivotal role in organizing cytoplasmic microtubules and contributes actively to maintaining cell polarity and shape. We examined the localization of self-extrachromosomal DNA circles during mitosis in relation to the microtubules using confocal microscopy for higher resolution. Interestingly, we did not observe direct end-to-end attachment of the circles to microtubule ends from metaphase to anaphase; instead, they seemed to be laterally connected to the microtubules. (Figure 14).

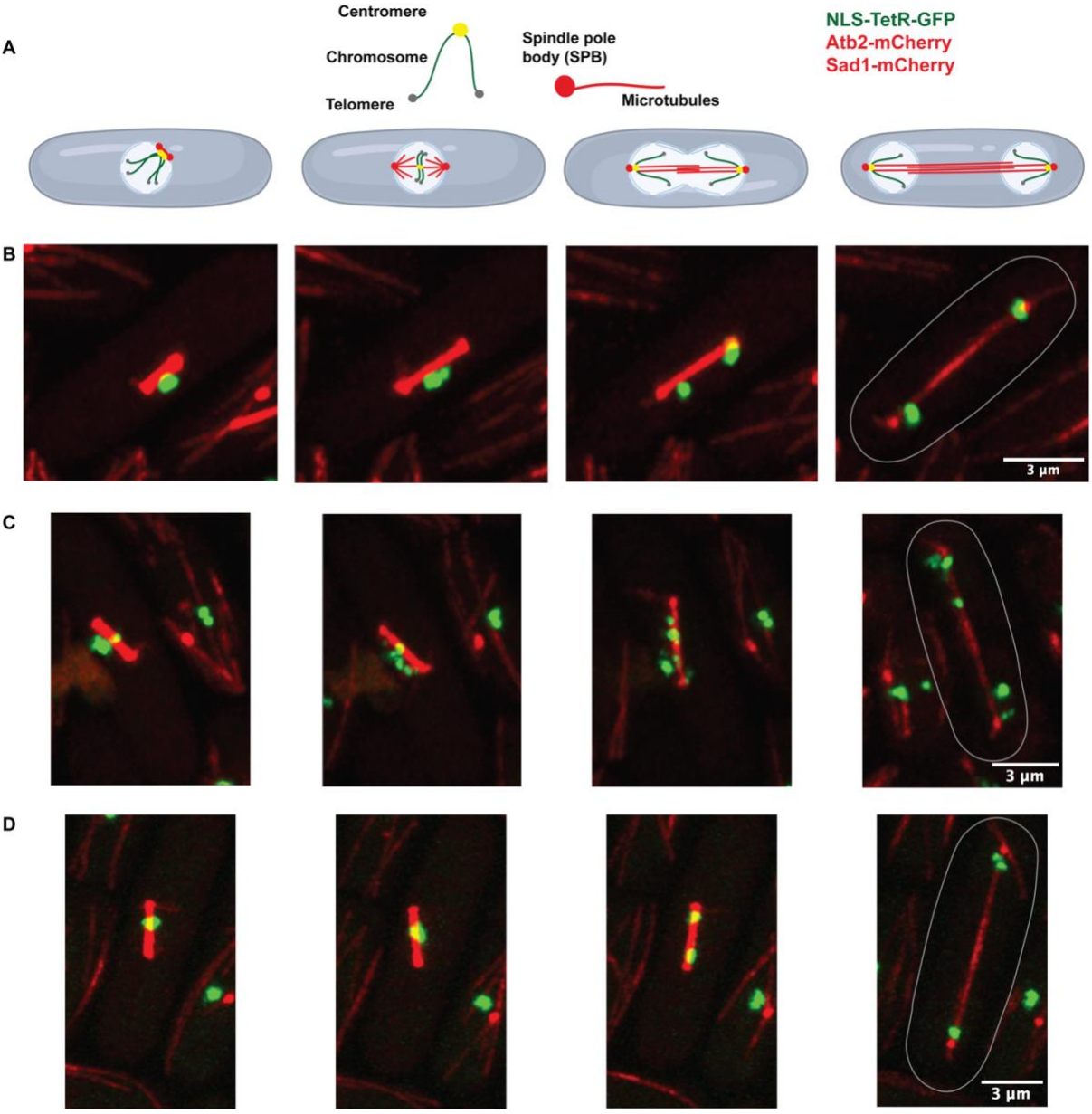

Figure 14: Dynamics of Chromosome-borne self-DNA circles with spindle microtubules. Microtubules are visualized by expression of Atb2-mCherry, spindle pole body with Sad1-mCherry, and DNA with TetR-GFP. Different microtubule structures depict different phases of the cell cycle. Prophase-metaphase corresponds to the initial spindle formation where the spindle elongates to about ~3 µm long. Metaphase-anaphase A is where the spindle length remains relatively unchanged, and anaphase B is where the spindle elongates to ~12 µm before breakdown. (A) Illustration of *S. pombe* mitotic phases focusing on DNA, microtubules, and spindle pole body. (B) Segregation of construct integrated at Chr. II arms. (C-D) Segregation of the extrachromosomal DNA construct after its excision from the genome, 16 hrs. and 3 days post-excision, respectively. The time resolution is 2 min/frame, and the scale bar is 3 µm. Prometaphase-Anaphase B is depicted here. The white lines in B,C, and D represent the outline of cells.

Although the resolution did not allow for a definitive view of individual microtubules interacting with the extrachromosomal DNA circles, their movement pattern and localisation

relative to the microtubules suggest a likely lateral connection, facilitating symmetric segregation. To explore further the possibility of end-to-end microtubule attachment, we engineered a strain with the microtubule plus-end-tracking protein Dis1 tagged with GFP and TetR tagged with mCherry.

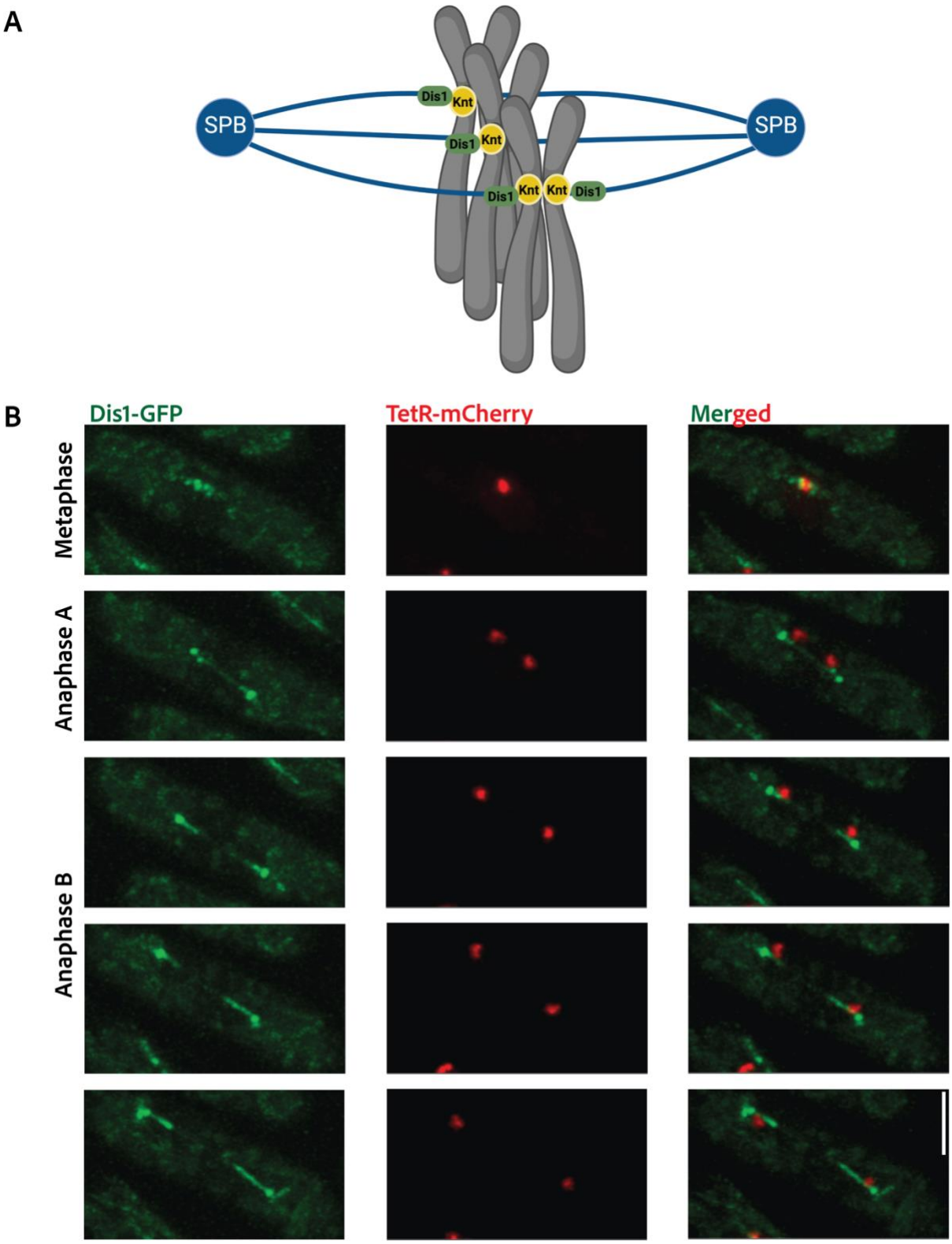

(figure legend on next page)

Figure 15: Dynamics of Chromosome-borne self-DNA circles with microtubule plus end tracking protein. Microtubule plus-end tracking protein is visualized by tagging Dis1 with GFP and extrachromosomal DNA with TetR-GFP. (A) Illustration Dis1 localization during metaphase with respect to the chromosomes. (B) Visualization of different mitotic phases in cells containing Dis1-GFP and TetR-mCherry. The time resolution is 2 min/frame, and the scale bar is 3 μm.

Dis1 accumulates near the tip of kinetochores during metaphase and establishes a microtubule-to-kinetochore connection (Murase et al., 2022; Ohkura et al., 2001). It has recently been implicated in microtubule shortening and proper chromosome pulling during the metaphase-to-anaphase transition. We examined the localisation of extrachromosomal DNA circles with respect to Dis1 during mitosis. Interestingly, they appear to localise with the Dis1 foci during metaphase, which is where the native centromeres are supposed to be at this phase. However, after anaphase A, they seemed to localise right after the Dis1 foci and follow them all the way till the end of mitosis (Figure 15). These results are consistent with our previous observation with α-tubulin, Atb2. Overall, it appears that extrachromosomal DNA circles interact with microtubules to segregate symmetrically, albeit through lateral attachment rather than end-to-end interaction.

2.7. Self-extrachromosomal DNA circles are stable during meiosis

DNA can be propagated within a population through two ways: mitosis and meiosis. Our observations thus have demonstrated that self-extrachromosomal DNA circles, just like chromosomes, undergo symmetric segregation during mitosis. Next, we aimed to understand the stability and fate of extrachromosomal DNA circles during meiosis.

It has been observed that extrachromosomal DNA circles that are transformed (non-self-extrachromosomal DNA), while they may persist within the population for a few mitotic generations, typically exhibit instability during meiosis (Heyer et al., 1986; Sakaguchi & Yamamoto, 1982). Additionally, it is widely believed that the vigorous back-and-forth movement observed in meiotic prophase across many eukaryotes (the horsetail movement in including *S. pombe*; see Figure 16A) serves as a mechanism to eliminate any unwanted chromosomal associations (Koszul & Kleckner, 2009). This means any unwanted connection a chromosome has will be eliminated by the contact shaking of the chromosomes by SPB movement.

To investigate if self-extrachromosomal DNA undergoes a similar fate to transformed circles and if they also get eliminated by the horsetail movement, we set up crosses between two

strains with insertions at identical loci. Along with tagged extrachromosomal DNA, we tagged *atb2* and *sad1* with mCherry to facilitate the visualisation of various meiotic phases (Fig. 16A). We designed our experiment to cross the following strains: (a) cross two strains with integrated construct at the same locus, (b) two strains with excised construct for 16 hrs, and (c) strains with excised construct for 3 days. After setting up the cross for a few hours, we examined the behaviour of each DNA molecule during each phase of meiosis. Utilising tagged Chr. II (integrated construct), as a control, we compared its behaviour and segregation with that of excised extrachromosomal DNA circles.

During meiosis, the following segregation patterns can be observed in the 4 spores: (a) 4:0, all spores inherit a particular genetic material; (b) 2:2, only two out of four spores inherit the genetic material; (c) 1:3, only one spore out of four inherit the genetic material. Our microscopic observations of meiosis revealed several key points: Cross with tagged Chr. II consistently displayed symmetric segregation with a ratio of 4:0 (Figure 16B, C), as we expected. Interestingly, crosses with excised extrachromosomal DNA circles predominantly exhibited symmetric segregation with ratios of either 4:0 or 2:0 (Figures 17,18,19). Notably, just like mitosis, the segregation of self-extrachromosomal DNA during meiosis also tended towards increased symmetry over time, with more instances of the 4:0 ratio with increasing time, as can be seen by crosses conducted with strains with 3 days excised extrachromosomal DNA circles (Figures 17, 18).

Upon closer examination of the horsetail movement, it becomes evident that extrachromosomal DNA circles, along with the chromosomal mass, remain within the meiotic nucleus and are not shaken off by SPB movement (Figures 17, 18). During this movement, the telomeres interact with the SPB while the centromeres detach from it, as illustrated in Figure 16-A (the bouquet orientation). As anticipated, the integrated construct marking the midpoint of chromosome II exhibits a localisation away from the spindle pole body and experiences substantial movement during this phase (Figure 16B, HT). Similarly, extrachromosomal DNA circles also demonstrate dynamic behaviour during this phase (Figure 17A, HT). However, it is noteworthy that extrachromosomal DNA circles in almost all cases do not consistently colocalise with the spindle pole body (SPB), suggesting a lack of interaction with telomeres and/or integration into chromosome ends. Additionally, their localisation differs from the integrated cassettes, indicating that they do not reintegrate at the same site from which they were excised.

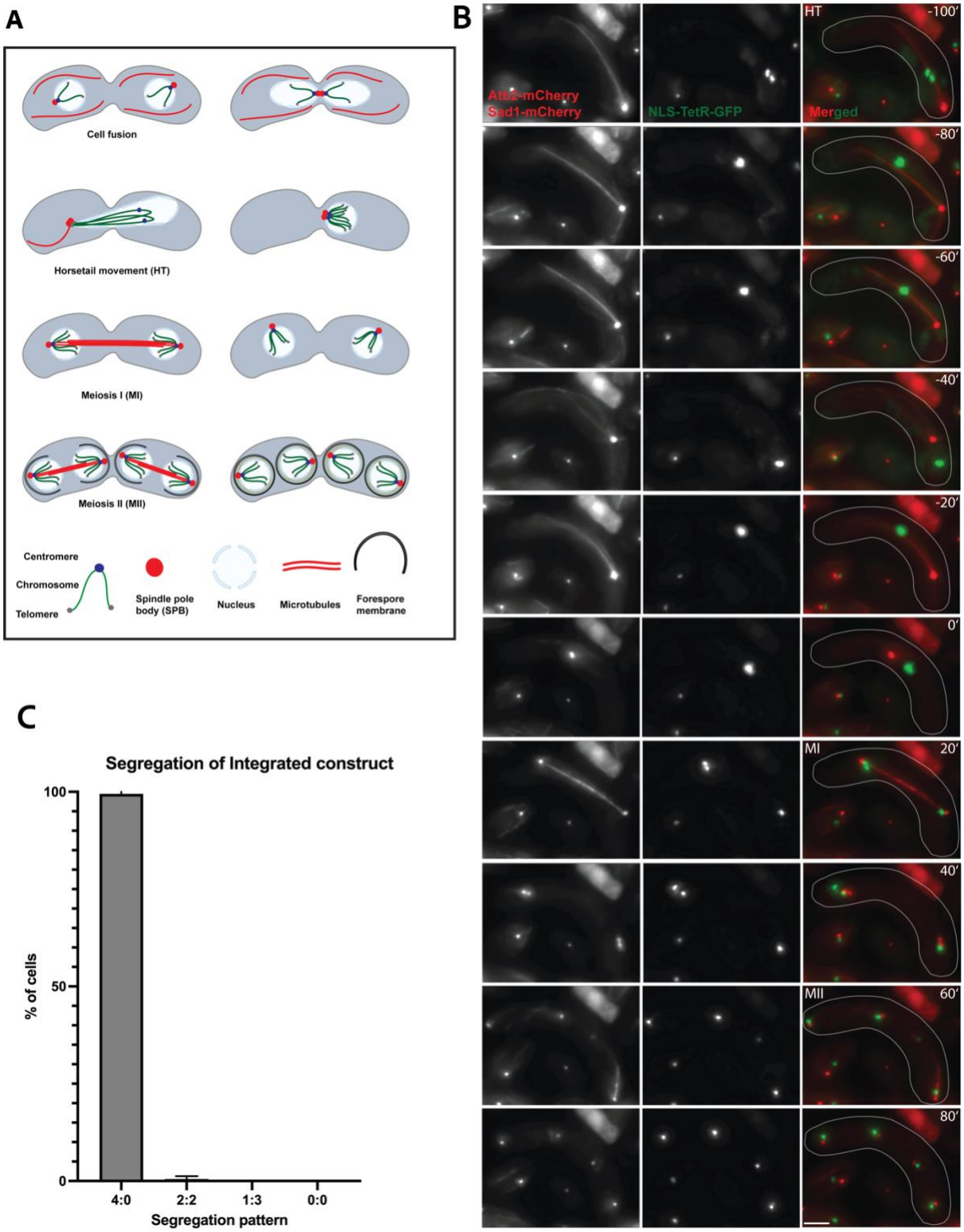

Figure 16: Chromosomal DNA segregation during meiosis. Microtubules are visualised by expression of *atb2-cherry,* spindle pole body with *sad1-mcherry* and DNA with *tetR-GFP.* (A) Illustration of *S. pombe* meiotic phases with respect to chromosome II, microtubules, and spindle pole body. (B) Segregation of construct integrated at chr. II arm. The time-lapse starts from the horsetail (HM) movement and ends at meiosis II (MTII), capturing metaphase I (MTI), meiosis I (MI), and metaphase II (MTII) in the middle. The images are a stack of 12 z stacks, which are 0.2 µm apart. The time resolution is 20 min/frame, and the scale bar is 3 µm. (C) Statistics of the segregation of the integrated construct. Columns show the mean of replicates, and error bars show SEM.

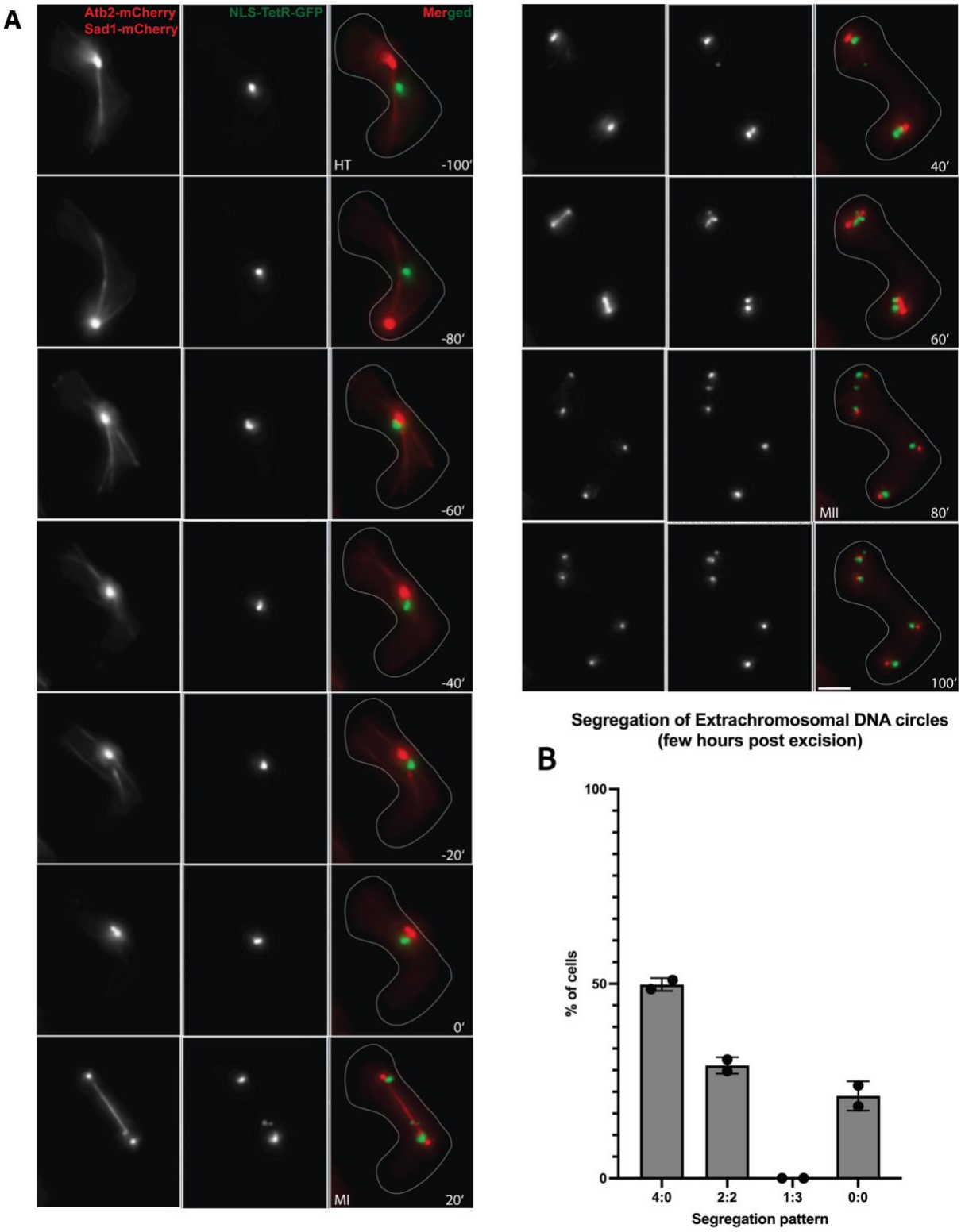

Figure 17: Segregation of self-extrachromosomal DNA during meiosis soon after their excision from the genome. (A) Segregation of extrachromosomal DNA 16hrs post excision. The images are a stack of 12 z stacks, which are 0.2 µm apart. The time resolution is 20 min/frame, and the scale bar is 3 µm. (B) Statistics of the segregation of the excised construct. Columns show the mean of replicates indicated by dots, and error bars show SEM.

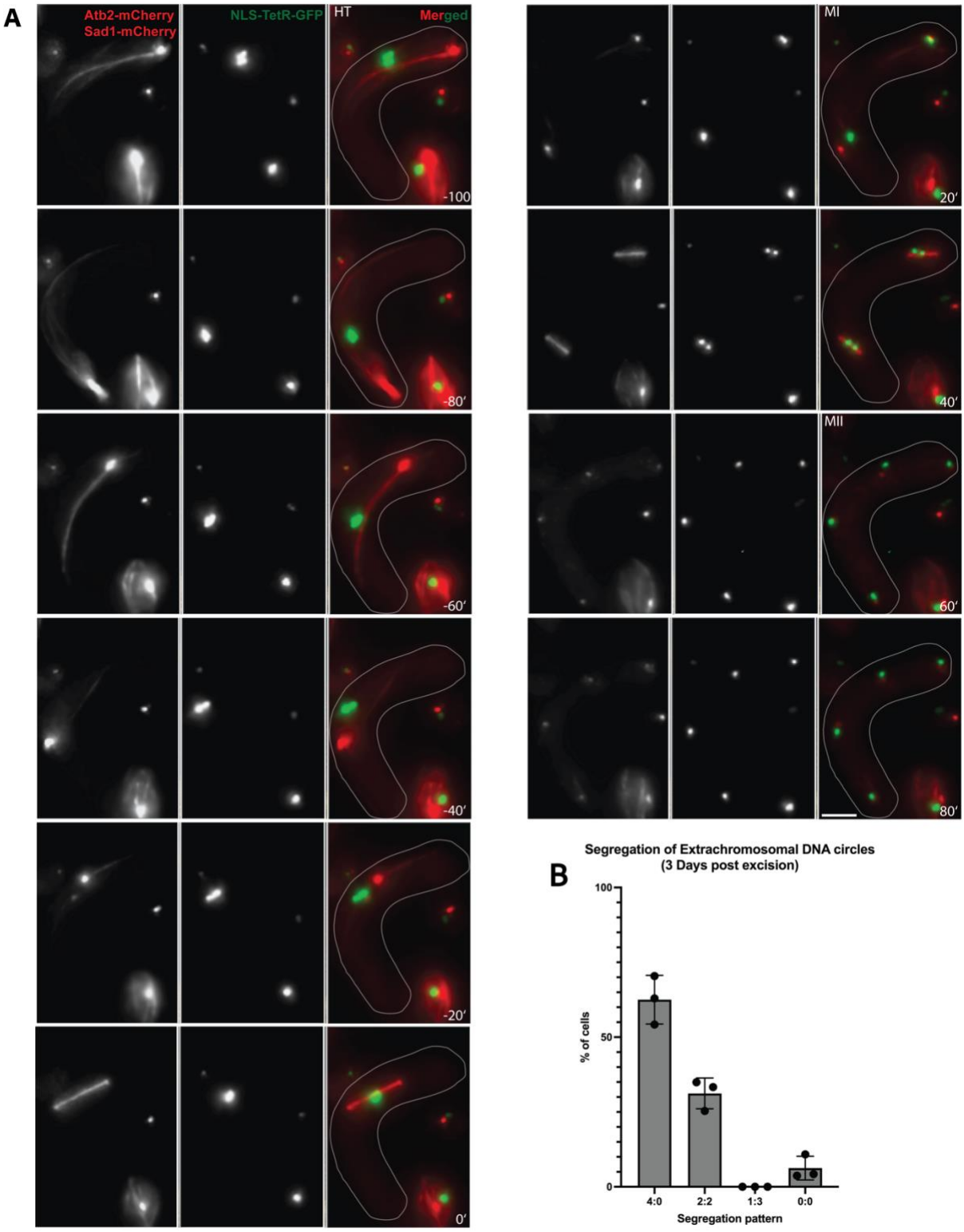

Figure 18: 3 Days excised extra-chromosomal DNA segregation during meiosis. (A) Segregation of extrachromosomal DNA 3 days post excision. The images are a stack of 12 z stacks, which are 0.2 µm apart. The time resolution is 20 min/frame, and the scale bar is 3 µm. (B) Statistics of the segregation of the excised construct. Columns show the mean of replicates indicated by dots, and error bars show SEM.

It is worth noting that extrachromosomal DNA circles lack telomeres, a crucial requirement for symmetric segregation during meiosis, yet they survive the horsetail movement and exhibit symmetrical segregation. Interestingly, Chr III also does not have telomere repeats in the end; rather, it has rDNA repeats but manages to attach to the SPB during the initial phases of meiosis. The mechanism by which it occurs or how extrachromosomal DNA circles might be interacting with the SPB is not very clear, but it is evident that self-extrachromosomal DNA circles are relatively stable and segregate symmetrically indicating a non-random segregation mechanism at play. Moreover, the horsetail movement phase is crucial for DNA synthesis and recombination (discussed in section 1.4.4). But, it is uncertain whether recombination occurs within extrachromosomal DNA circles. Investigating this aspect in future studies could provide valuable insights into their exact behaviour during meiosis.

Remarkably, we exclusively observed segregation patterns of 4:4 or 2:0 with occasional instances of 0:0 with extrachromosomal DNA circles. Among the 300+ crosses we examined, there was no occurrence of 3:1 segregation. This suggests that either they segregate symmetrically during both meiosis I and meiosis II, resulting in a distribution of 4:0, or they segregate symmetrically only during one of these phases. In either scenario, the segregation pattern has at least partial symmetry. Interestingly, in cases of 2:0 segregation, most segregation errors were observed during meiosis II, indicating symmetric segregation during meiosis I but asymmetric segregation during meiosis II, as depicted in Figure 19.

These observations suggest two key points: First, the segregation of extrachromosomal DNA circles is not random. Rather they appear to be stably propagated during meiosis. Second, it supports the notion that the excised construct does not reintegrate into the genome. If integration were to occur into one of the chromosomes, only that chromosome would inherit it, resulting in asymmetric meiosis I. However, segregation error during meiosis II is prominent. It indicates that extrachromosomal DNA circles remain independent post-excision. Furthermore, since the symmetric segregation is not 100%, it suggests that the mechanism facilitating symmetric segregation of extrachromosomal DNA circles may not be as robust as the chromosomal segregation machinery.

In conclusion, self-extrachromosomal DNA segregates symmetrically during meiosis, highlighting the existence of a mechanism ensuring the equitable distribution of these chromosome-borne DNA circles.

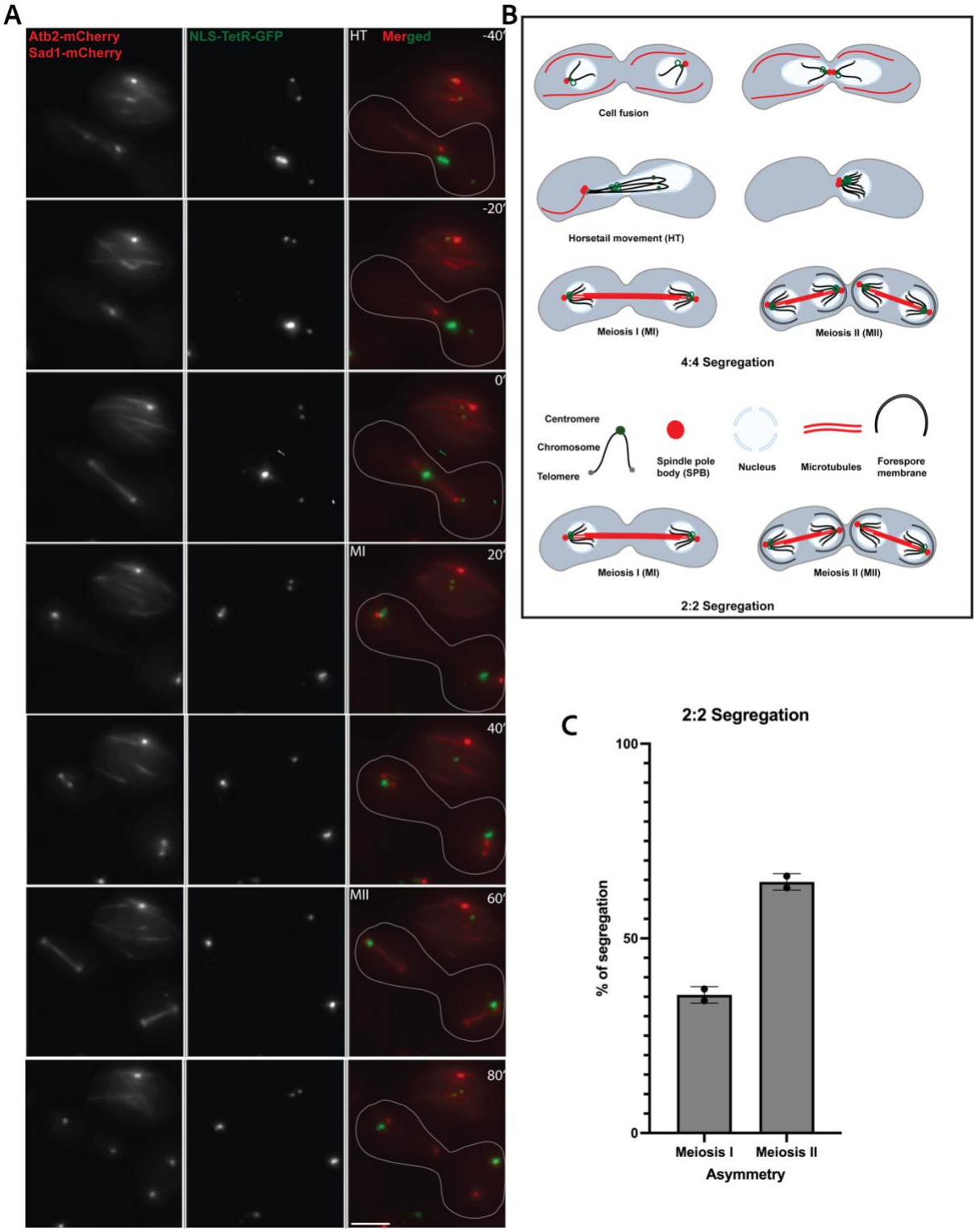

Figure 19: Asymmetric segregation of excised extra-chromosomal DNA segregation during meiosis. (A) Segregation of extrachromosomal DNA 3 days post excision. The images are a stack of 12 z stacks, which are 0.2µm apart. The time resolution is 20 min/frame, and the scale bar is 3 µm. (B) Illustration of 2:2 and 4:4 segregation of extrachromosomal DNA circles. (c) Statistics of the segregation of the excised construct. Columns show the mean of replicates indicated by dots, and error bars show SEM.

2.8. Chromosome segregation machinery plays a role in the segregation of self-extrachromosomal DNA circles

Next, we aimed to elucidate the factors underlying the symmetric segregation of self-extrachromosomal DNA circles. Given their observed interaction with the spindle pole body (SPB) during mitosis (Figure 13), we directed our attention to the chromosome segregation machinery known for its role in symmetric DNA segregation. This machinery orchestrates the separation of chromosomes during cell division, ensuring each daughter cell receives an equal amount of genetic material.

The most direct approach to testing this theory was to use genetics. We knocked out/ mutated different chromosome segregation machinery components and measured the influences on segregation patterns. By comparing the behaviour of the wild-type strain (WT) with self-extrachromosomal DNA circles to mutant strains harbouring extrachromosomal DNA circles, we aimed to identify key players in the process.

Among the mutants we tested, we particularly found interesting phenotypes with strains containing a mutation in the *mis6* gene. Mis6, a component of the inner centromere complex, is crucial for correct sister chromatid separation. It also forms a protein complex with Mal2 and Sim4, which recruits Cnp1/CENP-A at centromeres (Shiroiwa et al., 2011; Takahashi et al., 2000). Notably, mutations in this gene also lead to the loss of minichromosomes and chromosomes, hence the name *mis* (minichromosome instability). A temperature-sensitive (*ts*) *mis6-302* mutation has been shown to lose a minichromosome at 26°C (permissive temperature) and regular chromosomes at 36°C (restrictive temperature). We grew these mutants at semi-permissive temperatures (30°C), where chromosomal segregation remained somewhat stable (Kerres et al., 2004; Saitoh et al., 1997; Takahashi et al., 2000). At this temperature, the mutant disrupted the symmetric segregation phenotype of self-extrachromosomal DNA circles (Figure 20).

Studies have shown that *mis6* mutant allele also impact the clustering of centromeres as they lead to delustering at restrictive temperatures (Appelgren et al., 2003; Saitoh et al., 1997). Interestingly, the aggregation of extrachromosomal DNA circles was also affected in the *mis6-302 ts* mutant (Figure 20B).

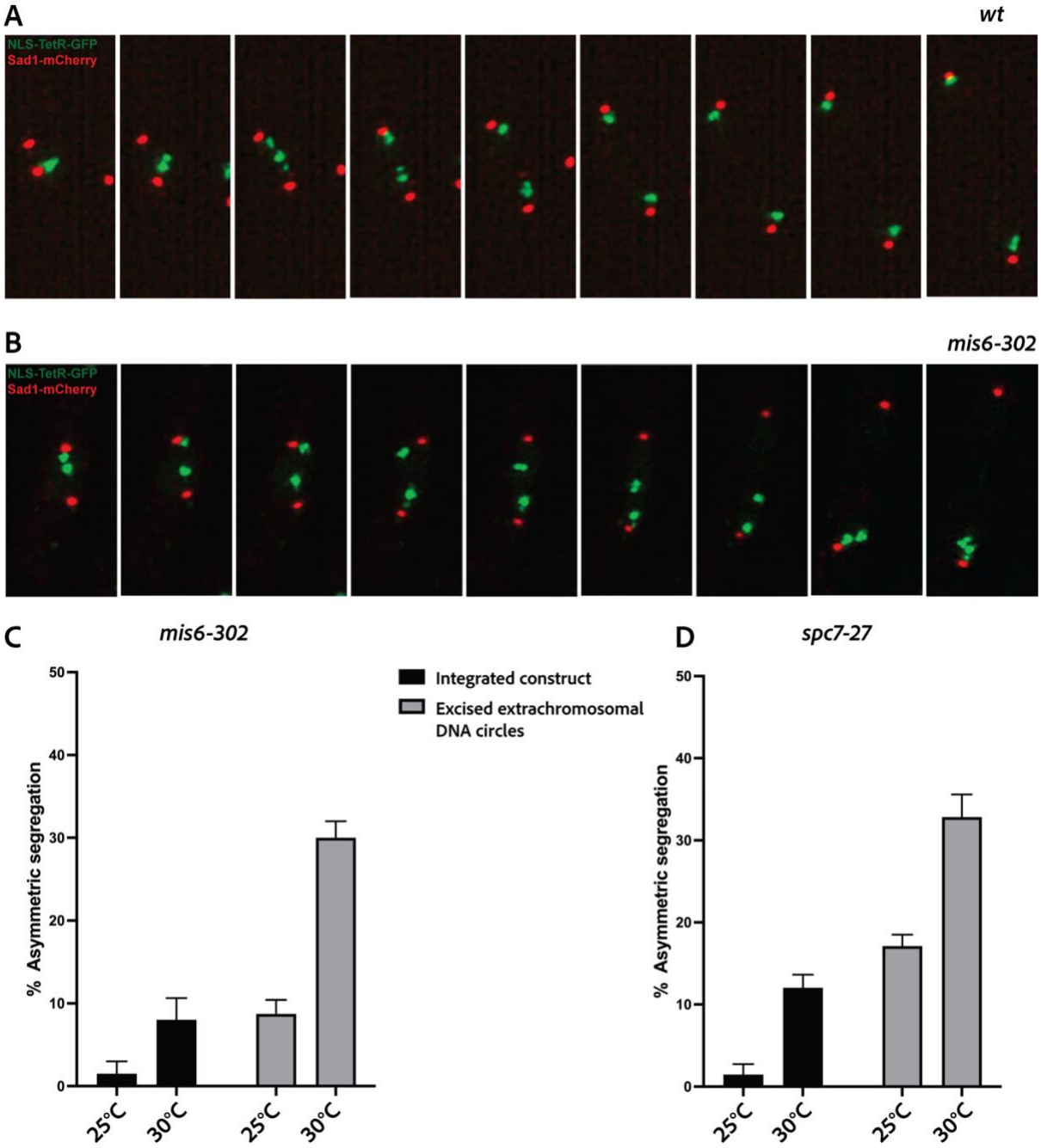

Figure 20: Symmetric segregation of self-extra-chromosomal DNA is disrupted by mutants involved in chromosome segregation machinery. The spindle pole body is visualised with Sad1-mCherry and DNA with TetR-GFP. Metaphase to anaphase transition is represented here. (A) Segregation of excised extrachromosomal DNA circles in *mis6-302 ts* mutant when grown at the permissive temperature (25°C). (B) Segregation of excised extrachromosomal DNA circles in *mis6-302 ts* mutant when grown at the semi-permissive temperature (30°C). The time resolution is 30sec/frame; images are maximum projections of 12 Z sections 0.4 µm apart. Metaphase to anaphase B is depicted in the images. (C) Quantification of mis-segregation of integrated construct and excised extrachromosomal DNA circles in *mis6-302 ts* mutant when grown at the permissive and semi-permissive temperatures. (D) Quantification of mis-segregation of integrated construct and excised extrachromosomal DNA circles in *spc7-27 ts* mutant when grown at the permissive and semi-permissive temperatures. Columns show the mean of replicates, and error bars show SEM.

Another mutant that exhibited a similar phenotype was the temperature-sensitive mutant *spc7-27.* Spc7 is a component of the Ndc80-MIND-Spc7 (NMS) super complex involved in kinetochore function (Liu et al., 2005). Mutations in this essential gene severely compromise kinetochore-microtubule interactions, leading to chromosome segregation errors (Kerres et al., 2004). Like *mis6-302* cells, we grew *spc7-27* cells at a semi-permissive temperature (30°C) to ensure minimal impact on the segregation of chromosomal DNA. Intriguingly, the symmetric segregation of self-extrachromosomal DNA was disrupted in these mutants, too (Figure 20).

These findings suggest that kinetochores and centromeric proteins may play a pivotal role in clustering and segregating self-extrachromosomal DNA circles. Furthermore, it was observed that the effect of these mutations was much more pronounced on the segregation of self-extrachromosomal DNA circles compared to the segregation of integrated construct. This increased sensitivity could be attributed to the robustness of chromosome segregation machinery, supported by backup mechanisms ensuring symmetric chromosome segregation. However, since the formation of extrachromosomal DNA circles is a relatively rare event in *S. pombe*, there may be fewer mechanisms ensuring their symmetric segregation, rendering them more susceptible to mutations.

2.9. Centromere and kinetochore proteins show mild localisation to the self-extrachromosomal DNA foci during mitosis

All the observations so far, including the interaction of self-extrachromosomal DNA circles to the SPB, their symmetric segregation and movement during mitosis and meiosis, and their sensitivity to the mutations in chromosome segregation machinery, indicated there might be centromeric proteins or a neocentromere on these circles. These neocentromeres could be fully functional matured centromeres or a rudimentary assembly ensuring even distribution of these small circles. Though the centromeric sequence (central core, cc) is a favoured sequence for centromere assembly in S. pombe, there is no obligate coupling of sequence and assembly (Castillo et al., 2013). In *S. pombe*, the centromere regions are epigenetically defined, and the assembly of CENP-A can happen irrespective of the underlying sequence; hence, neocentromeres can emerge at non-centromeric locations in the genome (Ishii et al.,

2008; Ogiyama et al., 2013). So, there is a good possibility of extrachromosomal DNA assembling a neocentromere.

To test this hypothesis, we tagged centromere/kinetochores protein to see if they colocalise with extrachromosomal DNA during mitosis. We used an N-terminal tagged GFP-Cnp1 strain for visualising centromeres and possibly neocentromeres (Takayama et al., 2008). *S. pombe* is quite small, and its centromeres stay clustered during interphase. We could observe centromere clusters as single foci in all the daughter nuclei during mitosis. Utilising the strain with Cnp1 tagged with GFP and TetR tagged with mCherry, we observed cells before and after the excision of extrachromosomal DNA circles. As expected, we rarely see the colocalisation of an integrated construct with the GFP-Cnp1, as the integration at *his7* locus which is away from the centromeric loci. Interestingly, after excision from the chromosomes, there are about 25% of cases where we could see the colocalisation of extrachromosomal foci with GFP-Cnp1. And this colocalisation also increased with time (Figure 21D). This increment was not much but points towards a trend similar to symmetric segregation. It is to be noted that we could only see colocalisation during interphase and Anaphase B. During metaphase, the extrachromosomal DNA foci do come approximately in the middle of the nucleus localising near other centromeres, but there was not much colocalisation indicating. Additionally, on the rare occasion where we could see three separate foci for each centromere, we could not see separate foci for the GFP-Cnp1 colocalising with the extrachromosomal DNA (Figure 21 B).

Interestingly, we observed something similar when we tagged a kinetochore protein Mis12 with GFP and TetR with mCherry. Just like before, we analysed cells before and after the excision from the chromosome arm, and we could see a similar trend again. Before the excision, TetR-mCherry rarely colocalised with Mis12-GFP, but after the excision, there was about 25% colocalisation (Figure 21E). And there was hardly any colocalisation during metaphase.

These results could mean one of these things: 1. There is no centromere on the extrachromosomal DNA circles. 2. There is a neocentromere, but it is so small that we cannot see it with a microscope.

Since the self-extrachromosomal DNA segregates symmetrically and shows all the phenotypes that a centromere-containing DNA molecule would show, there is a high

possibility that there is a neocentromere on this extrachromosomal DNA, but it is composed of very few Cnp1 molecules that are not detected by the microscope.

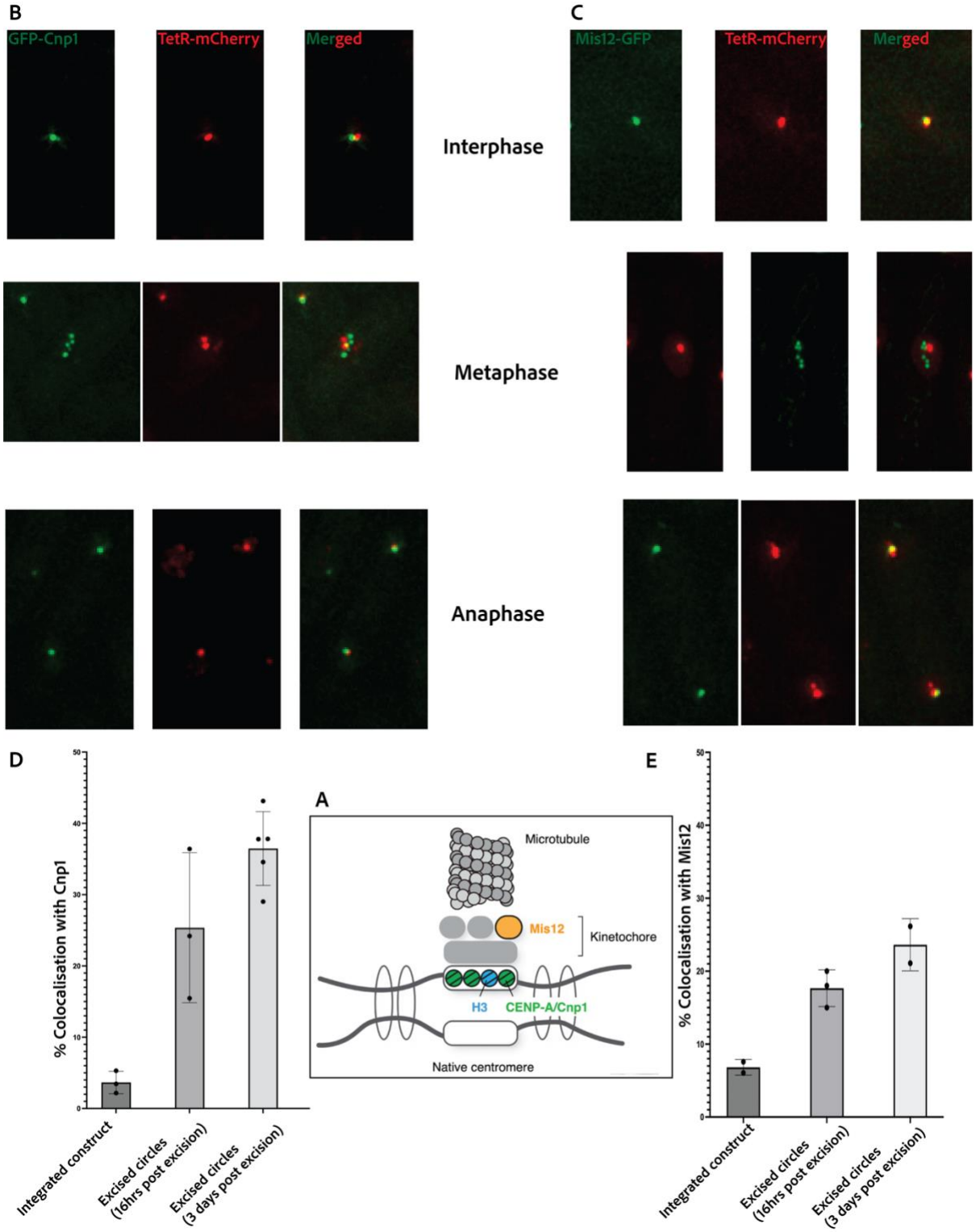

(figure legend on next page)

Figure 21: Self-extrachromosomal DNA circles colocalize with centromeric and kinetochore proteins. (A) Schematic representation of Cnp1 and Mis12 location on centromere/kinetochore complex. (B) Example cells with GFP-Cnp1 and excised extrachromosomal DNA circles tagged with TetR-mcherry. (C) Example cells with Mis12-GFP and excised extrachromosomal DNA circles tagged with TetR-mcherry. Microscopy images corresponding to interphase, metaphase, and anaphase are depicted here. (D) Quantification of colocalization of GFP-Cnp1 with integrated construct and excised extrachromosomal DNA circles (16hrs post excision and 3 days post excision). (E) Quantification of colocalisation of GFP-Cnp1 with integrated construct and excised extrachromosomal DNA circles (16hrs post excision and 3 days post excision). In D and E columns show the mean of replicates indicated by dots, and the error bars show SEM.

2.10. Cnp1 marks the chromosomal and the extrachromosomal DNA for memory:

To ascertain whether Cnp1 molecules are present on the self-extrachromosomal DNA circles that might not be detected with microscopy, we sought to perform a chromatin immunoprecipitation (ChIP) sequencing experiment to explore if self-extrachromosomal DNA could be pulled down of Cnp1 (Figure 22A). We utilised a strain which expresses GFP tagged to the N-terminus of Cnp1 (Figure 21), as this is less defective than the C-terminus tagging (Lando et al., 2012). We deleted the coding region for *tetR-mCherry* to ensure that the binding of TetR-mCherry did not hinder any potential interaction of Cnp1 with *tetO* repeats on self-extrachromosomal DNA circles (Figure 8). Immunoprecipitation was performed using an anti-GFP antibody, and ChIP was carried out on cells with both integrated constructs and excised extrachromosomal DNA circles a few hours and three days post-excision. The enriched DNA reads from the pull-down experiments in all three conditions were analysed. As anticipated, the majority of enriched reads were from the centromeres of all three chromosomes, validating the experiment (Figure 22C). Interestingly, we detected extrachromosomal DNA reads in clones with excised circles after 16 hours, albeit less enriched compared to centromeric DNA, which was expected due to the smaller size of extrachromosomal DNA and its limited capacity to assemble GFP-Cnp1-containing nucleosomes. This enrichment notably increased in clones with 3 days of excised extrachromosomal DNA circles. These findings suggest the presence of GFP-Cnp1 proteins on self-extrachromosomal DNA circles that nucleate more Cnp1 over time, consistent with the maturation process observed in spontaneously occurring neocentromeres in a recent study (Murillo-Pineda et al., 2021).

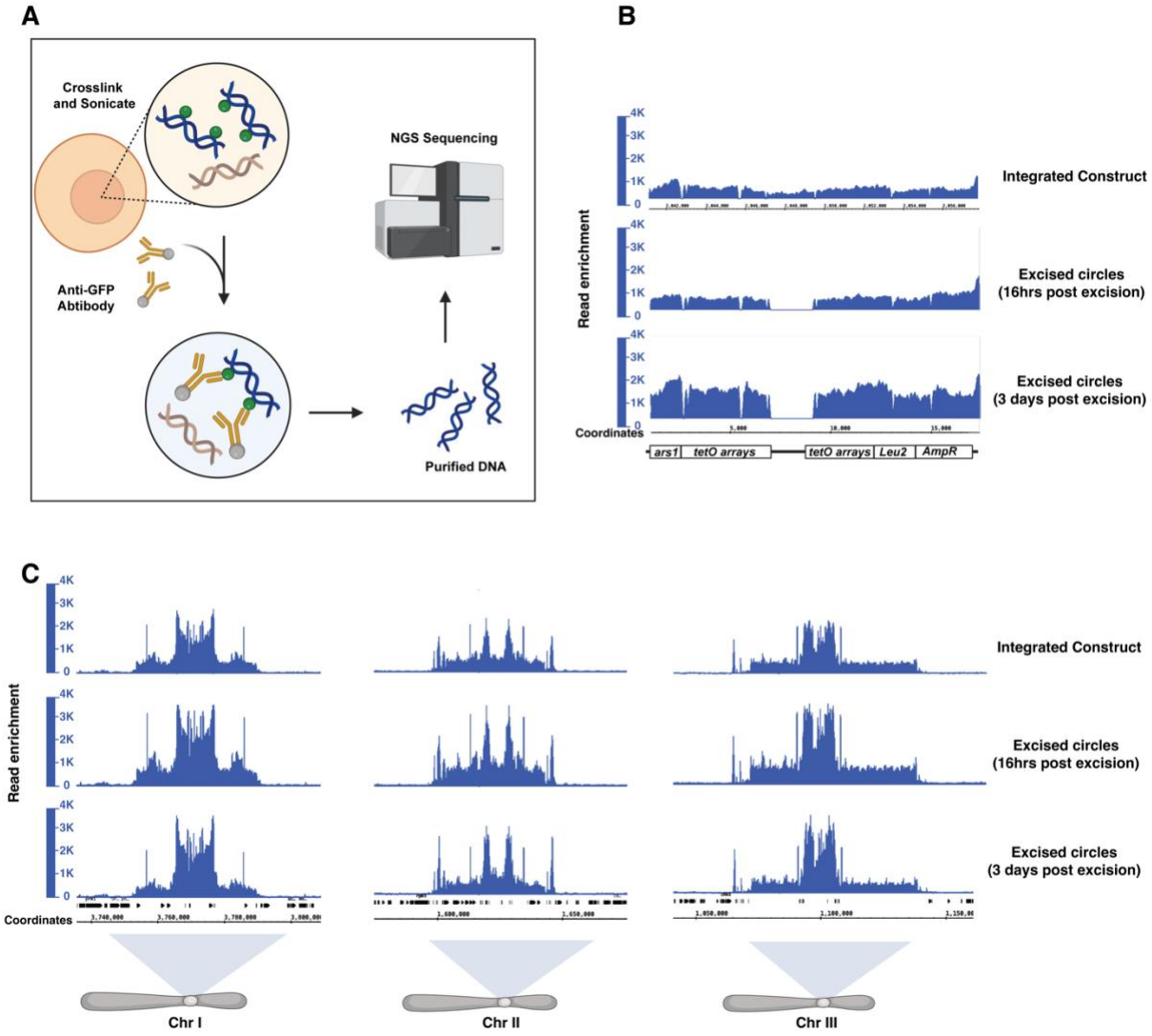

Figure 22: Cnp1 is distributed on extrachromosomal DNA before and after excision (A) Schematic representation of Chromatin immunoprecipitation (ChIP)-sequencing experiment. Strains expressing GFP Cnp1 were used for pull-down experiments (B) Distribution of Cnp1 nucleosomes across the extrachromosomal DNA construct before and after excision. (C) Distribution of Cnp1 nucleosomes across the centromeres of Chromosome I, II, and III in all the conditions (before excision and after excision). The X-axis represents the respective coordinates of the chromosomes and the extrachromosomal DNA. The Y-axis represent the read enrichment from the sequencing data for particular coordinates.

We observed the enrichment of Cnp1 all over the extrachromosomal DNA circles except for a small region. The enrichment on *tetO* repeats could be because the strain does not have *tetR;* we anticipate low or no enrichment in strains with *tetR,* which would occupy the *tetO* repeats. Additionally, we observed some enrichment in the *LEU2* sequence. The strain we used is auxotrophic and has a mutation in the *leu1* gene (*leu1-32*). As we cultivated these cells in a selection media (EMM-leu), the *LEU2* sequence must be transcribed to produce leucine for the survival of the cells. This indicates that despite the presence of an active

neocentromere, the underlying sequence can be transcribed, as shown by previous studies (Bergmann et al., 2011; Carone et al., 2009; Chan et al., 2012; Chueh et al., 2009; Topp et al., 2004; Wong et al., 2007). Another likely reason for the overall enrichment could be that every clone has Cnp1 nucleation at different loci. Because we collectively took many clones during our experiments, we observed Cnp1 enrichment at multiple places, as shown in figure 22B. It would be interesting to find if, indeed, there are multiple loci prone to Cnp1 nucleation of the entire extrachromosomal length act as nucleation sites.

We also observed mild enrichment of Cnp1 on the integrated construct. It was slightly less than the 16 hrs excised circles, but it was present, nonetheless. This observation will be further discussed in the subsequent section (2.10).

To investigate whether the neocentromere contributes to the symmetric segregation of self-extrachromosomal DNA circles, we examined the segregation pattern in conditions of cnp1 recruiting. Cnp1 is loaded onto new centromeres by specific chaperons Sim3 and Scn3, where Sim3 binds to Cnp1 and transfers it to the Cnp1 receptor Scm3 on centromere chromatin, facilitating its incorporation (Figure 23A) (Tanae et al., 2012). We created a strain with knocking-out the *sim3* gene and compared the degree of asymmetric segregation in cells with integrated construct and cells with excised extrachromosomal DNA circles (a few hours after excision and 3 days after excision). Interestingly, we observed a time-dependent increament the phenotype with this deletion: initially, there was little difference in segregation patterns between wild-type and sim3Δ strains containing extrachromosomal DNA circles a few hours post-excision; however, after 3 days, asymmetric segregation became more apparent (Figure 23). Additionally, we observed a clustering defect that was similar to *mis6-302* mutants. This indicated the role of Cnp1 in clustering the self-extrachromosomal DNA circles. These results suggest that the nucleation of Cnp1 on extrachromosomal DNA circles is crucial for their clustering, long-term maintenance and symmetric segregation. Segregation issues arise in the absence of a Cnp1 chaperone, such as Sim3.

Additionally, we noted that the impact of this deletion had a much higher impact on extrachromosomal DNA circle segregation compared to the integrated construct in Chr II, a pattern consistent with *mis6-302* and *spc7-27* mutants. This can be because, during metaphase, the preassembled centromere divides in half when sister chromatids separate, and the chaperons fill the rest half to create the whole centromere structure. The half-

centromere, which is still substantially big may allow for continued symmetric segregation for several more generations before issues arise.

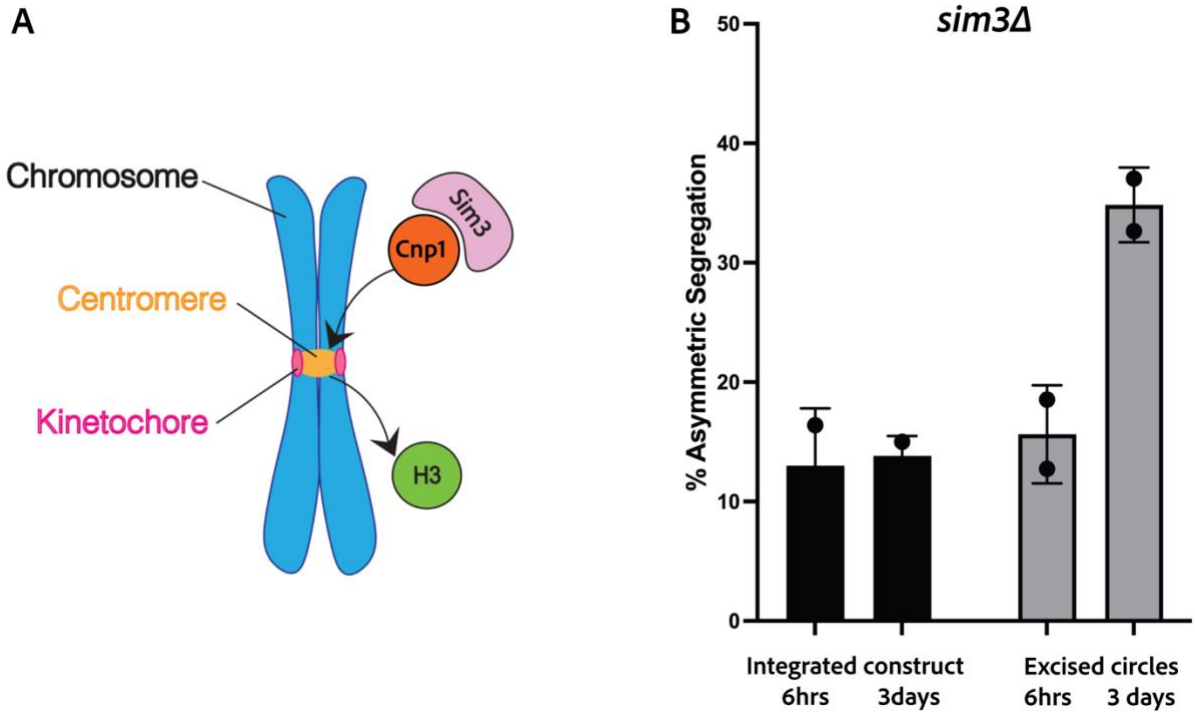

Figure 23: Symmetric segregation of self-extra-chromosomal DNA is disrupted by Cnp1 Chaperone Sim3 deletion. (A) Schematic representation of Sim3 function, i.e., replacement of H3 histone by Cnp1 at centromeres. (B) Quantification of mis-segregation of integrated construct and excised extrachromosomal DNA circles in *sim3* Δ cells. Columns show the mean of replicates, and error bars show SEM.

2.11. Cnp1 marking for memory is a global phenomenon:

An interesting observation we made with our ChIP-seq experiment was that Cnp1 was also slightly enriched on the integrated construct. This raised a question about Cnp1 distribution at locations other than centromeres.

Upon thorough examination of the sequencing data, we found that, indeed, Cnp1 was distributed in many locations on all three chromosomes along with centromeres. Mild to moderate enrichment was found at the rDNA locus, non-coding RNA, telomeres, LTR retrotransposons, and pseudogenes loci found across the chromosomes. An example of such enrichment is shown in Figure 24, which corresponds to the rDNA repeats at the end of chromosome III.

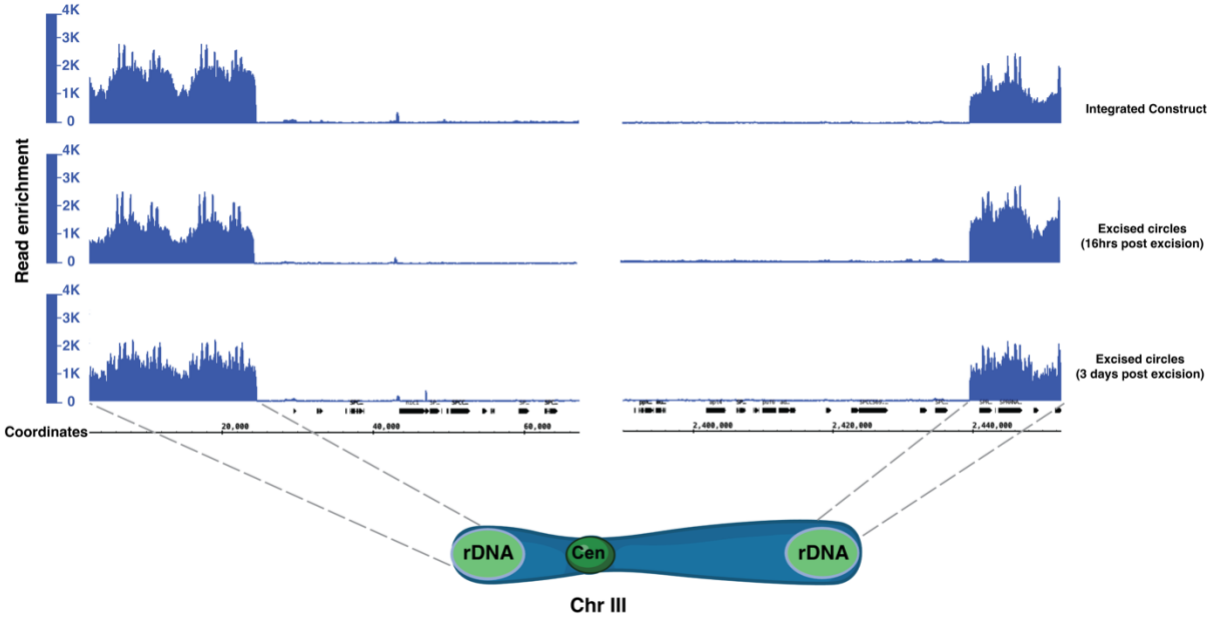

Figure 24: Cnp1 is distributed at rDNA locus of Chr III (A) Distribution of Cnp1 on the ends of Chromosome III depicted in three different clones with integrated construct, extrachromosomal DNA circles 16 hrs post excision, and three days post excision. The X-axis represents the coordinates of the chromosomes III. The Y-axis represents the read enrichment from the sequencing data for particular coordinates.

It has been reported that mild overexpression of Cnp1 in *S. pombe* leads to its accumulation in telomere and rDNA regions. It has been shown that telomere repeats are sufficient to promote CENP-A incorporation and assembly of neocentromere (Castillo et al., 2013b; M. Gonzalez et al., 2014). With this information and our observations, we believe that Cnp1 is distributed throughout the genome with more preference for some regions (e.g., telomere, rDNA repeats) than others.

3. Discussion

In this study, we aimed to investigate a potential DNA discrimination system that can distinguish self-DNA from non-self-DNA in *S. pombe.* We took advantage of extrachromosomal DNA circles as they can be both self (originating from the genome, for e.g., rDNA and telomere circles) and non-self (originating outside, for e.g. Viral DNA or eDNA). Indeed, our data supports the existence of such a discriminatory mechanism based on CENP-A-dependent labelling of DNA regions that are prone to making extrachromosomal DNA, which eventually leads to their self-identity in the events that they are excised from the genome.

3.1. DNA is distinguished based on its origin

The study of naturally occurring extrachromosomal DNA in *S. pombe* has been limited, with only a few documented investigations (Del Giudice et al., 1977; O'connor et al., 1975; Seitz-Mayr et al., 1978). This scarcity of prior research poses challenges in understanding the fate of self-extrachromosomal DNA within this organism. Our developed model provided a valuable platform for introducing and monitoring chromosome-borne and foreign DNA circles over long periods in living cells. Our observations revealed that both types of extrachromosomal DNA circles are dynamic entities exhibiting mobility within the nuclei. However, three days post excision, chromosome-borne DNA circles tended to aggregate and localise near the SPB.

We demonstrated *S. pombe*'s ability to discriminate DNA based on its origin rather than its sequence by utilising extrachromosomal DNA of distinct origins but with nearly identical sequences. Non-self-DNA undergoes asymmetric segregation, while self-extrachromosomal DNA undergoes symmetric segregation during mitosis. Extrachromosomal DNA of foreign origin segregating asymmetrically is somewhat common among organisms, as seen from the low transformation efficiency of most eukaryotic model organisms used in the lab. Interestingly, in contrast to the fate of chromosome-borne DNA circles in most other eukaryotes, we show that these kinds of extrachromosomal DNA are efficiently propagated in the population.

Overall, our findings shed light on the DNA discriminatory system in S. pombe, providing insights into its role in genomic maintenance.

3.2. Non-self-DNA is eliminated rapidly from the population, whereas Self-DNA is not

Many studies have been done to characterise the extrachromosomal DNA circle in different organisms. Typically, these DNA molecules exhibit either random segregation, as observed in human cells, or asymmetric segregation, particularly notable in budding yeast due to the absence of centromeres on extrachromosomal DNA circles (Lundberg et al., 2008; Sinclair & Guarente, 1997; S. Wu et al., 2022). However, exceptions exist within specialised parasitic or viral DNA, where segregation efficiency surpasses that of other extrachromosomal DNA entities. Notably, the Epstein-Barr virus (EBV) DNA serves as an example, employing the virally encoded EBNA-1 protein to facilitate its attachment to mitotic chromosomes and efficient segregation during cell division (Grogan et al., 1983; Marechal et al., 1999; Petti et al., 1990). The extrachromosomal DNA circles examined in our study lack sequences conducive to chromosome binding (Figure 8A, 8C) and looking at their behaviour and segregation pattern, they do not appear to attach to the chromosomes for faithful segregation.

Consistent with previous studies on extrachromosomal DNA in other organisms, our data shows that non-self-DNA is unstable during mitosis and segregates mostly asymmetrically in *S. pombe,* too. Intriguingly, while non-self-DNA quickly disappears from the population within approximately 40 generations, self-DNA, once excised from the genome, demonstrates remarkable stability, persisting across thousands of generations (Figure 11). This stark contrast in behaviour underscores a potential defence mechanism wherein asymmetric segregation facilitates the elimination of non-self-DNA, safeguarding the majority of the population from its presence.

As mentioned, no naturally occurring self-extrachromosomal DNA circles were found in *S. pombe*. This may suggest two possibilities: either *S. pombe* lacks naturally occurring extrachromosomal DNA circles altogether, or their prevalence is low, potentially due to fewer studies conducted on *S. pombe* than other organisms with extrachromosomal DNA. There is also a possibility that extrachromosomal DNA does not exist in lab strains such as *S. pombe* 972 strains but exists in wild strains. It is less plausible that *S. pombe* entirely lacks extrachromosomal DNA circles, as nearly all eukaryotic organisms harbour such entities originating from their genomes. For instance, budding yeast predominantly harbours extrachromosomal DNA circles derived from rDNA repeats, telomeres, and repeated

transposable elements (Møller et al., 2015), while mammalian cells also exhibit a plethora of extrachromosomal DNA circles (Sal'nokov, 1990). A notable distinction between these organisms and *S. pombe* lies in their divisional asymmetry. Typically, organisms like budding yeast and mammals divide mostly asymmetrically; as such, they segregate their extrachromosomal DNA circles asymmetrically, facilitating their accumulation and consequent detection. *S. pombe*, in contrast, is a symmetrically dividing organism, and our studies show that self-extrachromosomal DNA circles are evenly distributed among the diving cells, thereby reducing their overall abundance.

Moreover, studies have demonstrated the ability of rDNA circles in budding yeast to reintegrate into the genome, primarily due to their homology with the genomic rDNA repeats (Mansisidor et al., 2018). Given that extrachromosomal DNA circles often originate from repeat regions, they maintain a significant homology with the genome. Since *S. pombe* segregates extrachromosomal DNA circles symmetrically, and these circles potentially reintegrate into the genome after a few divisions, therefore, detecting these extrachromosomal DNA circles could be challenging. Our time course experiments revealed no instances of 100% symmetric segregation, suggesting that in our study, their lack of reintegration into the genome may be attributed to their reduced homology to the genome.

In conclusion, our study elucidates the differential sorting of extrachromosomal DNA circles in *S. pombe*, wherein self-originated DNA is retained within the population while non-self-DNA is systematically eliminated.

3.3. Self-extrachromosomal DNA is stable both during mitosis and meiosis

In budding yeast, it has been shown that both self and non-self-extrachromosomal DNA circles undergo asymmetrical segregation, except in cases where these circles harbour a centromeric sequence, resulting in a relatively symmetrical segregation pattern (Falcón & Aris, 2003). Similarly, investigations into various artificial linear and circular chromosomes in *S. pombe* have revealed that only those mini-chromosomes containing specific centromeric sequences—*cnt, imr,* and *otr*—exhibit symmetrical segregation (Niwa et al., 1986). These findings collectively suggest that the presence of a centromeric sequence is pivotal for achieving symmetrical segregation during mitosis.

Moreover, studies have indicated that while these mini-chromosomes remain stable during mitosis, their stability during meiosis is comparatively lower. According to these studies, these mini-chromosomes are not inherently defective for maintenance; rather, they often fail to form proper bivalent formations in meiosis metaphase (Niwa et al., 1986). Intriguingly, our investigation parallels these findings, revealing that self-extrachromosomal DNA also undergoes symmetrical segregation during mitosis and, to a lesser extent, during meiosis. Notably, self-extrachromosomal DNA lacks the centromeric sequences and is significantly smaller than the mini-chromosomes utilised in prior studies (approximately 500 kb). Despite these disparities, the behaviour of extrachromosomal DNA circles closely mirrors that of mini-chromosomes. Additionally, the slight instability of extrachromosomal DNA circles conserved could also stem from not forming proper bivalent formations in meiosis metaphase.

In summary, the ability of *S. pombe* to differentiate between self and non-self DNA enables it to sustain a population with intact genomic DNA, preventing the loss of genetic material through the asymmetric segregation of extrachromosomal DNA circles.

3.4. Cnp1 marks the DNA that is prone to making extrachromosomal DNA circles.

As mentioned earlier, a significant portion of extrachromosomal DNA circles originates from repetitive regions within the chromosome. Building on this understanding, we strategically inserted our construct into various genomic locations, including these repetitive regions. Remarkably, the excised extrachromosomal DNA exhibited symmetrical segregation irrespective of the insertion site. This intriguing finding suggests the presence of a mechanism in *S. pombe* that ensures equal representation of excised genome portions in subsequent generations. Notably, this mechanism likely relies on epigenetic markers present on the DNA fragment rather than its sequence, as supported by our experimental data. These epigenetic markers may function as identifiers of self-DNA, ensuring the faithful segregation of extrachromosomal DNA circles despite their non-chromosomal nature.

Notably, in cases of chromosomal fusion or the formation of additional centromeres on a chromosome, one of the centromeres is usually inactivated (Stimpson et al., 2012). Additionally, when a chromosome breaks, the resulting acentric fragment can assemble a neocentromere to facilitate equal segregation (Hasson et al., 2011). The precise determinant

governing whether there is more than one centromere, or no centromere is unclear. However, it is evident that cells have the capacity to form neocentromeres at non-centromeric locations following chromosomal DNA breakage or centromere deletion. We speculate that a similar mechanism may be at play with self-extrachromosomal DNA circles in *S. pombe*, as both chromosome breaking and excision events are comparable. Whatever facilitates the assembly of a neocentromere on broken chromosomal fragments may also be involved in regulating extrachromosomal DNA circles.

Research suggests that certain sequences, such as telomere repeats, exhibit a propensity to promote neocentromere assembly. For instance, mild overexpression of Cnp1 in *S. pombe* has been shown to accumulate at telomeric and rDNA regions, promoting neocentromere formation (Castillo et al., 2013b; M. Gonzalez et al., 2014). Our ChIP-Seq data supports these findings, revealing Cnp1 distribution across telomeric and rDNA repeat regions, although Cnp1 overexpression was not a factor in our study. Cnp1 is also mildly enriched to our integrated construct along with these repeats. Interestingly, Cnp1 nucleation increases upon extrachromosomal DNA excision, suggesting a mechanism by which telomeric and rDNA repeats are primed for neocentromere assembly. We propose that Cnp1 serves as a "self" identifier, preferentially localising to repetitive regions prone to recombination, including our construct. This localisation of Cnp1 promotes neocentromere assembly upon excision, promoting equal distribution of extrachromosomal DNA circles to mitigate DNA loss or copy number variation. However, we assume that neocentromere formation and maturation on rDNA circles, etc., should be extremely low compared to our extrachromosomal DNA circles, possibly because they integrated back into the genome in a few generations (you mentioned above).

However, whether the entire extrachromosomal DNA circle serves as a site for Cnp1 nucleation or if there are individual sites within different clones acting as Cnp1 nucleation sites remains to be confirmed. Additionally, we observed that extrachromosomal DNA circles excised from pericentromeric regions exhibited a notably high level of symmetric segregation. This observation suggests that their proximity to the centromere may contribute to their initial symmetrical segregation due to the abundance of Cnp1 in these regions.

Since *S. pombe* features monocentric chromosomes, it is likely that Cnp1 does not nucleate kinetochores on non-centromeric sites on the chromosomes already possessing a centromere. However, upon excision, Cnp1 presence on the excised circles prompts the

formation of functional neocentromeres by nucleating more Cnp1. Further exploration is warranted to ascertain whether Cnp1 nucleation also triggers the recruitment of other centromeric and kinetochore proteins or if it solely facilitates equal segregation until integration into the genome occurs.

3.5. Cnp1 is essential for the clustering and symmetric segregation of self-extrachromosomal DNA circles

We showed the distribution of Cnp1 across the genome and hypothesised its role as an identification mark on the excised extrachromosomal DNA. To validate this hypothesis and assess its contribution to the symmetrical segregation of self-extrachromosomal DNA circles, we disrupted the Cnp1 chaperon, Sim3. Our findings unequivocally showed that Cnp1 nucleation is indispensable for the symmetrical segregation of these extrachromosomal DNA circles. Initially, *sim3Δ* cells exhibited a segregation pattern akin to wild type; however, over time, they manifested disrupted symmetric segregation, indicating the necessity of accumulating Cnp1 over generations for proper segregation.

In *S. pombe*, chromosomes harbour large centromeres containing numerous Cnp1 molecules, which are evenly divided among sister chromatids during mitosis. These divided centromeres are then filled with more Cnp1 molecules with the help of Chaperons like Sim3. As these divided centromeres are still quite big after division, the impact of *sim3Δ* is quite low on chromosomes.

Similarly, the limited presence of Cnp1 on extrachromosomal DNA circles suggests that if these Cnp1 nucleosomes function as neocentromeres, they, too, are divided during symmetric segregation. Insufficient accumulation of Cnp1 over generations consequently leads to segregation issues quicker than chromosomal segregation problems because extrachromosomal DNA circles had quite a few Cnp1 molecules to begin with.

Furthermore, we observed the aggregation of self-extrachromosomal DNA circles over time, a phenomenon impaired in the *mis6-302* and the *sim3Δ* mutants. We propose that this aggregation resembles centromere clustering, with the Cnp1 marker facilitating the clustering of extrachromosomal DNA circles over time (W. Wu et al., 2021).

In conclusion, our study highlights the essential role of Cnp1 in mediating the aggregation of multiple extrachromosomal DNA circles and ensuring their long-term maintenance within the population.

3.6. Role of microtubules in symmetric segregation of extrachromosomal DNA

Chromosomes are segregated with precision through the establishment of biorientation, where sister kinetochores attach to microtubules extending from opposite spindle poles, known as end-on attachment. This attachment allows for chromosome movement via the elongation and shrinkage of microtubule bundles. Alternatively, kinetochores can also attach to the sides of microtubules, termed lateral attachment, and move along them with the assistance of motor proteins (Itoh et al., 2018). During mitosis, kinetochores can be efficiently captured by the lateral surfaces of microtubules and transported towards spindle poles (K. Tanaka, 2012). While some studies suggest that lateral attachment transitions into end-on attachment, bi-orientation can also be efficiently established for chromosome transport through lateral attachment (Itoh et al., 2018; Magidson et al., 2011, 2015; T. U. Tanaka et al., 2005). This suggests that lateral attachments are not just transient, unstable attachments but critical processes to chromosome transport and biorientation. This indicates that lateral attachments are not merely transient or unstable but are critical processes for chromosome transport and biorientation.

Our observation of self-extrachromosomal DNA circles being evenly distributed among the dividing cells, them not binding to chromosomal DNA and them rarely integrating back into the genome suggested that microtubule attachments must be established to facilitate their segregation. Our data, utilising tagged α-tubulin, Atb2 protein, and plus-end-tracking protein, indicates that this attachment is primarily lateral rather than end-on, yet still sufficient for the symmetrical segregation of these DNA molecules.

Further investigation is warranted to characterise these attachments precisely, and high-resolution microscopy could offer valuable insights into their nature and dynamics. Additionally, it would be interesting to explore if the surveillance system, the spindle assembly checkpoint (explained in section 1.4.3), affects the segregation pattern of self-extrachromosomal DNA circles.

3.7. Working model

The following model encapsulates the findings of our study (Figure 25). Replicative self-extrachromosomal DNA can spontaneously arise from repetitive regions within the chromosome by recombination or DNA breakage. These repetitive regions typically harbour a modest amount of Cnp1 molecules, which remain inactive due to the presence of endogenous centromere. However, upon excision from the chromosome, these Cnp1 molecules serve as sites for forming functional neocentromeres, facilitating the symmetrical segregation of chromosome-borne DNA circles. The presence of these neocentromeres ensures the faithful segregation of the circles until conditions permit their reintegration into the genome. It would be worth exploring in the homology does ensure the integration back into the genome after a successful propagation in the population.

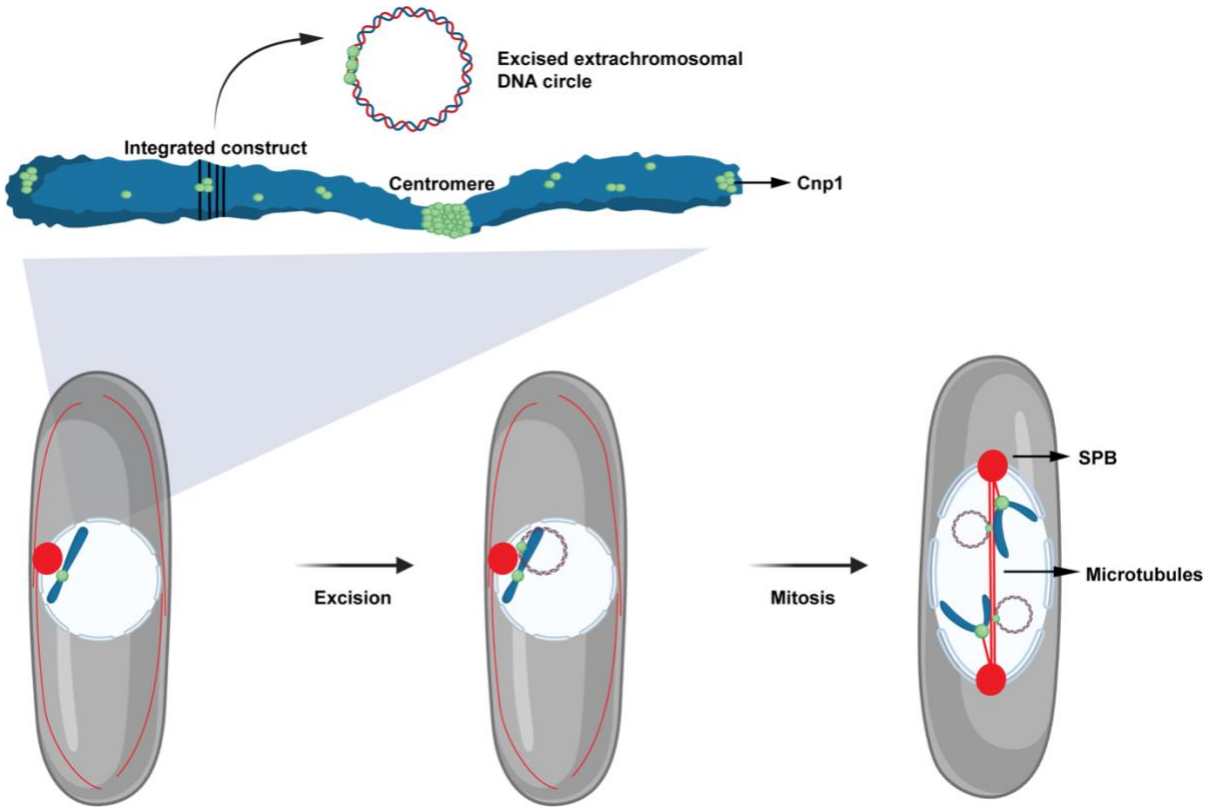

Figure 25: Model of self-extrachromosomal DNA circle dynamics in *S. pombe*. Chromosome-borne extrachromosomal DNA circles may originate from various genomic sites. The widespread presence of Cnp1 across the genome, particularly in regions susceptible to recombination, results in the inclusion of a few Cnp1 molecules within recombined circles. These Cnp1 molecules serve as nucleation points, facilitating the recruitment of additional Cnp1 and other essential protein complexes necessary for the accurate segregation and propagation of these circles.

3.8. Why segregate self-extrachromosomal DNA symmetrically?

The accumulation of extrachromosomal DNA circles has been implicated in various human pathologies, such as cancer and Inflammatory Bowel Disease (IBD), as well as in the ageing process of *S. cerevisiae* (Denoth Lippuner et al., 2014; Di Vincenzo et al., 2023; Kruitwagen et al., 2018; Sinclair & Guarente, 1997; Yang et al., 2022). Conversely, the loss of DNA copy number through extrachromosomal DNA recombination can also have adverse effects like telomere shortening and gene copy number variation, potentially harming the cells (Y.-A. Chen et al., 2017; Hull et al., 2019). Considering *S. pombe*'s unique characteristic of not undergoing ageing under normal conditions (Coelho et al., 2013) and its genome being relatively stable, (Rhind et al., 2011) it is conceivable that the organism employs mechanisms to prevent the accumulation of extrachromosomal DNA circles and ensures that it does not lose any DNA via genomic recombination. The symmetrical segregation of chromosome-borne DNA circles may serve as one such mechanism to maintain genome integrity and mitigate the toxicity associated with extrachromosomal DNA accumulation. This strategy is consistent with the symmetrical segregation observed for most other cellular components during *S. pombe* cell division, suggesting a coordinated mechanism for maintaining cellular homeostasis.

Also, the discrimination in segregation patterns may represent a strategy employed by *S. pombe* to safeguard its genome from unwanted genetic parasites by asymmetrically segregating them while ensuring the preservation of its genetic material through symmetric segregation.

4. Materials and Methods

4.1. Strain growth conditions

Schizosaccharomyces pombe was cultivated either on rich medium, yeast extract with supplements (YES) or minimal medium, Edinburgh minimal medium (EMM) described previously (Mitchison 1970). Cultures were grown at 30°*C* unless indicated otherwise for temperature-sensitive strains. The cultures were either grown in incubators without shaking of with shaking at 160 rpm. All the strains used in this study are a part of the Barral Lab Fission yeast strain collection. Some parent strains were gifts from Sophie Martin's lab, and some were bought from the Yeast Genetic Resource Center (YGRC). Most strains harboured a genomic construct expressing either stable TetR-GFP or TetR-cherry, regulated by Thiamine-repressible promoter Nmt81.

4.2. Strain Construction using mating

Fission yeast strains used for this study are listed in Table 5.10. Strains were primarily generated through genetic crossing, followed by either tetrad dissection or random sporulation. The strains were first resuscitated from -80°C on YES agar medium at 30°C or 25°C (temperature-sensitive strains) to initiate culture revival. After a recovery period typically lasting 2-3 days, equal quantities of both parental strains were combined in 20 µl dH20. Both the strains were thoroughly mixed, and 10 µl of this blend was spotted onto sporulation media (SPAS) agar to induce mating by invoking sudden nitrogen starvation shock. The cross was then incubated at room temperature for 24-48hrs. Spores were either harvested by random sporulation or by tetrad dissection.

For random sporulation, the genetic cross was suspended in 100 µl dH_20 and was treated with 2% β-glucuronidase/Arylsulfatase at 25°C with 160rpm shaking for 1hr. The vegetative cells were subsequently killed by adding 42 µl 100% EtOH for 5 min. The spores were then spread on a YES plate at 30°C or 25°C (~4000 spores/plate).

For tetrad dissection, the genetic cross was suspended in 50 µl dH_20. 25 µl of this suspension was dispensed on YES agar in a straight line down the middle of the plate. The plate was incubated at 30°C/25°C (depending on the kind of parental strain) for 3-4 hours, during which time the spores were released from the ascus. The spores were then dissected on both sides

of the distribution line. After dissection, the YES agar plate was incubated at 30°C/25°C for 3-5 days until the colonies appeared. The desired genotypes were then selected via replica plating onto various selection media.

4.3. Strain construction using homologous recombination

To generate deletion/mutation strains and perform C-terminal tagging of proteins with GFP or mCherry, we utilise pFA6a plasmids to amplify deletion or tagging cassettes (Bähler et al., 1998). Additionally, we incorporate flanking regions that homologously match the target gene loci through overlap extension PCR. Primers for this process are designed using the Bähler Laboratory PPPP online tool, allowing us to create primers with an 80-120 bp overhang while aligning with the constitutive binding sites on the template pFA6a plasmids Amplification of the respective cassette for transformation is performed using iProof High-Fidelity Polymerase (Bio-Rad) in HF buffer as per the manufacturer's instructions. Subsequently, the cassettes are transformed into the desired strain using the protocol outlined in section 5.4. Verification of the strains is carried out through colony PCR, growth on selection plates, and microscopic visualization. Details regarding the plasmids utilized for tagging/gene deletion are provided in Table [4.10]

4.4. Transformation

The strain with extrachromosomal DNA integration was revived from -80°C storage on a YES agar plate. Following revival, a preculture was established by inoculating 2-5ml of YES media and allowing it to incubate at 30°C overnight to achieve a desired optical density (OD) of 0.8-1. The next day, a main culture was inoculated to achieve an OD between 0.4-0.6 on the following day. Centrifugation steps were conducted at room temperature at 380 rcf for 3 minutes. The cells were then washed with 1ml dH2O and resuspended in 100 µl LiOAc+TE buffer (containing 0.1M lithium acetate, 10mM Tris pH 7.5, and 1 mM EDTA). A mixture was prepared with 0.1-1 µg DNA (10 µl), 5 µl ssDNA, 100ul of the culture in LiOAc+TE, and 240 µl of 40% fresh PEG 4000 (Sigma), followed by incubation at 30°C for 1-2 hours. After incubation, 43 µl of fresh DMSO was added to the mixture, followed by a 10-minute heat shock at 42°C. The cells were then pelleted, resuspended in 100 µl, and plated either on a selection plate or YES agar. In the case of auxotrophic markers, cells were directly plated on the selection plate.

However, for antibiotic selection markers, cells were first revived on YES agar for 18-24 hours at 30°C before being replica plated on antibiotic-containing plates.

4.5. Excision of integrated circles

As described before, the strain intended for transformation was revived from -80°C storage. Following revival, a preculture was established by inoculating 2-5ml of YES media and allowing it to incubate at 30°C overnight to achieve a desired optical density (OD) of 0.8-1. The next day, a main culture was inoculated in EMM -leu liquid media + 1µM β-estradiol to achieve an OD between 0.4-0.6 on the following day.

The excised circles were confirmed by visual inspections under the microscope.

4.6. Widefield microscopy Imaging

To assess the behaviour of extrachromosomal DNA during mitosis, wild-type strains were revived on YES medium at 30°C. Subsequently, strains were cultured in liquid EMM -leu or EMM complete medium until reaching OD600 = 0.4-0.6, followed by imaging. Temperature-sensitive mutants were cultivated at 25°C and served as controls. Subsequently, the same cells were exposed to the permissive temperature of 30°C for 6-16 hours to observe the phenotype. Imaging of the cells was conducted under the permissive temperature condition. For live cell imaging, cells were gently pelleted at 350g for 3 minutes at room temperature, resuspended in liquid EMM-leu or EMM complete medium, and then a 1 µl aliquot was placed on an agar pad of corresponding medium for imaging. Chromosomal and extrachromosomal DNA circle segregation were observed using a Deltavision microscope (Applied Biosystems) equipped with a CCD HQ (Roper) camera, solid-state LEDs, an Olympus 100x/1.4NA objective, Softworx software (Applied Precision), and a temperature-controlled chamber.

Still images were captured with exposure times of 0.5 seconds for the TRITC (red) channel, 0.5 seconds for the FITC (green) channel, and 0.1 seconds for the POL channel across 12 Z-stacks spaced 0.2 µm apart, followed by deconvolution using DeltaVision software. Time-lapse movies were recorded with exposure times of 0.15 seconds for TRITC, 0.15 seconds for FITC, and 0.015 seconds for POL across 9 Z-stacks spaced 0.4 µm apart, with images taken every 2 minutes over a 30-minute period, also deconvolved using DeltaVision software.

Data analysis was performed using Fiji image processing software. Cells in Anaphase B were identified by either separated nuclei or spindle pole body positioning. Foci number was determined by visual inspection, while total foci intensity per nucleus was measured by drawing a region of interest around the nucleus periphery, background subtraction, and calculating mean intensity per nucleus for mean z-stack projection. A minimum of 500 cells were measured for each condition.

For observation of meiosis, cells were cultured on an EMM medium at 30°C. Cells with integrated constructs or excised circles were mixed in equal amounts with their opposite mating partner in dH_20, spotted on a SPA medium, and observed. Genetic crosses were incubated overnight at room temperature, then spotted onto SPA agar pads for observation of meiosis using a Nikon MMi microscope with Orca Fusion BT camera, Spectra III LEDs, 60x/1.4NA objective, NIS-elements software, and temperature control at 25°C. Time-lapse movies were captured with 0.5 seconds exposure for GFP and mCherry channels, acquiring 9 z-stacks with 0.4 µm spacing every 10 minutes over 6 hours, with subsequent analysis using NIS-elements.ai software.

4.7. Confocal microscopy Imaging

To achieve high-quality imaging, we utilised a Zeiss LSM 510 confocal microscope equipped with a 488-nm argon laser (with a maximum output of 25 mW) from Zeiss Microimaging. The instrument was controlled by ZEN 2010 software provided by Carl Zeiss.

Prior to colocalisation experiments, cells were fixed. They were initially cultured in EMM-leu liquid media until reaching an optical density (OD600) between 0.4 and 0.6. Subsequently, cells were harvested via centrifugation at 350g for 3 minutes. The cell pellet was then resuspended in 70% ice-cold ethanol and kept at -20°C for a minimum of 1 hour before being placed on slides for imaging.

Image acquisition involved capturing images with a 0.1-second exposure for both mCherry and GFP channels across 14 Z stacks spaced 0.2 µm apart. Additionally, time-lapse movies were generated with images acquired every minute for a duration of 10 minutes. Image analysis was performed using ImageJ.

4.8. Chromatin immunoprecipitation (ChIP)

Fission yeast cells were cultured in selective liquid media (EMM-leu) at 30°C until reaching an optical density (OD600) of 0.6-1.0 in a 100ml volume. Formaldehyde was then added to a final concentration of 3% and the culture was incubated with moderate shaking for 20 minutes at room temperature (RT). The formaldehyde cross-linking reaction was quenched by adding 2.5M glycine to a final concentration of 250mM and further incubated with shaking for 5 minutes at RT. After incubation, the cells were harvested by centrifugation at 3500g for 5 minutes at 4°C, washed twice with 25ml of ice-cold 1xPBS and aliquoted into 2ml screw cap tubes. The cell pellets were snap-frozen and stored at -80°C until further use.

For chromatin preparation, the frozen cell pellets were thawed on ice and lysed by adding 2 PCR-sized scoops of zirconia beads (~ 250 µl vol equivalent) and 500 µl of ice-cold lysis buffer (50mM HEPES/KOH pH 7.5, 140mM NaCl, 1mM EDTA, 1% Triton X-100, 0.1% Na-Deoxycholate) supplemented with protease inhibitors (1mM AEBSF, 100 µg/ml Leupeptin, Roche complete protease inhibitor cocktail). Cells were then beaten using a FastPrep-24 (MP Biomedicals) cell disruptor with 8 rounds of 30-second bursts at 6m/s with 1-minute intervals in a cold room. This was followed by puncturing the screw-cap tubes containing lysed cells with a 22-gauge needle and putting them in 2ml Eppendorf tubes. Tubes were centrifugated for 3 minutes at 700g at 4°C. The lysates were transferred to fresh tubes and sonicated in a water bath sonicator for 30 minutes (30 seconds on/30 seconds off cycles) in a cold room to shear chromatin. The sonicated material was then centrifuged at 16,000g for 10 minutes at 4°C to remove debris. The supernatant (lysate) containing DNA fragments was further cleared by centrifugation one more time.

For immunoprecipitation (IP), 5 OD of lysate material was used as input and stored at -20°C after topping up to 200µl with TE/1% SDS. For IP of cnp1-GFP, 30OD of lysate material was incubated overnight at 4°C with 0.4µg antibodie (Roche 11814460001) on a nutator for constant mixing. 25µl Magnetic ProtG/Dynabeads(Invitrogen™ 10003D) were washed 2x with PBS/.1% Tween, then 1x with lysis buffer. Beads were eventually resuspended in 100µl of lysis buffer and were added to the IP samples. IP samples were incubated overnight at 4°C on a nutator. The samples were then washed subsequently 2x with ice-cold lysis buffers and

2X with High salt lysis buffer(50mM HEPES/KOH pH 7.5, 500mM NaCl, 1mM EDTA, 1% Triton X-100, 0.1% Na-Deoxycholate), 2x with Wash buffer (10mM Tris/HCl pH 8, 250mM LiCl, 1mM EDTA, 0.5% NP-40, 0.5% Na-Deoxycholate) and 1x with TE(10mM Tris/HCl, 10mM EDTA). The IP samples were resuspended in elution buffer (50 mM Tris/HCl pH 8, 10 mM EDTA, 0.8% SDS). The cross-links were reversed by incubating both the IP and the input samples at 95°C for 10 minutes with maximum shaking followed by 3 hrs incubation at 65°C with shaking at 500 rpm. Subsequently, the samples were treated with 50µg Proteinase K and incubated at 55°C for 2 hours with shaking at 500 rpm. IP and Input samples were cleaned using a ChIP DNA Clean & Concentrator kit. Functional Genomics Center Zurich performed high-throughput sequencing of purified DNA fragments using Illumina.

4.9. Sequencing and Analysis

Functional Genomics Center Zurich performed raw reads analysis with specific modifications in the genome. Briefly, a recombinant genome, including chromosome II-specific integration, was generated. A new gene annotation adjusted for changes in chromosome name and position was also generated. A 17,447bp integration was added between Chr II: 2042146-2040893 as they were located at his7 locus of Chr II. The integrated sequence present in the strain was removed afterβ-estradiol treatment as the contract would be excised at this time. Raw reads generated from stain with unexcised construct a few hours after excision and three days after excision were then aligned to their corresponding genome. We also generated chromosome size files and genome files for IGV visualisation.

Quantification of ChiP-seq reads on whole chromosomes was performed by the Functional Genomics Center Zurich. Briefly, all chromosomes were divided in 500 equally sized bins. After trimming the barcodes and performing quality control on the reads, the number of reads in each bin for IP and input samples was quantified using bedtools multicov and normalised the values for sequencing depth before subtracting the input values. Reads were counted separately for samples not treated and treated withβ-estradiol (because they have different headers). Samples were then merged, and column headers were added and normalised to sequencing depth.

4.10. Illustrations

The illustrations in Figures 1, 3, 4, 5, 6, 7, 8A, 8C, 9, 10A, 12A, 14A, 15A, 16A, 19B, 22C, and 24 were created with BioRender.com. All the graphs were generated by GraphPad Prism.

4.11. Strains used in this study

Strain number (FYB)	Genotype	Mating type
31	h- Z::Padh15-mCh-atb2-NatMX leu1-	M
60	h+ ade6+ leu1-32 ura4-294 Pnmt81-NLStetR-GFP::ura4+	P
67	h- ura4 cut3-477	M
97	h+ ade6+ leu1-32 ura4-294 Pnmt81-NLStetR-GFP::ura4+ cut11-mCh::KanMX	P
108	h- leu1 Sad1mCherry::kanR	M
166	h+ ura4-294 his7-366 leu1-32	P
176	h+ ade6+ leu1-32 ura4-294 his7-366 Pnup211-NLStetR-GFP Pnmt81-creEBD :: ura4+	P
192	h+ ade6+ leu1-32 ura4-294 his7-366 Pnup211-NLStetR-GFP Pnmt81-creEBD :: ura4+ sad1-mCh::NatMX tetO-GmR LEU2 :: loxP>cen1f1 (lys1frag) loxP>	P
197	h+ ade6+ leu1-32 ura4-294 his7-366 tetO-GmR ARS LEU2 :: loxP>his7+ loxP> Pnup211-NLStetR-GFP Pnmt81-creEBD :: ura4+ sad1-mCh::NatMX	P
202	h- ade6? leu1-32 ura4-294 his7-366 tetO-GmR ARS LEU2 :: loxP>his7+ loxP> Pnup211-NLStetR-GFP Pnmt81-creEBD :: ura4+ sad1-mCh::NatMX	M
216	h+ ade6+ leu1-32 ura4-294 his7-366 tetO-GmR ARS LEU2 :: loxP>his7+ loxP> Pnup211-NLStetR-GFP Pnmt81-creEBD :: ura4+ sad1-mCh::NatMX cut3-477	P
255	h+ ade6+ leu1-32 ura4-294 his7-366 tetO-GmR LEU2 :: loxP>sTeloI loxP> Pnup211-NLStetR-GFP Pnmt81-creEBD :: ura4+ sad1-mCh::NatMX	P
256	h+ ade6+ leu1-32 ura4-294 his7-366 tetO-GmR LEU2 :: loxP>rDNA18S loxP> Pnup211-NLStetR-GFP Pnmt81-creEBD :: ura4+ sad1-mCh::NatMX	P
257	h+ ade6+ leu1-32 ura4-294 his7-366 tetO-GmR LEU2 :: loxP>rDNA18S loxP> Pnup211-NLStetR-GFP Pnmt81-creEBD :: ura4+ sad1-mCh::NatMX	P

274	h+ ade6+ leu1-32 ura4-294 his7-366 tetO-GmD ARS1::hphMX6 LEU2 :: loxP>sTeloI loxP> Pnup211-NLStetR-GFP Pnmt81-creEBD :: ura4+ sad1-mCh::NatMX	P
276	h+ ade6+ leu1-32 ura4-294 his7-366 tetO-GmD ARS1::hphMX6 LEU2 :: loxP>rDNA 18SloxP> Pnup211-NLStetR-GFP Pnmt81-creEBD :: ura4+ sad1-mCh::NatMX	P
277	h+ ade6+ leu1-32 ura4-294 his7-366 tetO-GmR LEU2 :: loxP>lys2f loxP> Pnup211-NLStetR-GFP Pnmt81-creEBD :: ura4+ sad1-mCh::NatMX	P
278	h+ ade6+ leu1-32 ura4-294 his7-366 tetO-GmR LEU2 :: loxP>lys2f loxP> Pnup211-NLStetR-GFP Pnmt81-creEBD :: ura4+ sad1-mCh::NatMX	P
292	h+ ade6+ leu1-32 ura4-294 his7-366 tetO-GmR ARS LEU2 :: loxP>his7+ loxP> Pnup211-NLStetR-GFP Pnmt81-creEBD :: ura4+ sad1-mCh::NatMX sim3Delta::hphMX	P
294	h- leu1 mis6-302	M
296	h- spc7-27-myc::KanR leu1 ura4	M
300	h+ ura4-294 his7-366 leu1-32 Pnup211-TetRmCh_Pnmt81-creEBD :: ura4+	P
319	h+ ade6+ leu1-32 ura4-294 his7-366 tetO-GmR ARS LEU2 :: loxP>his7+ loxP> Pnup211-NLStetR-GFP Pnmt81-creEBD :: ura4+ sad1-mCh::NatMX mis6-302	P
320	h+ ade6+ leu1-32 ura4-294 his7-366 tetO-GmR ARS LEU2 :: loxP>his7+ loxP> Pnup211-NLStetR-GFP Pnmt81-creEBD :: ura4+ sad1-mCh::NatMX mis6-302	P
324	h+ ade6+ leu1-32 ura4-294 his7-366 tetO-GmR ARS LEU2 :: loxP>his7+ loxP> Pnup211-NLStetR-GFP Pnmt81-creEBD :: ura4+ sad1-mCh::NatMX spc7-27-myc::kanR	P
330	h+ ura4-294 his7-366 leu1-32 Pnup211-TetRmCh_Pnmt81-creEBD :: ura4+ cnp1-GFP::lys1+ his7-366 tetO-GmR ARS LEU2 :: loxP>his7+ loxP>	P
333	h+ ura4-294 his7-366 leu1-32 Pnup211-TetRmCh_Pnmt81-creEBD :: ura4+ his7-366 tetO-GmR ARS LEU2 :: loxP>his7+ loxP>	P
530	h- ade6? leu1-32 ura4-294 Pnmt81-NLStetR-GFP::ura4+ cut11-mCh::KanMX CFP-atb2-NatMX	M
540	h- leu1 Mis12-GFP::LEU2	M
627	h? ura4-294 his7-366 leu1-32 Pnup211-TetRmCh_Pnmt81-creEBD :: ura4+ his7-366 tetO-GmR ARS LEU2 :: loxP>his7+ loxP> Mis12-GFP::LEU2	?

629	h+ ura4-294 his7-366 leu1-32 Pnmt81-creEBD :: ura4+ cnp1-GFP::lys1+ his7-366 tetO-GmR ARS LEU2 :: loxP>his7+ loxP>	P
630	h+ ura4-294 his7-366 leu1-32 Pnmt81-creEBD :: ura4+ cnp1-GFP::lys1+ his7-366 tetO-GmR ARS LEU2 :: loxP>his7+ loxP>	P
646	h? Ade6? leu1-32 ura4-294 his7-366 tetO-GmR ARS LEU2 :: loxP>his7+ loxP> Pnup211-NLStetR-GFP Pnmt81-creEBD :: ura4+ sad1-mCh::NatMX Z::Padh15-mCh-atb2-NatMX	?
699	h- GFP-cnp1-NAT leu1-32 ura4-D18 lys1	M
826	h? leu1-32 ura4-294::P.nup211-NLS-tetR-mCh:P3nmt81-Cre-ERT2:ura4+ his7-366::LoxP:(tetO repeats):LEU2:ori:ars1:(tetO repeats):GmR:LoxP:his7+ GFP-cnp1:NAT	?

4.12. Plasmids used in this study

Plasmid number (pYB)	**Description**
1555	pFA6a-mCherry-kanMX6 ampR
1591	pFA6a-mCherry-NatMX6
1657	pFA6a-hphMX6 ampR
1761	pBAL2-tetO-GmR LEU2 ars1 ampR
1840	pBAL2h7L-tetO-GmR LEU2 ars1 ampR his7+<LoxP>
1846	CEN TRP Pnmt81-creEBD-term Pnup211-NLS-tetR-GFP-term ura4+
1847	pBH7L-tetO-GmR his7+<LoxP> ampR
1897	pBAL2-tetO-GmR LEU2 ars1 ampR >loxp-cen1lys1fr-loxp>
1899	pBAL2-tetO-GmR LEU2 ampR >loxp-cen1lys1fr-loxp>
1900	pBAL2-tetO-GmR LEU2 ars1 ampR >loxp-cen3L-loxp>
2016	pFA6a-(s.*pombe*)ars1-hphMX6
2036	CEN TRP Pnmt81-creEBD-term Pnup211-NLS-tetR-mCherry-term ura4+

5. References

Ahmad, K., & Henikoff, S. (2002). Histone H3 variants specify modes of chromatin assembly. *Proceedings of the National Academy of Sciences*, *99*(suppl_4), 16477–16484. https://doi.org/10.1073/pnas.172403699

Akiyoshi, B., & Gull, K. (2014). Discovery of Unconventional Kinetochores in Kinetoplastids. *Cell*, *156*(6), 1247–1258. https://doi.org/10.1016/j.cell.2014.01.049

Alfredsson-Timmins, J., Henningson, F., & Bjerling, P. (2007). The Clr4 methyltransferase determines the subnuclear localization of the mating-type region in fission yeast. *Journal of Cell Science*, *120*(11), 1935–1943. https://doi.org/10.1242/jcs.03457

Allshire, R. C., & Karpen, G. H. (2008a). Epigenetic regulation of centromeric chromatin: Old dogs, new tricks? *Nature Reviews Genetics*, *9*(12), Article 12. https://doi.org/10.1038/nrg2466

Allshire, R. C., & Karpen, G. H. (2008b). Epigenetic regulation of centromeric chromatin: Old dogs, new tricks? *Nature Reviews Genetics*, *9*(12), Article 12. https://doi.org/10.1038/nrg2466

Andersson, J. O. (2005). Lateral gene transfer in eukaryotes. *Cellular and Molecular Life Sciences CMLS*, *62*(11), 1182–1197. https://doi.org/10.1007/s00018-005-4539-z

Appelgren, H., Kniola, B., & Ekwall, K. (2003). Distinct centromere domain structures with separate functions demonstrated in live fission yeast cells. *Journal of Cell Science*, *116*(19), 4035–4042. https://doi.org/10.1242/jcs.00707

Aravind, L., Watanabe, H., Lipman, D. J., & Koonin, E. V. (2000). Lineage-specific loss and divergence of functionally linked genes in eukaryotes. *Proceedings of the National Academy of Sciences*, *97*(21), 11319–11324. https://doi.org/10.1073/pnas.200346997

Arber, W. (1965). Host specificity of DNA produced by *Escherichia coli*. *Journal of Molecular Biology*, *11*(2), 247–256. https://doi.org/10.1016/S0022-2836(65)80055-9

Arber, W. (2000). Genetic variation: Molecular mechanisms and impact on microbial evolution. *FEMS Microbiology Reviews*, *24*(1), 1–7. https://doi.org/10.1111/j.1574-6976.2000.tb00529.x

Arber, W., & Dussoix, D. (1962). Host specificity of DNA produced by *Escherichia coli*. *Journal of Molecular Biology*, *5*(1), 18–36. https://doi.org/10.1016/S0022-2836(62)80058-8

Arber, W., & Linn, S. (1969). DNA Modification and Restriction. *Annual Review of Biochemistry*, *38*(1), 467–500. https://doi.org/10.1146/annurev.bi.38.070169.002343

Ardeljan, D., Taylor, M. S., Ting, D. T., & Burns, K. H. (2017). The Human Long Interspersed Element-1 Retrotransposon: An Emerging Biomarker of Neoplasia. *Clinical Chemistry*, *63*(4), 816–822. https://doi.org/10.1373/clinchem.2016.257444

Asakawa, H., Haraguchi, T., & Hiraoka, Y. (2007). Reconstruction of the kinetochore: A prelude to meiosis. *Cell Division*, *2*(1), 17. https://doi.org/10.1186/1747-1028-2-17

Baan, B. (2009). *The role of ATF2 in insulin action* [Leiden University]. https://hdl.handle.net/1887/13861

Bähler, J., Wu, J. Q., Longtine, M. S., Shah, N. G., McKenzie, A., Steever, A. B., Wach, A., Philippsen, P., & Pringle, J. R. (1998). Heterologous modules for efficient and versatile PCR-based gene targeting in Schizosaccharomyces pombe. *Yeast (Chichester, England)*, *14*(10), 943–951. https://doi.org/10.1002/(SICI)1097-0061(199807)14:10<943::AID-YEA292>3.0.CO;2-Y

Baker, R. T. (1977). Humic acid-associated organic phosphate. *New Zealand Journal of Science*, *20*, 439–441.

Barbalat, R., Ewald, S. E., Mouchess, M. L., & Barton, G. M. (2011). Nucleic Acid Recognition by the Innate Immune System. *Annual Review of Immunology*, *29*(1), 185–214. https://doi.org/10.1146/annurev-immunol-031210-101340

Barra, V., & Fachinetti, D. (2018). The dark side of centromeres: Types, causes and consequences of structural abnormalities implicating centromeric DNA. *Nature Communications*, *9*(1), 4340. https://doi.org/10.1038/s41467-018-06545-y

Bass, H. W., Marshall, W. F., Sedat, J. W., Agard, D. A., & Cande, W. Z. (1997). Telomeres Cluster De Novo before the Initiation of Synapsis: A Three-dimensional Spatial Analysis of Telomere Positions before and during Meiotic Prophase. *Journal of Cell Biology*, *137*(1), 5–18. https://doi.org/10.1083/jcb.137.1.5

Bergmann, J. H., Rodríguez, M. G., Martins, N. M. C., Kimura, H., Kelly, D. A., Masumoto, H., Larionov, V., Jansen, L. E. T., & Earnshaw, W. C. (2011). Epigenetic engineering shows H3K4me2 is required for HJURP targeting and CENP-A assembly on a synthetic human kinetochore. *The EMBO Journal*, *30*(2), 328–340. https://doi.org/10.1038/emboj.2010.329

Black, B. E., & Cleveland, D. W. (2011). Epigenetic Centromere Propagation and the Nature of CENP-A Nucleosomes. *Cell*, *144*(4), 471–479. https://doi.org/10.1016/j.cell.2011.02.002

Bodor, D. L., Mata, J. F., Sergeev, M., David, A. F., Salimian, K. J., Panchenko, T., Cleveland, D. W., Black, B. E., Shah, J. V., & Jansen, L. E. (2014). The quantitative architecture of centromeric chromatin. *eLife*, *3*, e02137. https://doi.org/10.7554/eLife.02137

Boeke, J. D., LaCroute, F., & Fink, G. R. (1984). A positive selection for mutants lacking orotidine-5'-phosphate decarboxylase activity in yeast: 5-fluoro-orotic acid resistance. *Molecular & General Genetics: MGG*, *197*(2), 345–346. https://doi.org/10.1007/BF00330984

Bolivar, F., Rodriguez, R. L., Greene, P. J., Betlach, M. C., Heyneker, H. L., Boyer, H. W., Crosa, J. H., & Falkow, S. (1977). Construction and characterization of new cloning vehicles. II. A multipurpose cloning system. *Gene*, *2*(2), 95–113.

Briggs, E. M., Ha, S., Mita, P., Brittingham, G., Sciamanna, I., Spadafora, C., & Logan, S. K. (2018). Long interspersed nuclear element-1 expression and retrotransposition in prostate cancer cells. *Mobile DNA*, *9*(1), 1. https://doi.org/10.1186/s13100-017-0106-z

Buchwitz, B. J., Ahmad, K., Moore, L. L., Roth, M. B., & Henikoff, S. (1999). A histone-H3-like protein in C. elegans. *Nature*, *401*(6753), Article 6753. https://doi.org/10.1038/44062

Cam, H. P., Noma, K., Ebina, H., Levin, H. L., & Grewal, S. I. S. (2008). Host genome surveillance for retrotransposons by transposon-derived proteins. *Nature*, *451*(7177), Article 7177. https://doi.org/10.1038/nature06499

Campos, M., Capilla, R., Naya, F., Futami, R., Coque, T., Moya, A., Fernandez-Lanza, V., Cantón, R., Sempere, J. M., Llorens, C., & Baquero, F. (2019). Simulating Multilevel Dynamics of Antimicrobial Resistance in a Membrane Computing Model. *mBio*, *10*(1), 10.1128/mbio.02460-18. https://doi.org/10.1128/mbio.02460-18

Cao, X., Wang, S., Ge, L., Zhang, W., Huang, J., & Sun, W. (2021). Extrachromosomal Circular DNA: Category, Biogenesis, Recognition, and Functions. *Frontiers in Veterinary Science*, *8*. https://www.frontiersin.org/articles/10.3389/fvets.2021.693641

Carone, D. M., Longo, M. S., Ferreri, G. C., Hall, L., Harris, M., Shook, N., Bulazel, K. V., Carone, B. R., Obergfell, C., O'Neill, M. J., & O'Neill, R. J. (2009). A new class of retroviral and satellite encoded small RNAs

emanates from mammalian centromeres. *Chromosoma*, *118*(1), 113–125. https://doi.org/10.1007/s00412-008-0181-5

Castellano-Castillo, D., Moreno-Indias, I., Sanchez-Alcoholado, L., Ramos-Molina, B., Alcaide-Torres, J., Morcillo, S., Ocaña-Wilhelmi, L., Tinahones, F., Queipo-Ortuño, M. I., & Cardona, F. (2019). Altered Adipose Tissue DNA Methylation Status in Metabolic Syndrome: Relationships Between Global DNA Methylation and Specific Methylation at Adipogenic, Lipid Metabolism and Inflammatory Candidate Genes and Metabolic Variables. *Journal of Clinical Medicine*, *8*(1), Article 1. https://doi.org/10.3390/jcm8010087

Castillo, A. G., Pidoux, A. L., Catania, S., Durand-Dubief, M., Choi, E. S., Hamilton, G., Ekwall, K., & Allshire, R. C. (2013). Telomeric Repeats Facilitate CENP-ACnp1 Incorporation via Telomere Binding Proteins. *PLoS ONE*, *8*(7), e69673. https://doi.org/10.1371/journal.pone.0069673

Chan, F. L., Marshall, O. J., Saffery, R., Won Kim, B., Earle, E., Choo, K. H. A., & Wong, L. H. (2012). Active transcription and essential role of RNA polymerase II at the centromere during mitosis. *Proceedings of the National Academy of Sciences*, *109*(6), 1979–1984. https://doi.org/10.1073/pnas.1108705109

Chen, Y.-A., Shen, Y.-L., Hsia, H.-Y., Tiang, Y.-P., Sung, T.-L., & Chen, L.-Y. (2017). Extrachromosomal telomere repeat DNA is linked to ALT development via cGAS-STING DNA sensing pathway. *Nature Structural & Molecular Biology*, *24*(12), 1124–1131. https://doi.org/10.1038/nsmb.3498

Chen, Z. J., Parent, L., & Maniatis, T. (1996). Site-Specific Phosphorylation of IκBα by a Novel Ubiquitination-Dependent Protein Kinase Activity. *Cell*, *84*(6), 853–862. https://doi.org/10.1016/S0092-8674(00)81064-8

Chikashige, Y., Ding, D., Imai, Y., Yamamoto, M., Haraguchi, T., & Hiraoka, Y. (1997). Meiotic nuclear reorganization: Switching the position of centromeres and telomeres in the fission yeast Schizosaccharomyces pombe. *The EMBO Journal*, *16*(1), 193–202. https://doi.org/10.1093/emboj/16.1.193

Chikashige, Y., Ding, D.-Q., Funabiki, H., Haraguchi, T., Mashiko, S., Yanagida, M., & Hiraoka, Y. (1994). Telomere-Led Premeiotic Chromosome Movement in Fission Yeast. *Science*, *264*(5156), 270–273. https://doi.org/10.1126/science.8146661

Chikashige, Y., Yamane, M., Okamasa, K., Tsutsumi, C., Kojidani, T., Sato, M., Haraguchi, T., & Hiraoka, Y. (2009). Membrane proteins Bqt3 and -4 anchor telomeres to the nuclear envelope to ensure chromosomal bouquet formation. *Journal of Cell Biology*, *187*(3), 413–427. https://doi.org/10.1083/jcb.200902122

Chueh, A. C., Northrop, E. L., Brettingham-Moore, K. H., Choo, K. H. A., & Wong, L. H. (2009). LINE Retrotransposon RNA Is an Essential Structural and Functional Epigenetic Component of a Core Neocentromeric Chromatin. *PLOS Genetics*, *5*(1), e1000354. https://doi.org/10.1371/journal.pgen.1000354

Clyne, R. K., & Kelly, T. J. (1995). Genetic analysis of an ARS element from the fission yeast Schizosaccharomyces pombe. *The EMBO Journal*, *14*(24), 6348–6357.

Coelho, M., Dereli, A., Haese, A., Kühn, S., Malinovska, L., DeSantis, M. E., Shorter, J., Alberti, S., Gross, T., & Tolić-Nørrelykke, I. M. (2013). Fission Yeast Does Not Age under Favorable Conditions, but Does So after Stress. *Current Biology*, *23*(19), 1844–1852. https://doi.org/10.1016/j.cub.2013.07.084

Collins, K. A., Furuyama, S., & Biggins, S. (2004). Proteolysis Contributes to the Exclusive Centromere Localization of the Yeast Cse4/CENP-A Histone H3 Variant. *Current Biology*, *14*(21), 1968–1972. https://doi.org/10.1016/j.cub.2004.10.024

Connell, J. H. (1980). Diversity and the Coevolution of Competitors, or the Ghost of Competition Past. *Oikos*, *35*(2), 131–138. https://doi.org/10.2307/3544421

Costa, L., Marques, A., Buddenhagen, C. E., Pedrosa-Harand, A., & Souza, G. (2023). Investigating the diversification of holocentromeric satellite DNA *Tyba* in *Rhynchospora* (Cyperaceae). *Annals of Botany*, *131*(5), 813–825. https://doi.org/10.1093/aob/mcad036

Costello, K. R., & Schones, D. E. (2018). Chromatin modifications in metabolic disease: Potential mediators of long-term disease risk. *WIREs Systems Biology and Medicine*, *10*(4), e1416. https://doi.org/10.1002/wsbm.1416

DeFlaun, M., Paul, J., & Jeffrey, W. (1987). Distribution and molecular weight of dissolved DNA in subtropical estuarine and oceanic environments. *Marine Ecology Progress Series*, *38*, 65–73. https://doi.org/10.3354/meps038065

Del Giudice, L., Wolf, K., Seitz, G., Burger, G., Lang, B., & Kaudewitz, F. (1977). Extrachromosomal inheritance inSchizosaccharomyces pombe. *Molecular and General Genetics MGG*, *152*(3), 319–324. https://doi.org/10.1007/BF00693086

Deniz, Ö., Frost, J. M., & Branco, M. R. (2019). Regulation of transposable elements by DNA modifications. *Nature Reviews Genetics*, *20*(7), Article 7. https://doi.org/10.1038/s41576-019-0106-6

Denoth Lippuner, A., Julou, T., & Barral, Y. (2014). Budding yeast as a model organism to study the effects of age. *FEMS Microbiology Reviews*, *38*(2), 300–325. https://doi.org/10.1111/1574-6976.12060

Deyter, G. M. R., & Biggins, S. (2014). The FACT complex interacts with the E3 ubiquitin ligase Psh1 to prevent ectopic localization of CENP-A. *Genes & Development*, *28*(16), 1815–1826. https://doi.org/10.1101/gad.243113.114

Di Vincenzo, F., Yadid, Y., Petito, V., Emoli, V., Masi, L., Gerovska, D., Araúzo-Bravo, M. J., Gasbarrini, A., Regenberg, B., & Scaldaferri, F. (2023). Circular and Circulating DNA in Inflammatory Bowel Disease: From Pathogenesis to Potential Molecular Therapies. *Cells*, *12*(15), 1953. https://doi.org/10.3390/cells12151953

Dimitriu, T., Szczelkun, M. D., & Westra, E. R. (2020). Evolutionary Ecology and Interplay of Prokaryotic Innate and Adaptive Immune Systems. *Current Biology*, *30*(19), R1189–R1202. https://doi.org/10.1016/j.cub.2020.08.028

Drinnenberg, I. A., deYoung, D., Henikoff, S., & Malik, H. S. (2014). Recurrent loss of CenH3 is associated with independent transitions to holocentricity in insects. *eLife*, *3*, e03676. https://doi.org/10.7554/eLife.03676

Dubnau, D. (1999). DNA Uptake in Bacteria. *Annual Review of Microbiology*, *53*(1), 217–244. https://doi.org/10.1146/annurev.micro.53.1.217

Ebrahimi, H., Masuda, H., Jain, D., & Cooper, J. P. (2018). Distinct 'safe zones' at the nuclear envelope ensure robust replication of heterochromatic chromosome regions. *eLife*, *7*, e32911. https://doi.org/10.7554/eLife.32911

Egel, R., & Egel-Mitani, M. (1974). Premeiotic DNA synthesis in fission yeast. *Experimental Cell Research*, *88*(1), 127–134. https://doi.org/10.1016/0014-4827(74)90626-0

Emamalipour, M., Seidi, K., Zununi Vahed, S., Jahanban-Esfahlan, A., Jaymand, M., Majdi, H., Amoozgar, Z., Chitkushev, L. T., Javaheri, T., Jahanban-Esfahlan, R., & Zare, P. (2020). Horizontal Gene Transfer: From Evolutionary Flexibility to Disease Progression. *Frontiers in Cell and Developmental Biology*, *8*. https://www.frontiersin.org/articles/10.3389/fcell.2020.00229

Emerson, J. J., & Li, W.-H. (2010). The genetic basis of evolutionary change in gene expression levels. *Philosophical Transactions of the Royal Society B: Biological Sciences*, *365*(1552), 2581–2590. https://doi.org/10.1098/rstb.2010.0005

Endler, J. (1986). Natural Selection in the Wild. *Monogr Popul Biol*, *21*. https://doi.org/10.2307/2260553

Falcón, A. A., & Aris, J. P. (2003). Plasmid Accumulation Reduces Life Span in Saccharomyces cerevisiae *. *Journal of Biological Chemistry*, *278*(43), 41607–41617. https://doi.org/10.1074/jbc.M307025200

Flemming, W. (1882). *Zellsubstanz, Kern und Zelltheilung*. Vogel.

Forsburg, S. L. (2003). Overview of Schizosaccharomyces pombe. *Current Protocols in Molecular Biology*, *64*(1), 13.14.1-13.14.3. https://doi.org/10.1002/0471142727.mb1314s64

Forsburg, S. L., & Nurse, P. (1991). *Cell Cycle Regulation in the Yeasts Saccharomyces cerevisiae and Schizosaccharomyces pombe*.

Funabiki, H., Hagan, I., Uzawa, S., & Yanagida, M. (1993). Cell cycle-dependent specific positioning and clustering of centromeres and telomeres in fission yeast. *Journal of Cell Biology*, *121*(5), 961–976. https://doi.org/10.1083/jcb.121.5.961

Gallardo, P., Barrales, R. R., Daga, R. R., & Salas-Pino, S. (2019). Nuclear Mechanics in the Fission Yeast. *Cells*, *8*(10), Article 10. https://doi.org/10.3390/cells8101285

Gammon, D. B., & Mello, C. C. (2015). RNA interference-mediated antiviral defense in insects. *Current Opinion in Insect Science*, *8*, 111–120. https://doi.org/10.1016/j.cois.2015.01.006

Gómez, E. B., & Forsburg, S. L. (2004). Analysis of the Fission Yeast Schizosaccharomyces pombe Cell Cycle. In H. B. Lieberman (Ed.), *Cell Cycle Checkpoint Control Protocols* (pp. 93–111). Humana Press. https://doi.org/10.1385/1-59259-646-0:93

Gonzalez, M., He, H., Dong, Q., Sun, S., & Li, F. (2014). Ectopic Centromere Nucleation by CENP-A in Fission Yeast. *Genetics*, *198*(4), 1433–1446. https://doi.org/10.1534/genetics.114.171173

Gonzalez, S., González-Rodríguez, A. P., Suárez-Álvarez, B., López-Soto, A., Huergo-Zapico, L., & Lopez-Larrea, C. (2011). Conceptual aspects of self and nonself discrimination. *Self Nonself*, *2*(1), 19–25. https://doi.org/10.4161/self.2.1.15094

Grallert, B., Nurse, P., & Patterson, T. E. (1993). A study of integrative transformation in Schizosaccharomyces pombe. *Molecular and General Genetics MGG*, *238*(1), 26–32. https://doi.org/10.1007/BF00279526

Grogan, E. A., Summers, W. P., Dowling, S., Shedd, D., Gradoville, L., & Miller, G. (1983). Two Epstein-Barr viral nuclear neoantigens distinguished by gene transfer, serology, and chromosome binding. *Proceedings of the National Academy of Sciences*, *80*(24), 7650–7653. https://doi.org/10.1073/pnas.80.24.7650

Hassold, T., & Hunt, P. (2001). To err (meiotically) is human: The genesis of human aneuploidy. *Nature Reviews Genetics*, *2*(4), Article 4. https://doi.org/10.1038/35066065

Hasson, D., Alonso, A., Cheung, F., Tepperberg, J. H., Papenhausen, P. R., Engelen, J. J. M., & Warburton, P. E. (2011). Formation of novel CENP-A domains on tandem repetitive DNA and across chromosome breakpoints on human chromosome 8q21 neocentromeres. *Chromosoma*, *120*(6), 621–632. https://doi.org/10.1007/s00412-011-0337-6

Hayles, J., & Nurse, P. (2016). Introduction of fission yeast as a model system. *(No Title)*. https://cir.nii.ac.jp/crid/1130282269910953088

Heckman, D. S., Geiser, D. M., Eidell, B. R., Stauffer, R. L., Kardos, N. L., & Hedges, S. B. (2001). Molecular Evidence for the Early Colonization of Land by Fungi and Plants. *Science*, *293*(5532), 1129–1133. https://doi.org/10.1126/science.1061457

Heckmann, S., Macas, J., Kumke, K., Fuchs, J., Schubert, V., Ma, L., Novák, P., Neumann, P., Taudien, S., Platzer, M., & Houben, A. (2013). The holocentric species Luzula elegans shows interplay between centromere and large-scale genome organization. *The Plant Journal: For Cell and Molecular Biology*, *73*(4), 555–565. https://doi.org/10.1111/tpj.12054

Henikoff, S., Ahmad, K., & Malik, H. S. (2001). The Centromere Paradox: Stable Inheritance with Rapidly Evolving DNA. *Science*. https://doi.org/10.1126/science.1062939

Henikoff, S., & Furuyama, T. (2012). The unconventional structure of centromeric nucleosomes. *Chromosoma*, *121*(4), 341–352. https://doi.org/10.1007/s00412-012-0372-y

Henikoff, S., & Smith, M. M. (2015). Histone Variants and Epigenetics. *Cold Spring Harbor Perspectives in Biology*, *7*(1), a019364. https://doi.org/10.1101/cshperspect.a019364

Heyer, W. D., Sipiczki, M., & Kohli, J. (1986). Replicating plasmids in Schizosaccharomyces pombe: Improvement of symmetric segregation by a new genetic element. *Molecular and Cellular Biology*, *6*(1), 80–89.

Hiraoka, Y. (1998). Meiotic telomeres: A matchmaker for homologous chromosomes. *Genes to Cells*, *3*(7), 405–413. https://doi.org/10.1046/j.1365-2443.1998.00205.x

Hoffman, C. S., Wood, V., & Fantes, P. A. (2015). An Ancient Yeast for Young Geneticists: A Primer on the Schizosaccharomyces pombe Model System. *Genetics*, *201*(2), 403–423. https://doi.org/10.1534/genetics.115.181503

Hofstatter, P. G., Thangavel, G., Lux, T., Neumann, P., Vondrak, T., Novak, P., Zhang, M., Costa, L., Castellani, M., Scott, A., Toegelová, H., Fuchs, J., Mata-Sucre, Y., Dias, Y., Vanzela, A. L. L., Huettel, B., Almeida, C. C. S., Šimková, H., Souza, G., … Marques, A. (2022). Repeat-based holocentromeres influence genome architecture and karyotype evolution. *Cell*, *185*(17), 3153-3168.e18. https://doi.org/10.1016/j.cell.2022.06.045

Holoch, D., & Moazed, D. (2015). RNA-mediated epigenetic regulation of gene expression. *Nature Reviews Genetics*, *16*(2), Article 2. https://doi.org/10.1038/nrg3863

Hou, H., Zhou, Z., Wang, Y., Wang, J., Kallgren, S. P., Kurchuk, T., Miller, E. A., Chang, F., & Jia, S. (2012). Csi1 links centromeres to the nuclear envelope for centromere clustering. *Journal of Cell Biology*, *199*(5), 735–744. https://doi.org/10.1083/jcb.201208001

Hull, R. M., King, M., Pizza, G., Krueger, F., Vergara, X., & Houseley, J. (2019). Transcription-induced formation of extrachromosomal DNA during yeast ageing. *PLOS Biology*, *17*(12), e3000471. https://doi.org/10.1371/journal.pbio.3000471

Ishii, K., Ogiyama, Y., Chikashige, Y., Soejima, S., Masuda, F., Kakuma, T., Hiraoka, Y., & Takahashi, K. (2008). Heterochromatin Integrity Affects Chromosome Reorganization After Centromere Dysfunction. *Science*, *321*(5892), 1088–1091. https://doi.org/10.1126/science.1158699

Ishikawa, H., Ma, Z., & Barber, G. N. (2009). STING regulates intracellular DNA-mediated, type I interferon-dependent innate immunity. *Nature*, *461*(7265), Article 7265. https://doi.org/10.1038/nature08476

Itoh, G., Ikeda, M., Iemura, K., Amin, M. A., Kuriyama, S., Tanaka, M., Mizuno, N., Osakada, H., Haraguchi, T., & Tanaka, K. (2018). Lateral attachment of kinetochores to microtubules is enriched in prometaphase rosette and facilitates chromosome alignment and bi-orientation establishment. *Scientific Reports*, *8*(1), 3888. https://doi.org/10.1038/s41598-018-22164-5

Iwasaki, O., Tanaka, A., Tanizawa, H., Grewal, S. I. S., & Noma, K. (2010). Centromeric Localization of Dispersed Pol III Genes in Fission Yeast. *Molecular Biology of the Cell*, *21*(2), 254–265. https://doi.org/10.1091/mbc.e09-09-0790

Janeway, C. A. (2001). How the immune system protects the host from infection. *Microbes and Infection*, *3*(13), 1167–1171. https://doi.org/10.1016/s1286-4579(01)01477-0

Keeling, P. J., & Palmer, J. D. (2008). Horizontal gene transfer in eukaryotic evolution. *Nature Reviews Genetics*, *9*(8), Article 8. https://doi.org/10.1038/nrg2386

Keeney, J. B., & Boeke, J. D. (1994). Efficient targeted integration at leu1-32 and ura4-294 in Schizosaccharomyces pombe. *Genetics*, *136*(3), 849–856. https://doi.org/10.1093/genetics/136.3.849

Kerres, A., Vietmeier-Decker, C., Ortiz, J., Karig, I., Beuter, C., Hegemann, J., Lechner, J., & Fleig, U. (2004). The Fission Yeast Kinetochore Component Spc7 Associates with the EB1 Family Member Mal3 and Is Required for Kinetochore–Spindle Association. *Molecular Biology of the Cell*, *15*(12), 5255–5267. https://doi.org/10.1091/mbc.e04-06-0443

Ketel, C., Wang, H. S. W., McClellan, M., Bouchonville, K., Selmecki, A., Lahav, T., Gerami-Nejad, M., & Berman, J. (2009). Neocentromeres Form Efficiently at Multiple Possible Loci in Candida albicans. *PLOS Genetics*, *5*(3), e1000400. https://doi.org/10.1371/journal.pgen.1000400

Kim, M., & Costello, J. (2017). DNA methylation: An epigenetic mark of cellular memory. *Experimental & Molecular Medicine*, *49*(4), Article 4. https://doi.org/10.1038/emm.2017.10

Kitagawa, T., Ishii, K., Takeda, K., & Matsumoto, T. (2014). The 19S proteasome subunit Rpt3 regulates distribution of CENP-A by associating with centromeric chromatin. *Nature Communications*, *5*(1), Article 1. https://doi.org/10.1038/ncomms4597

Koonin, E. V. (2016). Viruses and mobile elements as drivers of evolutionary transitions. *Philosophical Transactions of the Royal Society B: Biological Sciences*, *371*(1701), 20150442. https://doi.org/10.1098/rstb.2015.0442

Koszul, R., & Kleckner, N. (2009). Dynamic chromosome movements during meiosis: A way to eliminate unwanted connections? *Trends in Cell Biology*, *19*(12), 716–724. https://doi.org/10.1016/j.tcb.2009.09.007

Krawchuk, M. D., & Wahls, W. P. (1999). High-efficiency gene targeting in Schizosaccharomyces pombe using a modular, PCR-based approach with long tracts of flanking homology. *Yeast*, *15*(13), 1419–1427. https://doi.org/10.1002/(SICI)1097-0061(19990930)15:13<1419::AID-YEA466>3.0.CO;2-Q

Kruitwagen, T., Chymkowitch, P., Denoth-Lippuner, A., Enserink, J., & Barral, Y. (2018). Centromeres License the Mitotic Condensation of Yeast Chromosome Arms. *Cell*, *175*(3), 780-795.e15. https://doi.org/10.1016/j.cell.2018.09.012

Lacroix, B., & Citovsky, V. (2016). Transfer of DNA from Bacteria to Eukaryotes. *mBio*, *7*(4), e00863-16. https://doi.org/10.1128/mBio.00863-16

Lando, D., Endesfelder, U., Berger, H., Subramanian, L., Dunne, P. D., McColl, J., Klenerman, D., Carr, A. M., Sauer, M., Allshire, R. C., Heilemann, M., & Laue, E. D. (2012). Quantitative single-molecule microscopy reveals that CENP-ACnp1 deposition occurs during G2 in fission yeast. *Open Biology*, *2*(7), 120078. https://doi.org/10.1098/rsob.120078

Leupold, U. (1949). *Die Vererbung von Homothallie und Heterothallie bei Schizosaccharomyces Pombe*. Luno.

Lewontin, R. C. (1974). THE GENETIC BASIS OF EVOLUTIONARY CHANGE. *Columbia University Press*.

Linder, S. J., & Mostoslavsky, R. (2017). Chapter 15—Interaction Between Cellular Metabolic States and Chromatin Dynamics. In A. Göndör (Ed.), *Chromatin Regulation and Dynamics* (pp. 373–398). Academic Press. https://doi.org/10.1016/B978-0-12-803395-1.00015-0

Liu, X., McLeod, I., Anderson, S., Yates, J. R., & He, X. (2005). Molecular analysis of kinetochore architecture in fission yeast. *The EMBO Journal*, *24*(16), 2919–2930. https://doi.org/10.1038/sj.emboj.7600762

Lodish, H. F. (Ed.). (2000). *Molecular cell biology* (4th ed). W.H. Freeman.

Loidl, J., & Scherthan, H. (2004). Organization and pairing of meiotic chromosomes in the ciliate Tetrahymena thermophila. *Journal of Cell Science*, *117*(24), 5791–5801. https://doi.org/10.1242/jcs.01504

Lorenz, M. G., & Wackernagel, W. (1994). Bacterial gene transfer by natural genetic transformation in the environment. *Microbiological Reviews*, *58*(3), 563–602. https://doi.org/10.1128/mr.58.3.563-602.1994

Lundberg, G., Rosengren, A. H., Håkanson, U., Stewénius, H., Jin, Y., Stewénius, Y., Påhlman, S., & Gisselsson, D. (2008). Binomial Mitotic Segregation of MYCN-Carrying Double Minutes in Neuroblastoma Illustrates the Role of Randomness in Oncogene Amplification. *PLOS ONE*, *3*(8), e3099. https://doi.org/10.1371/journal.pone.0003099

Magidson, V., O'Connell, C. B., Lončarek, J., Paul, R., Mogilner, A., & Khodjakov, A. (2011). The Spatial Arrangement of Chromosomes during Prometaphase Facilitates Spindle Assembly. *Cell*, *146*(4), 555–567. https://doi.org/10.1016/j.cell.2011.07.012

Magidson, V., Paul, R., Yang, N., Ault, J. G., O'Connell, C. B., Tikhonenko, I., McEwen, B. F., Mogilner, A., & Khodjakov, A. (2015). Adaptive changes in the kinetochore architecture facilitate proper spindle assembly. *Nature Cell Biology*, *17*(9), 1134–1144. https://doi.org/10.1038/ncb3223

Malik, H. S., & Henikoff, S. (2009). Major evolutionary transitions in centromere complexity. *Cell*, *138*(6), 1067–1082. https://doi.org/10.1016/j.cell.2009.08.036

Mansisidor, A., Molinar, T., Srivastava, P., Dartis, D. D., Pino Delgado, A., Blitzblau, H. G., Klein, H., & Hochwagen, A. (2018). Genomic Copy-Number Loss Is Rescued by Self-Limiting Production of DNA Circles. *Molecular Cell*, *72*(3), 583-593.e4. https://doi.org/10.1016/j.molcel.2018.08.036

Marechal, V., Dehee, A., Chikhi-Brachet, R., Piolot, T., Coppey-Moisan, M., & Nicolas, J.-C. (1999). Mapping EBNA-1 Domains Involved in Binding to Metaphase Chromosomes. *Journal of Virology*, *73*(5), 4385–4392. https://doi.org/10.1128/jvi.73.5.4385-4392.1999

Matsuda, A., Asakawa, H., Haraguchi, T., & Hiraoka, Y. (2017). Spatial organization of the Schizosaccharomyces pombe genome within the nucleus. *Yeast*, *34*(2), 55–66. https://doi.org/10.1002/yea.3217

McKinley, K. L., & Cheeseman, I. M. (2016). The molecular basis for centromere identity and function. *Nature Reviews Molecular Cell Biology*, *17*(1), Article 1. https://doi.org/10.1038/nrm.2015.5

Molecular Biology of the Fission Yeast. (2012). Elsevier.

Møller, H. D., Parsons, L., Jørgensen, T. S., Botstein, D., & Regenberg, B. (2015). Extrachromosomal circular DNA is common in yeast. *Proceedings of the National Academy of Sciences of the United States of America*, *112*(24), E3114–E3122. https://doi.org/10.1073/pnas.1508825112

Montévil, M., & Mossio, M. (2020). The Identity of Organisms in Scientific Practice: Integrating Historical and Relational Conceptions. *Frontiers in Physiology*, *11*, 611. https://doi.org/10.3389/fphys.2020.00611

Murase, Y., Yamagishi, M., Okada, N., Toya, M., Yajima, J., Hamada, T., & Sato, M. (2022). Fission yeast Dis1 is an unconventional TOG/XMAP215 that induces microtubule catastrophe to drive chromosome pulling. *Communications Biology*, *5*(1), 1–11. https://doi.org/10.1038/s42003-022-04271-2

Murillo-Pineda, M., Valente, L. P., Dumont, M., Mata, J. F., Fachinetti, D., & Jansen, L. E. T. (2021). Induction of spontaneous human neocentromere formation and long-term maturation. *Journal of Cell Biology*, *220*(3), e202007210. https://doi.org/10.1083/jcb.202007210

Nagaki, K., Cheng, Z., Ouyang, S., Talbert, P. B., Kim, M., Jones, K. M., Henikoff, S., Buell, C. R., & Jiang, J. (2004). Sequencing of a rice centromere uncovers active genes. *Nature Genetics*, *36*(2), Article 2. https://doi.org/10.1038/ng1289

Nasmyth, K., Nurse, P., & Fraser, R. S. S. (1979). The effect of cell mass on the cell cycle timing and duration of S-phase in fission yeast. *Journal of Cell Science*, *39*(1), 215–233. https://doi.org/10.1242/jcs.39.1.215

Neitz, M., & Carbon, J. (1985). Identification and Characterization of the Centromere from Chromosome XIV in Saccharomyces cerevisiae. *Molecular and Cellular Biology*, *5*(11), 2887–2893. https://doi.org/10.1128/mcb.5.11.2887-2893.1985

Niwa, O., Matsumoto, T., & Yanagida, M. (1986). Construction of a mini-chromosome by deletion and its mitotic and meiotic behaviour in fission yeast. *Molecular and General Genetics MGG*, *203*(3), 397–405. https://doi.org/10.1007/BF00422063

Noma, K., Allis, C. D., & Grewal, S. I. S. (2001). Transitions in Distinct Histone H3 Methylation Patterns at the Heterochromatin Domain Boundaries. *Science*, *293*(5532), 1150–1155. https://doi.org/10.1126/science.1064150

Noma, K., Cam, H. P., Maraia, R. J., & Grewal, S. I. S. (2006). A Role for TFIIIC Transcription Factor Complex in Genome Organization. *Cell*, *125*(5), 859–872. https://doi.org/10.1016/j.cell.2006.04.028

O'connor, R. M., McARTHUR, C. R., & Clark-Walker, G. D. (1975). Closed-Circular DNA from Mitochondrial-Enriched Fractions of Four Petite-Negative Yeasts. *European Journal of Biochemistry*, *53*(1), 137–144. https://doi.org/10.1111/j.1432-1033.1975.tb04050.x

Ogiyama, Y., Ohno, Y., Kubota, Y., & Ishii, K. (2013). Epigenetically induced paucity of histone H2A.Z stabilizes fission-yeast ectopic centromeres. *Nature Structural & Molecular Biology*, *20*(12), Article 12. https://doi.org/10.1038/nsmb.2697

Ohkura, H., Garcia, M. A., & Toda, T. (2001). Dis1/TOG universal microtubule adaptors—One MAP for all? *Journal of Cell Science*, *114*(21), 3805–3812. https://doi.org/10.1242/jcs.114.21.3805

Payer, L. M., & Burns, K. H. (2019). Transposable elements in human genetic disease. *Nature Reviews Genetics*, *20*(12), Article 12. https://doi.org/10.1038/s41576-019-0165-8

Pazhenkova, E. A., & Lukhtanov, V. A. (2023). Whole-Genome Analysis Reveals the Dynamic Evolution of Holocentric Chromosomes in Satyrine Butterflies. *Genes*, *14*(2), Article 2. https://doi.org/10.3390/genes14020437

Petti, L., Sample, C., & Kieff, E. (1990). Subnuclear localization and phosphorylation of Epstein-Barr virus latent infection nuclear proteins. *Virology*, *176*(2), 563–574. https://doi.org/10.1016/0042-6822(90)90027-O

Polizzi, C., & Clarke, L. (1991). The chromatin structure of centromeres from fission yeast: Differentiation of the central core that correlates with function. *Journal of Cell Biology*, *112*(2), 191–201. https://doi.org/10.1083/jcb.112.2.191

Polleys, E. J., & Freudenreich, C. H. (2021). Homologous recombination within repetitive DNA. *Current Opinion in Genetics & Development*, *71*, 143–153. https://doi.org/10.1016/j.gde.2021.08.005

Rancurel, C., Legrand, L., & Danchin, E. G. J. (2017). Alienness: Rapid Detection of Candidate Horizontal Gene Transfers across the Tree of Life. *Genes*, *8*(10), Article 10. https://doi.org/10.3390/genes8100248

Rhind, N., Chen, Z., Yassour, M., Thompson, D. A., Haas, B. J., Habib, N., Wapinski, I., Roy, S., Lin, M. F., Heiman, D. I., Young, S. K., Furuya, K., Guo, Y., Pidoux, A., Chen, H. M., Robbertse, B., Goldberg, J. M., Aoki, K., Bayne, E. H., … Nusbaum, C. (2011). Comparative functional genomics of the fission yeasts. *Science (New York, N.Y.)*, *332*(6032), 930–936. https://doi.org/10.1126/science.1203357

Saitoh, S., Takahashi, K., & Yanagida, M. (1997). Mis6, a Fission Yeast Inner Centromere Protein, Acts during G1/S and Forms Specialized Chromatin Required for Equal Segregation. *Cell*, *90*(1), 131–143. https://doi.org/10.1016/S0092-8674(00)80320-7

Sakaguchi, J., & Yamamoto, M. (1982). Cloned ural locus of Schizosaccharomyces pombe propagates autonomously in this yeast assuming a polymeric form. *Proceedings of the National Academy of Sciences of the United States of America*, *79*(24), 7819–7823.

Sal'nokov, K. V. (1990). [Extrachromosomal DNA in mammalian cells]. *Tsitologiia*, *32*(11), 1061–1071.

Sauer, B., & Henderson, N. (1988). Site-specific DNA recombination in mammalian cells by the Cre recombinase of bacteriophage P1. *Proceedings of the National Academy of Sciences*, *85*(14), 5166–5170. https://doi.org/10.1073/pnas.85.14.5166

Scherthan, H., Weich, S., Schwegler, H., Heyting, C., Härle, M., & Cremer, T. (1996). Centromere and telomere movements during early meiotic prophase of mouse and man are associated with the onset of chromosome pairing. *Journal of Cell Biology*, *134*(5), 1109–1125. https://doi.org/10.1083/jcb.134.5.1109

Seitz-Mayr, G., Wolf, K., & Kaudewitz, F. (1978). Extrachromosomal inheritance in Schizosaccharomyces pombe. *Molecular and General Genetics MGG*, *164*(3), 309–320. https://doi.org/10.1007/BF00333162

Sender, R., Fuchs, S., & Milo, R. (2016). Revised Estimates for the Number of Human and Bacteria Cells in the Body. *PLOS Biology*, *14*(8), e1002533. https://doi.org/10.1371/journal.pbio.1002533

Shiroiwa, Y., Hayashi, T., Fujita, Y., Villar-Briones, A., Ikai, N., Takeda, K., Ebe, M., & Yanagida, M. (2011). Mis17 Is a Regulatory Module of the Mis6-Mal2-Sim4 Centromere Complex That Is Required for the Recruitment of CenH3/CENP-A in Fission Yeast. *PLOS ONE*, *6*(3), e17761. https://doi.org/10.1371/journal.pone.0017761

Sinclair, D. A., & Guarente, L. (1997). Extrachromosomal rDNA Circles—A Cause of Aging in Yeast. *Cell*, *91*(7), 1033–1042. https://doi.org/10.1016/S0092-8674(00)80493-6

Sipiczki, M. (2000). Where does fission yeast sit on the tree of life? *Genome Biology*, *1*(2), reviews1011.1. https://doi.org/10.1186/gb-2000-1-2-reviews1011

Stearns, S. C. (1994). Hoffman, A. A. and Parsons, P. A. 1991. Evolutionary Genetics and Environmental Stress. Oxford University Press. paper .ix + 284 pp., illus. ISBN: 0-19-854081-7. *Journal of Evolutionary Biology*, *7*(5), 634–635. https://doi.org/10.1046/j.1420-9101.1994.7050634.x

Steiner, F. A., & Henikoff, S. (2014). Holocentromeres are dispersed point centromeres localized at transcription factor hotspots. *eLife*, *3*, e02025. https://doi.org/10.7554/eLife.02025

Stimpson, K. M., Matheny, J. E., & Sullivan, B. A. (2012). Dicentric chromosomes: Unique models to study centromere function and inactivation. *Chromosome Research*, *20*(5), 595–605. https://doi.org/10.1007/s10577-012-9302-3

Strahl, B. D., & Allis, C. D. (2000). The language of covalent histone modifications. *Nature*, *403*(6765), Article 6765. https://doi.org/10.1038/47412

Sundararajan, K., & Straight, A. F. (2022). Centromere Identity and the Regulation of Chromosome Segregation. *Frontiers in Cell and Developmental Biology*, *10*, 914249. https://doi.org/10.3389/fcell.2022.914249

Sveiczer, A. (2004). Modelling the fission yeast cell cycle. *Briefings in Functional Genomics and Proteomics*, *2*(4), 298–307. https://doi.org/10.1093/bfgp/2.4.298

Szittya, G., & Burgyán, J. (2013). RNA Interference-Mediated Intrinsic Antiviral Immunity in Plants. In B. R. Cullen (Ed.), *Intrinsic Immunity* (pp. 153–181). Springer. https://doi.org/10.1007/978-3-642-37765-5_6

Takahashi, K., Chen, E. S., & Yanagida, M. (2000). Requirement of Mis6 Centromere Connector for Localizing a CENP-A-Like Protein in Fission Yeast. *Science*, *288*(5474), 2215–2219. https://doi.org/10.1126/science.288.5474.2215

Takayama, Y., Sato, H., Saitoh, S., Ogiyama, Y., Masuda, F., & Takahashi, K. (2008). Biphasic incorporation of centromeric histone CENP-A in fission yeast. *Molecular Biology of the Cell*, *19*(2), 682–690. https://doi.org/10.1091/mbc.e07-05-0504

Tanae, K., Horiuchi, T., Yamakawa, T., Matsuo, Y., & Kawamukai, M. (2012). Sim3 shares some common roles with the histone chaperone Asf1 in fission yeast. *FEBS Letters*, *586*(23), 4190–4196. https://doi.org/10.1016/j.febslet.2012.10.020

Tanaka, K. (2012). Dynamic regulation of kinetochore–microtubule interaction during mitosis. *The Journal of Biochemistry*, *152*(5), 415–424. https://doi.org/10.1093/jb/mvs109

Tanaka, T. U., Stark, M. J. R., & Tanaka, K. (2005). Kinetochore capture and bi-orientation on the mitotic spindle. *Nature Reviews Molecular Cell Biology*, *6*(12), 929–942. https://doi.org/10.1038/nrm1764

Thomas, C. M., & Nielsen, K. M. (2005). Mechanisms of, and barriers to, horizontal gene transfer between bacteria. *Nature Reviews. Microbiology*, *3*(9), 711–721. https://doi.org/10.1038/nrmicro1234

Topp, C. N., Zhong, C. X., & Dawe, R. K. (2004). Centromere-encoded RNAs are integral components of the maize kinetochore. *Proceedings of the National Academy of Sciences*, *101*(45), 15986–15991. https://doi.org/10.1073/pnas.0407154101

Trelles-Sticken, E., Loidl, J., & Scherthan, H. (1999). Bouquet formation in budding yeast: Initiation of recombination is not required for meiotic telomere clustering. *Journal of Cell Science*, *112*(5), 651–658. https://doi.org/10.1242/jcs.112.5.651

Trevors, J. T. (1996). DNA in soil: Adsorption, genetic transformation, molecular evolution and genetic microchip. *Antonie van Leeuwenhoek*, *70*(1), 1–10. https://doi.org/10.1007/BF00393564

Turcot, V., Tchernof, A., Deshaies, Y., Pérusse, L., Bélisle, A., Marceau, S., Biron, S., Lescelleur, O., Biertho, L., & Vohl, M.-C. (2012). LINE-1 methylation in visceral adipose tissue of severely obese individuals is associated with metabolic syndrome status and related phenotypes. *Clinical Epigenetics*, *4*(1), 10. https://doi.org/10.1186/1868-7083-4-10

Uzawa, S., & Yanagida, M. (1992). Visualization of centromeric and nucleolar DNA in fission yeast by fluorescence in situ hybridization. *Journal of Cell Science*, *101*(2), 267–275. https://doi.org/10.1242/jcs.101.2.267

Uzman, A. (2003). Molecular biology of the cell (4th ed.): Alberts, B., Johnson, A., Lewis, J., Raff, M., Roberts, K., and Walter, P. *Biochemistry and Molecular Biology Education*, *31*(4), 212–214. https://doi.org/10.1002/bmb.2003.494031049999

Vasu, K., & Nagaraja, V. (2013). Diverse Functions of Restriction-Modification Systems in Addition to Cellular Defense. *Microbiology and Molecular Biology Reviews : MMBR*, *77*(1), 53–72. https://doi.org/10.1128/MMBR.00044-12

Vazquez-Martin, A., Van den Haute, C., Cufí, S., Corominas-Faja, B., Cuyàs, E., Lopez-Bonet, E., Rodriguez-Gallego, E., Fernández-Arroyo, S., Joven, J., Baekelandt, V., & Menendez, J. A. (2016). Mitophagy-

driven mitochondrial rejuvenation regulates stem cell fate. *Aging*, *8*(7), 1330–1352. https://doi.org/10.18632/aging.100976

Vyas, A., Freitas, A. V., Ralston, Z. A., & Tang, Z. (2021a). Correction: Fission Yeast Schizosaccharomyces pombe: A Unicellular "Micromammal" Model Organism. *Current Protocols*, *1*(7), e225. https://doi.org/10.1002/cpz1.225

Vyas, A., Freitas, A. V., Ralston, Z. A., & Tang, Z. (2021b). Fission Yeast Schizosaccharomyces pombe: A Unicellular "Micromammal" Model Organism. *Current Protocols*, *1*(6), e151. https://doi.org/10.1002/cpz1.151

Weaver, B. A. A., & Cleveland, D. W. (2007). Aneuploidy: Instigator and Inhibitor of Tumorigenesis. *Cancer Research*, *67*(21), 10103–10105. https://doi.org/10.1158/0008-5472.CAN-07-2266

Westhorpe, F. G., & Straight, A. F. (2015). The Centromere: Epigenetic Control of Chromosome Segregation during Mitosis. *Cold Spring Harbor Perspectives in Biology*, *7*(1), a015818. https://doi.org/10.1101/cshperspect.a015818

Wieland, G., Orthaus, S., Ohndorf, S., Diekmann, S., & Hemmerich, P. (2004). Functional Complementation of Human Centromere Protein A (CENP-A) by Cse4p from Saccharomyces cerevisiae. *Molecular and Cellular Biology*, *24*(15), 6620–6630. https://doi.org/10.1128/MCB.24.15.6620-6630.2004

Wong, L. H., Brettingham-Moore, K. H., Chan, L., Quach, J. M., Anderson, M. A., Northrop, E. L., Hannan, R., Saffery, R., Shaw, M. L., Williams, E., & Choo, K. H. A. (2007). Centromere RNA is a key component for the assembly of nucleoproteins at the nucleolus and centromere. *Genome Research*, *17*(8), 1146–1160. https://doi.org/10.1101/gr.6022807

Wood, V. (2006). How to get the most from fission yeast genome data: A report from the 2006 European Fission Yeast Meeting computing workshop. *Yeast*, *23*(13), 905–912. https://doi.org/10.1002/yea.1419

Woolcock, K. J., Stunnenberg, R., Gaidatzis, D., Hotz, H.-R., Emmerth, S., Barraud, P., & Bühler, M. (2012). RNAi keeps Atf1-bound stress response genes in check at nuclear pores. *Genes & Development*, *26*(7), 683–692. https://doi.org/10.1101/gad.186866.112

Wu, S., Bafna, V., Chang, H. Y., & Mischel, P. S. (2022). Extrachromosomal DNA: An Emerging Hallmark in Human Cancer. *Annual Review of Pathology*, *17*, 367–386. https://doi.org/10.1146/annurev-pathmechdis-051821-114223

Wu, W., McHugh, T., Kelly, D. A., Pidoux, A. L., & Allshire, R. C. (2021). *Centromere identity is dependent on nuclear spatial organization* [Preprint]. Cell Biology. https://doi.org/10.1101/2021.12.16.473016

Yang, L., Jia, R., Ge, T., Ge, S., Zhuang, A., Chai, P., & Fan, X. (2022). Extrachromosomal circular DNA: Biogenesis, structure, functions and diseases. *Signal Transduction and Targeted Therapy*, *7*(1), 1–21. https://doi.org/10.1038/s41392-022-01176-8

Yuen, K. W. Y., Nabeshima, K., Oegema, K., & Desai, A. (2011). Rapid De Novo Centromere Formation Occurs Independently of Heterochromatin Protein 1 in C. elegans Embryos. *Current Biology*, *21*(21), 1800–1807. https://doi.org/10.1016/j.cub.2011.09.016

Zhao, Y., Yu, L., Zhang, S., Su, X., & Zhou, X. (2022). Extrachromosomal circular DNA: Current status and future prospects. *eLife*, *11*, e81412. https://doi.org/10.7554/eLife.81412

Zhou, R., & Rana, T. M. (2013). RNA-based mechanisms regulating host–virus interactions. *Immunological Reviews*, *253*(1), 97–111. https://doi.org/10.1111/imr.12053